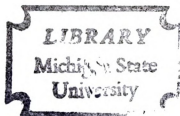


SYNTHESIS AND ADSORPTION OF
PORPHYRINS AND PORPHYRIN
INTERMEDIATES ON THE INTRACRYSTAL
SURFACES OF MONTMORILLONITE

Dissertation for the Degree of Ph. D.
MICHIGAN STATE UNIVERSITY
SHARMAINE S. CADY
1976



This is to certify that the

thesis entitled

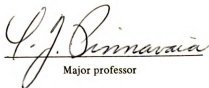
**SYNTHESIS AND ADSORPTION OF PORPHYRINS AND
PORPHYRIN INTERMEDIATES ON THE INTRACRYSTAL
SURFACES OF MONTMORILLONITE**

presented by

Sharmaine S. Cady

has been accepted towards fulfillment
of the requirements for

Ph.D. degree in **Chemistry**


Major professor

Date March 31, 1976

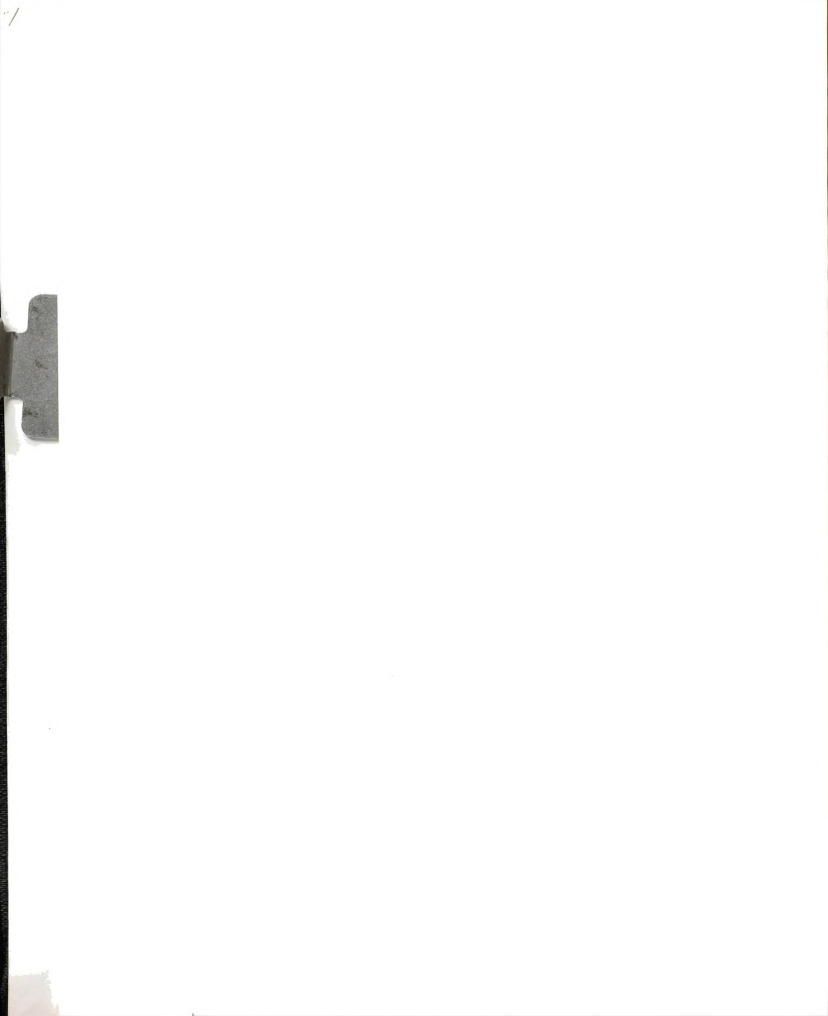












G994/35

ABSTRACT

SYNTHESIS AND ADSORPTION OF PORPHYRINS AND
PORPHYRIN INTERMEDIATES ON THE INTRACRYSTAL
SURFACES OF MONTMORILLONITE

By

Sharmaine S. Cady

The adsorption of pyrrole and benzaldehyde on the interlayer surfaces of various cation exchanged montmorillonites under aerobic and anaerobic aqueous conditions at room temperature results in the formation of a porphyrin intermediate which is assigned a porphodimethene structure. This condensation to a macrocyclic structure is achieved at pyrrole and benzaldehyde concentrations of 0.015 M or less and M^{n+} to pyrrole molar ratios of 1:2, where $M^{n+} = Fe^{3+}, Cu^{2+}, Zn^{2+}, Co^{2+}, VO^{2+}, Mg^{2+},$ and Na^{+} . The H^{+} and TPA^{+} exchange forms of montmorillonite are also investigated.

During the course of the condensation reaction, the aqueous clay slurries gradually change from pale pink to a deep purple over a 24-hour period. The elapsed time before the initial appearance of the pink color is dependent on the acidity of the cation in the interlamellar region. $Fe(III), Cu(II), VO(II),$ and H^{+} require only minutes to initiate the condensation while the other metal ions require a half hour or more before any color change is



observed. TPA^+ montmorillonite does not catalyze the reaction.

Freeze-drying of the clays with the adsorbed reaction product yields purple clays whose Nujol mull, visible absorption spectra exhibit an intense absorption near 500 nm characteristic of porphyrin intermediates with a dipyrromethene chromophore. X-ray diffraction data indicate a basal spacing of $5.1 \overset{\circ}{\text{A}}$, which is the approximate thickness of a porphyrin ring and indicates the intermediate is oriented parallel to the silicate layers. This "sandwiching" of the intermediate between the layers may result in the flattening of the pyrrole and benzene rings which increases the resonance interaction of the phenyl rings with the porphyrin nucleus. This increased resonance interaction accounts for the bathochromic shift of the visible absorption band observed for the intermediate adsorbed on montmorillonite from that obtained in acetic acid solution.

Desorption of the intermediate from the montmorillonite surface in the presence of a large excess of exchangeable cation results in its oxidation to the free base porphyrin and/or the diprotonated cation of the porphyrin. The highest yields of porphyrin (10 to 12 per cent based on pyrrole) are obtained when the condensation reaction is allowed to proceed in the presence of an exchangeable cation.

The porphyrin intermediate may be adsorbed onto the external surfaces of Cu(II) and TPA^+ montmorillonites from a chloroform solution that is $1.1 \times 10^{-2} \text{ M}$ in pyrrole and



Sharmaine S. Cady

benzaldehyde and contains 0.1 ml concentrated HCl. Maximum absorption occurs at 485 nm for TPA⁺ montmorillonite and at 505 nm for Cu(II) montmorillonite. The bathochromic shift of the absorption in the case of Cu(II) montmorillonite is believed to arise from chelation of the porphyrin intermediate with the Cu(II) ions.

In studies on the adsorption of free base meso-tetraphenylporphyrin by metal ion exchange forms of montmorillonite, solutions of porphyrin in acetone are allowed to react with montmorillonite at M²⁺ to porphyrin molar ratios of 14:1, 2:1, 1:1, and 1:2. The adsorbed free base porphyrin undergoes two distinct reactions with the metal exchange ions: formation of the dication, which remains mineral-bound, and formation of metalloporphyrins, which are desorbed into solution.

Dication formation is found to be dependent on the acidity of the exchangeable cation, as measured by its ability to hydrolyze in the interlamellar region. X-ray diffraction data, infrared pleochroic measurements, and visible absorption spectra for the dication exchange form of montmorillonite indicate that the dication orients itself parallel to the silicate layers upon intercalation.

Cu(II), Zn(II), and Co(II) are the only metal exchange ions incorporated into the porphyrin ring with the order of the rate of incorporation being given by Cu(II) > Zn(II) >> Co(II). Dication formation also occurs during metalloporphyrin formation; however, the metallation reaction



Sharmaine S. Cady

predominates. The neutral porphyrin complexes CuTPP and CoTPP are physically adsorbed onto the external surfaces of montmorillonite.

SYNTHESIS AND ADSORPTION OF PORPHYRINS AND
PORPHYRIN INTERMEDIATES ON THE INTRACRYSTAL
SURFACES OF MONTMORILLONITE

By

Sharmaine S. Cady ^{andra}

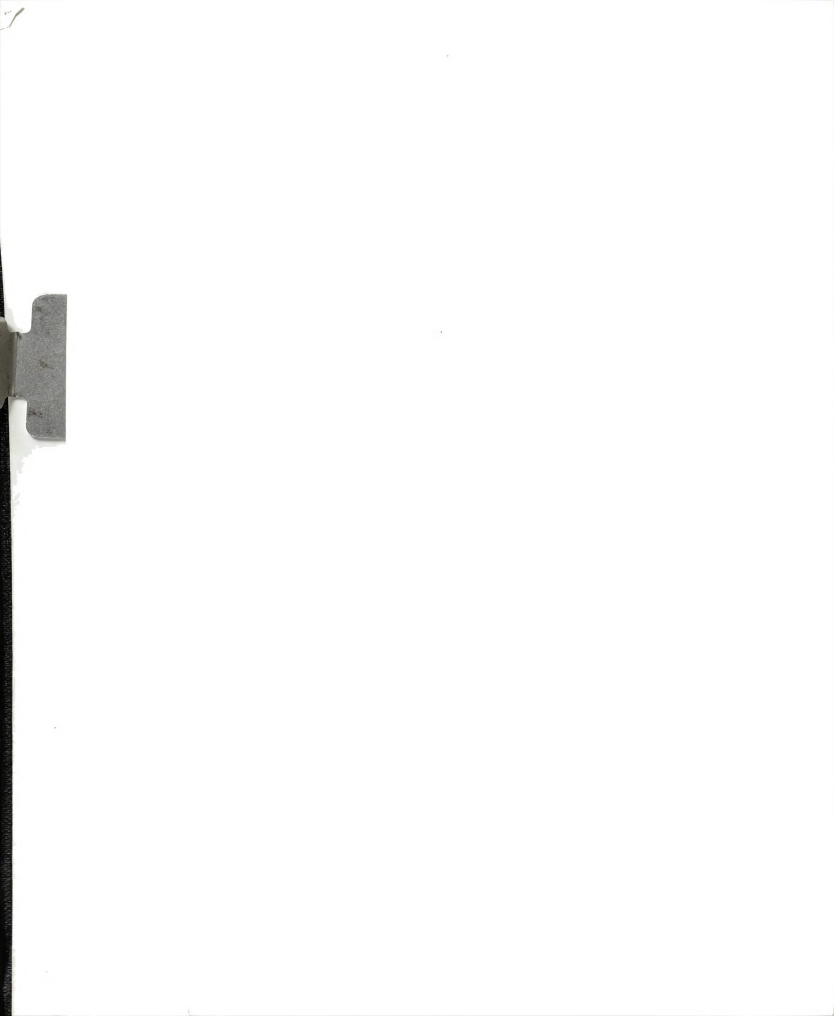
A DISSERTATION

Submitted to
Michigan State University
in partial fulfillment of the requirements
for the degree of

DOCTOR OF PHILOSOPHY

Department of Chemistry

1976



To
my parents
and
my husband



ACKNOWLEDGMENTS

I wish to express my appreciation to Professor Thomas J. Pinnavaia for the patience, guidance, and support which he has shown me during the past five years. I wish to thank Professor C. H. Brubaker, Jr. for being my second reader and overseeing my grammar. I also wish to thank Professor M. M. Mortland of the Department of Crops and Soil Science for the interest he has expressed in my research and for the helpful suggestions he has given me.

A special note of thanks is due Mr. Vaughn E. Berkheiser for his invaluable assistance in obtaining and interpreting the X-ray diffraction data.

Finally, I am deeply grateful to my husband, Skip, for the love and encouragement he has given me throughout my graduate studies. I am especially grateful to my parents, Mr. and Mrs. Leon J. Shive, for their continued love and encouragement and for the many sacrifices made on my behalf which have enabled me to pursue my education.



TABLE OF CONTENTS

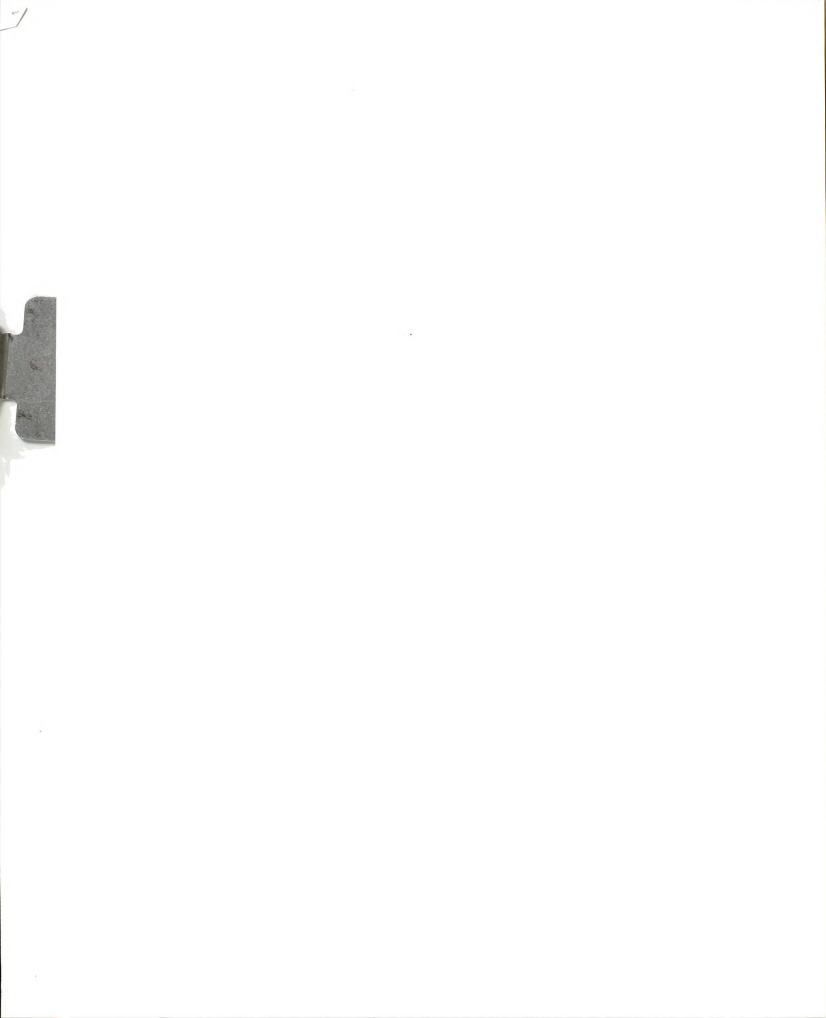
Chapter	Page
1. STATEMENT OF PURPOSE	1
2. INTRODUCTION	4
2.1 Clay Minerals	4
Definition	4
Structure	4
Exchange cations	6
Swelling properties	6
2.2 Porphyrins	9
Structure	9
Ionization	13
Metalloporphyrins	14
Spectra	15
Adsorption on clay minerals	17
2.3 <u>meso</u> -Tetraphenylporphyrin	19
Synthesis	19
Mechanisms of formation	19
2.4 Chemical Evolution of Porphyrins	27
2.5 Prebiotic Syntheses on Clay Minerals	30
3. EXPERIMENTAL SECTION	33
3.1 Preparation of Homoionic Montmorillonites	33
M ⁿ⁺ montmorillonites	33
TPA ⁺ and H ⁺ montmorillonites	34
TPPH ₄ ⁺⁺ montmorillonite	34
3.2 Synthesis of TPPH ₂	35
3.3 Adsorption of TPPH ₂ onto Montmorillonite	35



Chapter	Page	
3.4	Reaction between Pyrrole and Benzaldehyde in the Presence of Montmorillonite	40
	Aerobic synthesis	40
	Anaerobic synthesis	41
3.5	Reaction between Pyrrole and Benzaldehyde in Water	42
3.6	Desorption of the Condensation Product	42
	Method A	42
	Method B	43
	Method C	44
	Method D	44
3.7	Porphyrin Intermediates	45
	Synthesis	45
	Adsorption on montmorillonite	46
3.8	Spectroscopy	51
	Visible absorption	51
	Infrared absorption	51
	Electron spin resonance	51
	X-ray diffraction	51
3.9	Chemical Analyses	51
4.	RESULTS AND DISCUSSION	52
4.1	Interaction of <u>meso</u> -Tetraphenylporphyrin with Montmorillonite	52
	VO(II) and Fe(III) montmorillonite	52
	Cu(II) and Zn(II) montmorillonite	57
	Co(II) montmorillonite	63
	Na(I) and Mg(II) montmorillonite	63
	Mechanism of <u>meso</u> -tetraphenylporphyrin adsorption	68
	Conclusion	73



Chapter	Page
4.2 Synthesis of Porphyrin Intermediates on the Intracrystal Surfaces of Montmorillonite	75
Visible absorption spectra	75
Desorption studies	81
Adsorption of the porphyrin intermediate from solution	84
Mechanism of <u>meso</u> -tetraphenylporpho- dimethene formation	86
Conclusion	92
BIBLIOGRAPHY	93



LIST OF TABLES

Table	Page
1. Ultraviolet and Visible Absorption Spectra for the Reaction of TPPH_2 with Montmorillonite .	54
2. Hydrolysis Constants for Selected Metal Ions . .	70
3. Visible Absorption Spectra of the Pyrrole- Benzaldehyde Condensation Product Adsorbed on Various Montmorillonites	76



LIST OF FIGURES

Figure	Page
1. Structure of montmorillonite.	8
2. Molecular structures of (a) porphine, (b) chlorin, (c) tetrahydroporphyrin, (d) porphyrinogen, (e) porphomethene, (f) phlorin, (g) porphodimethene, (h) phlorin monocation, and (i) porphodimethene dication.	11
3. Molecular structures of (a) <u>meso</u> -tetraphenylporphyrin, (b) <u>meso</u> -tetraphenylporphyrin dication, and (c) metal chelate of <u>meso</u> -tetraphenylporphyrin	21
4. Mechanism proposed by Badger <u>et al</u> for the Rothmund reaction.	23
5. Summary of Dolphin's proposed mechanism for <u>meso</u> -tetraarylporphyrin formation	26
6. Electronic absorption spectra of $TPPH_4^{++}$ in glacial acetic acid, $TPPH_4^+$ montmorillonite, and $Fe(III)$ montmorillonite after adsorption of $TPPH_2$	37
7. Infrared absorption spectra of (A) $Cu(II)$ montmorillonite dried 1 week at $110^{\circ} C$ and (B) $Cu(II)$ montmorillonite after exchange with $TPPH_4^+$ and drying 4 weeks at $130^{\circ} C$ to remove adsorbed acetone	39
8. Electronic absorption spectra of an $HCl-CHCl_3$ solution of pyrrole and benzaldehyde after 2^3 hours of reaction time and after exposure to air overnight	48
9. Electronic absorption spectra of TPA^+ montmorillonite after the adsorption of the porphyrin intermediate from $HCl-CHCl_3$ solution and $Cu(II)$ montmorillonite after adsorption of the intermediate from $HCl-CHCl_3$ solution	50



Figure	Page
10. Schematic drawing showing the orientation of the porphyrin skeleton between montmorillonite layers	56
11. (A) Spectrophotometric changes after various time intervals in the absorption spectrum of the TPPH ₂ -acetone solution after the addition of Cu(II) montmorillonite. (B) and (C) Visible and Soret absorptions of the TPPH ₂ -acetone solution before and 24 hours after the addition of Cu(II) montmorillonite	59
12. (A) Spectrophotometric changes after various time intervals in the absorption spectrum of the TPPH ₂ -acetone solution after the addition of Zn(II) montmorillonite. (B) and (C) Visible and Soret absorptions of the TPPH ₂ -acetone solution before and 24 hours after the addition of Zn(II) montmorillonite	61
13. Electronic absorption spectrum of CoTPP on Co(II) montmorillonite	65
14. (A) Spectrophotometric changes after various time intervals in the absorption spectrum of the TPPH ₂ -acetone solution after the addition of Co(II) montmorillonite at reflux temperature. (B) and (C) Visible and Soret absorptions of the TPPH ₂ -acetone solution before and 24 hours after the addition of Co(II) montmorillonite.	67
15. Electronic absorption spectra of the pyrrole-benzaldehyde condensation product adsorbed on Cu(II) montmorillonite and H ⁺ montmorillonite . .	78
16. Electronic absorption spectra of the chloroform extraction solution 2 hours and 24 hours after the desorption of the pyrrole-benzaldehyde condensation product from Cu(II) montmorillonite in the presence of TPA ⁺	83
17. Mechanism of <u>meso</u> -tetraphenylporphodimethene formation on the intracrystal surfaces of montmorillonite	89

CHAPTER 1

STATEMENT OF PURPOSE

The interaction of porphyrins with clay minerals has been studied by petroleum geochemists to determine if clay surfaces played a role in the degradation of chlorophyll to a homologous series of porphyrins similar to that found in petroleum, oil shale, and coal. Although numerous researchers have concentrated on the relation between porphyrins and clay minerals in the origin of petroleum, no attention has been given to the formation of porphyrins in the presence of clay minerals from simple precursor molecules available on the prebiotic, primitive Earth 4.5 to 3.5 billion years ago. The presence of porphyrins on the primitive Earth was necessary for the emergence of the first living organism and the subsequent plant and animal life that developed. The research presented here provides in part a plausible mechanism for the prebiotic synthesis of porphyrins by reaction of pyrrole and an aldehyde on a clay mineral surface.

The kinetics of meso-tetraarylporphyrin formation indicate that at least one step in the reaction mechanism

is acid-catalyzed.¹⁻⁴ Since transition metal ions exchanged onto the intracrystal surfaces of montmorillonite generate an acidic medium in the interlamellar region by transferring protons to interlayer water molecules, it is feasible that montmorillonite may act as an effective heterogeneous catalyst for the prebiotic synthesis of porphyrins or their intermediate precursors from simple molecules present during chemical evolution.

The M^{n+} montmorillonite-pyrrole-benzaldehyde-water system was chosen for investigation, where $M^{n+} = Fe^{3+}$, Cu^{2+} , Zn^{2+} , Co^{2+} , VO^{2+} , Mg^{2+} , and Na^+ . An expanding layer lattice silicate, such as montmorillonite, was required for the experiments in order to allow the reactant molecules to penetrate the interlamellar region and come in contact with the catalytic surface. Water was selected as the solvent to simulate the environment provided by the prebiotic ocean. In order for synthesis to occur, the montmorillonite clay must concentrate the reactant molecules from the aqueous solution, catalyze their condensation to macrocycles, and then provide for the storage of the reaction products until their incorporation into the first living cell.

Pyrrole and benzaldehyde were ideal for the reactant molecules because the reactions between pyrroles and benzaldehydes offer several diversified pathways and intermediates leading to the formation of meso-tetraaryl-porphyrins. It was of interest to determine whether the

structure of the silicate layer lattices of clay minerals and the increased acidic nature of the interlayer water molecules would influence the mechanism by which porphyrin synthesis may occur.

Since free base meso-tetraphenylporphyrin, the diacid, and several of the reaction intermediates have distinct and characteristic absorption spectra, the condensation products formed on the clay surface could be easily identified from their electronic absorption spectra. In addition, X-ray diffraction data could be employed to determine whether the products were intercalated or only externally adsorbed.

It was also necessary in the present studies to prepare free base meso-tetraphenylporphyrin and study its adsorption on montmorillonite saturated with various metal ions in order to compare its interaction with the clay surface with that exhibited by the condensation reaction products.

CHAPTER 2

INTRODUCTION

2.1 Clay Minerals

Definition. Naturally occurring clay minerals invariably contain varying percentages of coarse, nonclay-mineral material. A clay particle size of 2μ is frequently the optimum size fraction for the best separation of the clay-mineral components from the nonclay-mineral components in the natural source materials. The term "clay" in the context of the research presented here indicates that the minerals employed does not exceed 2μ as the upper limit.

Structure. Clay minerals are essentially composed of silica, alumina, and water, often with appreciable quantities of iron, alkali cations, and alkaline earth cations. Based on structural characteristics, clay minerals can be classified into two groups: amorphous and crystalline. The crystalline group can be further subdivided into layer- and chain-type structures. Montmorillonite is a crystalline-type, expanding layer lattice clay mineral with the approximate unit cell formula $\text{Na}_{0.66}[\text{Si}_8(\text{Al}_{3.34}, \text{Mg}_{0.66})\text{O}_{20}(\text{OH})_4]$.

Two basic structural units compose the lattices of

most of the clay minerals. One unit consists of a central aluminum, magnesium or iron atom octahedrally coordinated to six oxygen atoms or hydroxyl groups. When aluminum is the central atom, only two thirds of the octahedral positions are filled to maintain electrical neutrality in the octahedral sheet. If magnesium is substituted for aluminum in the octahedral layer, all the positions must be filled to balance the electrical charge.

The second structural unit is the silica tetrahedron. Each tetrahedron contains a central silicon atom bound to the four oxygen atoms occupying the apices of the tetrahedron. Occasionally a hydroxyl group is located at one of the apices in order to balance the charge. These silica tetrahedra are arranged in an open hexagonal network which is repeated indefinitely to form a sheet. In addition, the tips of all the tetrahedra point in the same direction, and the triangular bases all lie in the same plane.

The montmorillonite lattice structure is composed of three-layer units consisting of two silica tetrahedral sheets with a central alumina octahedral sheet. The tetrahedral and octahedral layers are arranged so that the tips of the silica tetrahedra and one of the hydroxyl layers of the octahedral sheet form a common layer, and each tetrahedron shares its apex oxygen with an octahedron.

The layers composing the montmorillonite lattice are continuous in the a and b directions and are stacked one above the other in the c direction. The c-axis dimension

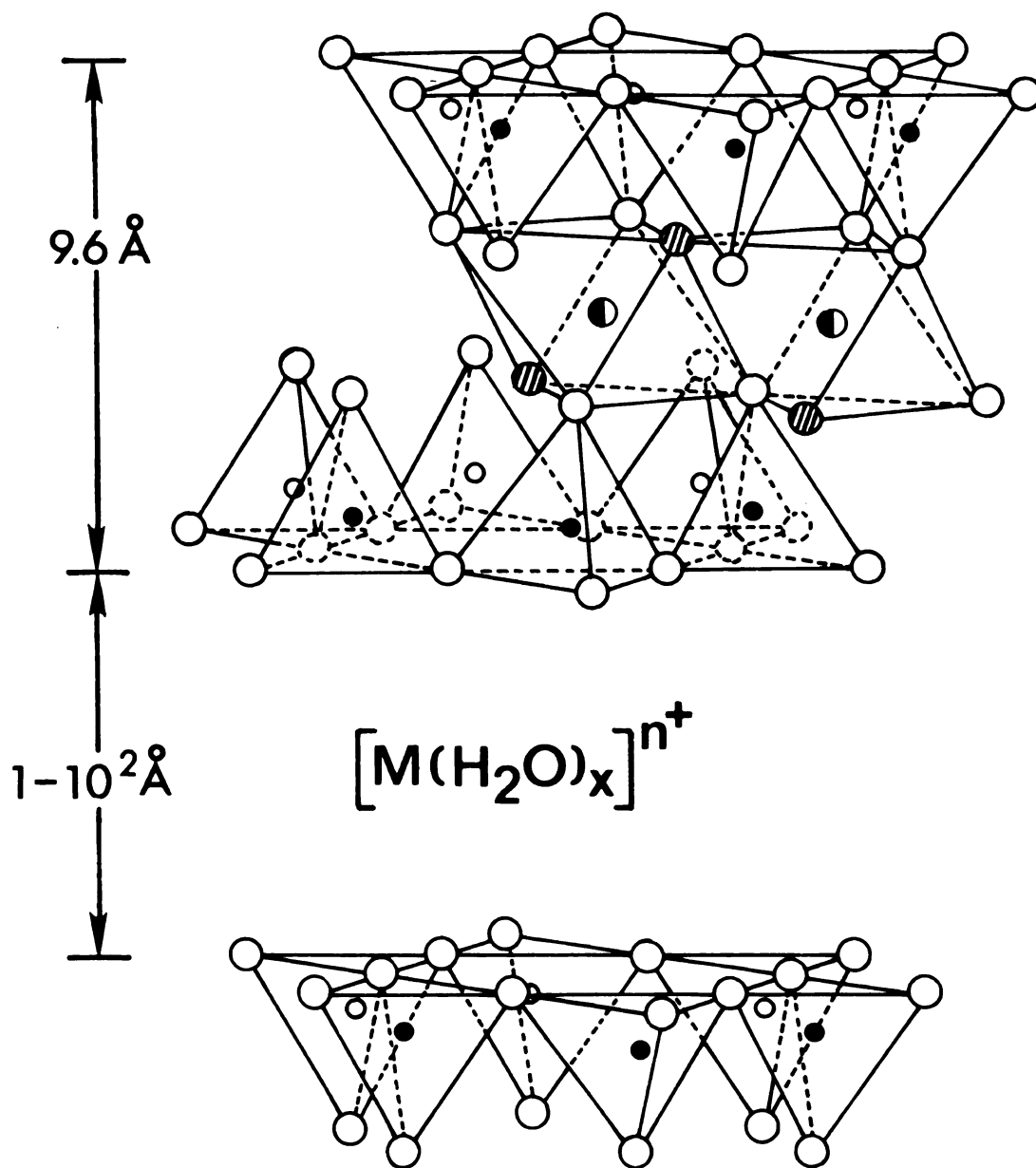
of the three-layer structural unit is $9.6 \overset{0}{\text{A}}$. Figure 1 shows a diagrammatic sketch of this structure of montmorillonite.

Exchange cations. The layer lattice units always have a net negative charge per unit cell of -0.66 associated with them as a result of substitutions within the lattice of Al^{3+} for Si^{4+} in the tetrahedral sheet and/or Mg^{2+} for Al^{3+} or Li^+ for Mg^{2+} in the octahedral sheet. This charge deficiency is balanced by exchangeable cations adsorbed between the unit silicate layers and around their edges.

These exchangeable cations are of fundamental importance in clay chemistry for they have a pronounced effect on many of the physical properties of clay minerals. The c-axis spacing of completely dehydrated montmorillonite is dependent to some extent on the size of the intercalated cation, the c-axis spacing being larger for larger cations. It is also of significant importance to the research presented here that the intercalated cations adsorbed in the natural state can be exchanged for other cations by treatment with such ions in a water solution or other suitable solvent. The exchange reaction is also stoichiometric with montmorillonite having an approximate exchange capacity of 90 meq/100 g clay.

Swelling properties. Co-adsorbed with the exchangeable cations into the interlayer region are the solvent molecules, usually water. The thickness of the water layer between

Figure 1. Structure of montmorillonite.



- Al^{3+} , Mg^{2+} , Fe^{3+}
- Oxygens
- ◐ Hydroxyls
- } Si^{4+} , occasionally Al^{3+}
- }

the silicate units is dependent on the nature of the exchangeable cation at a given relative humidity; however, the thickness of the water layer is normally restricted to an integral number of molecular water layers, usually one or two.

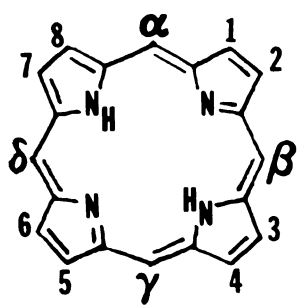
The existence of a very weak bond between the silica-alumina-silica structural units in the c direction allows the penetration of inorganic and organic molecules between the silicate layers. This ability of the montmorillonite lattice to expand in the c direction is of primary importance in studies of heterogeneous catalysis on clay surfaces.

2.2 Porphyrins

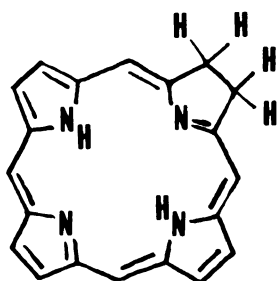
Structure. Porphyrins are a class of highly conjugated tetrapyrrole macrocycles which are formally derived from the parent free base compound, porphine(PH_2)(Fig. 2a), by substitution of some or all of the hydrogen atoms in positions 1-8 and/or the meso- positions α - δ . The porphyrins of animal origin, including the metalloporphyrins such as the iron heme complexes, are completely substituted at all eight pyrrole carbon atoms. Substitution at the meso- positions has not been found in the naturally occurring porphyrins.

Crystal studies on the porphine molecule^{5,6} show it to be essentially planar; however, the porphyrin ring system is flexible, having a low energy barrier with

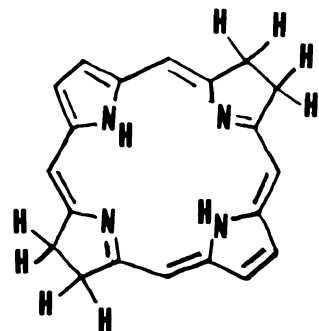
Figure 2. Molecular structures of (a) porphine, (b) chlorin, (c) tetrahydroporphyrin, (d) porphyrinogen, (e) porphomethene, (f) phlorin, (g) porphodimethene, (h) phlorin monocation, and (i) porphodimethene dication.



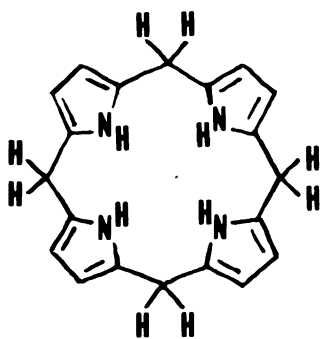
a



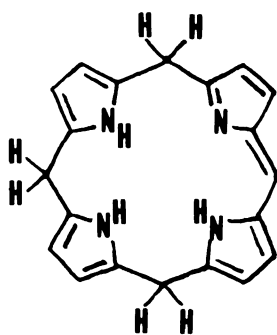
b



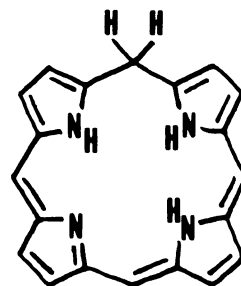
c



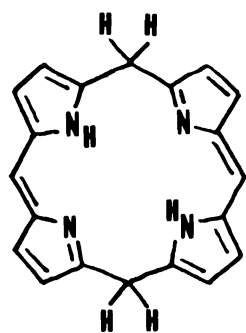
d



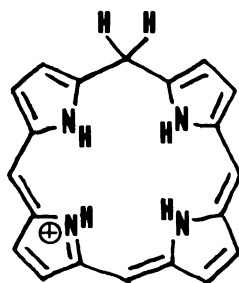
e



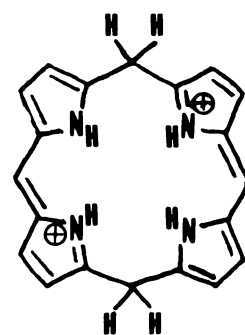
f



g



h



i

respect to deviations from planarity. Intramolecular crystal interactions and bulky substituents can greatly influence the geometry of the molecule. Falk⁷ estimates the porphyrin skeleton to be 8.5 Å in diameter and 4.7 Å thick based on the crystal structure obtained for the Ni(II) aetioporphyrin I complex.⁸

Reduction of the porphyrin nucleus in which some of the pyrrole carbon atoms are hydrogenated yields dihydroporphyrins or tetrahydroporphyrins (Fig. 2c). Chlorin (Fig. 2b) is a dihydroporphyrin from which chlorophylls a and b are derived while bacteriochlorophyll is related to the tetrahydroporphyrin structure.

Hydrogenation of some or all of the pyrroline nitrogen atoms and bridge carbon atoms yields porphyrinogens and related compounds as the reduction products. The porphyrinogens are hexahydroporphyrins having the four methene bridge carbon atoms and the two pyrroline nitrogen atoms hydrogenated (Fig. 2d). The conjugation of the porphyrin ring is absent in porphyrinogens, and they therefore lack the planarity and color of the porphyrin molecule. The porphyrinogens may be chemically or photolytically oxidized to porphyrins, with the oxidation pathway involving tetra- and dihydroporphyrin intermediates.

The tetrahydroporphyrin structure known as a porphomethene (Fig. 2e) has three methene bridge carbons and one pyrroline nitrogen hydrogenated. There is some evidence⁹⁻¹² to suggest that tetrahydroporphyrins are

intermediates in the biological oxidation of porphyrinogens to porphyrins.

The dihydroporphyrins phlorin(Fig. 2f) and porphodimethene(Fig. 2g) are isomers. In the porphodimethene only two methene bridge carbons are hydrogenated while the phlorin structure requires that one pyrroline nitrogen be hydrogenated in addition to the methene bridge carbon. The protonation of a monocationic phlorin salt (Fig. 2h) to form a dicationic porphodimethene(Fig. 2i) is known to occur under strongly acidic conditions.¹³ Both the phlorin and the porphodimethene, including their cations, can be oxidized to porphyrins by chemical and photolytic methods.

Ionization. Porphyrins are amphoteric in nature with ionization occurring at either the two pyrroline nitrogen atoms(-N=) or at the two pyrrole-type nitrogens(-NH-). Both the pyrroline and pyrrole-type nitrogens are capable of accepting a proton and therefore acting as basic centers. The pyrrole-type nitrogens are also capable of acting as acidic centers through the loss of their protons. Thus, there are six charged species possible: PH^- , P^{2-} , PH_3^+ , PH_4^{2+} , PH_5^{3+} , and PH_6^{4+} . Only three of these ionic porphyrins have been observed spectroscopically, namely, P^{2-} , PH_3^+ , and PH_4^{2+} ; and only the dianion and dication have been chemically isolated as salts.

Porphyrins are extremely weak acids even in concentrated sodium hydroxide solutions, the dianion being formed only in

the more strongly basic alkoxide solutions. Porphyrins are, however, readily soluble in dilute mineral acids in which the formation of the dication is usually observed.

Metalloporphyrins. The two protons attached to the pyrrole-type nitrogens in porphyrins are readily displaced by metal ions to form metalloporphyrins. It is in this form that the macrocyclic porphyrins perform their most important biological functions: as Mg(II) complexes in the chlorophylls, as Co(II) complexes in Vitamin B₁₂, and as Fe(II) or Fe(III) complexes in the hemoproteins. Once coordinated, the metal ion is incorporated into the highly resonant aromatic system of the porphyrin ring.

A number of monovalent cations(e.g., Na(I), K(I), and Li(I)) form metal complexes with porphyrins in which one of the two metal ions required to balance the charge of the porphyrin ring is believed to lie above and the other below the plane of the nucleus.

Numerous divalent metal ion complexes of porphyrins have been prepared in which the metal ion is four-coordinate and the resulting complex is square planar in geometry. However, some metalloporphyrins containing divalent ions, such as Mg(II), Cd(II), and Zn(II), readily add an axial ligand to their square planar structure to form five-coordinate square pyramidal complexes. The addition of two axial ligands to form six-coordinate complexes with distorted octahedral geometry also occurs with divalent metal chelates(e.g., Fe(II), Co(II), and Mn(II)) of

porphyrins. The latter metal ions are also capable of undergoing oxidation to the trivalent state in which the metalloporphyrin complexes carry a unit positive charge and have an anionic counter-ligand associated with them, often in the axial position.

The thermodynamic stabilities of the metalloporphyrins as deduced from spectroscopic data as well as from replacement and dissociation reactions follow the order:¹⁴ Pt(II) > Pd(II) > Ni(II) > Co(II) > Ag(II) > Cu(II) > Fe(II) > Zn(II) > Mg(II) > Cd(II) > Sn(II) > Li₂ > Na₂ > Ba(II) > K₂ > [Ag(I)]₂. The order¹⁵ of the rates of incorporation of various metal ions into porphyrins in aqueous solutions does not correspond to the thermodynamic stability order, the order of reactivity being Cu(II) > Zn(II) > Mn(II) > Co(II) > Fe(II) > Ni(II) > Cd(II).

Spectra. The electronic absorption spectra of the porphyrins, metalloporphyrins, and their derivatives are their most useful and most characteristic property. The neutral tetrapyrrole macrocycles are characterized by four absorption bands in the visible region (450 nm to 700 nm), numbered sequentially I to IV from the red end of the spectrum, and by a single intense absorption in the near ultraviolet (~400 nm) known as the Soret band after J. L. Soret who first discovered this band in hemoglobin in 1883. These electronic absorptions have been assigned to $\pi-\pi^*$ transitions between molecular orbitals delocalized over the porphyrin framework.

The Soret band is observed for all tetrapyrroles in which the nucleus is fully conjugated. It is the most intense absorption band in the porphyrin compounds, having molar extinction coefficients of the order of 2 to 5×10^5 , which are 10 to 20 times as intense as the strongest visible band. The Soret absorption can be easily measured in absorption cells of 1-cm path length at concentrations of the order of 10^{-5} and 10^{-6} M. The positions of the Soret and visible absorptions are influenced by changes in the π -electron density at the periphery of the porphyrin nucleus. Factors which increase the π -electron density cause bathochromic shifts in the absorption bands.

Chlorin and related dihydroporphyrins in which one pyrrole double bond is reduced are characterized by an intense absorption in the red region (band I) and Soret absorptions less intense than those observed for the fully oxidized porphyrins. Band I and the Soret band absorb at higher energies in the chlorin dications.

Unlike the porphyrins and chlorins, the Soret band is absent in the porphyrinogens and related hydroporphyrins since the conjugation of the porphyrin ring is destroyed at the methene bridge carbons. The porphyrinogens also lack absorption bands in the visible region, but an absorption near 200 nm does occur in the ultraviolet region. The porphomethene and porphodimethene are characterized by an intense absorption near 500 nm, while phlorin compounds have two main absorptions in the visible near 440 nm and 735 nm.

In the porphyrin dications, dianions, and chelates with divalent metal ions, the porphyrin molecule more closely approaches square symmetry, and the four visible absorption bands are reduced to two main visible bands. The Soret bands of the dication and dianion shift to longer wavelength with respect to that observed for the neutral porphyrin. A Soret and three visible absorptions are observed for porphyrin monocations, with the Soret band occurring at a shorter wavelength than that found in the neutral porphyrin.

The square planar metalloporphyrins with divalent ions are characterized by a Soret absorption in addition to the two visible absorptions, usually called the α and β bands, with the α band assigned to the absorption of longest wavelength. In general, the coordination of either one or two extra ligands to the square planar metalloporphyrins results in a bathochromic shift of the absorption bands.

Adsorption on clay minerals. Because crude oils and ancient sediments generally contain porphyrins believed to be derived from chlorophyll, the interaction of porphyrins with clay minerals has received recent attention. Hodgson and Casagrande^{16,17} recently succeeded in generating a homologous series of porphyrins from a single porphyrin under simulated geochemical conditions known to be important in petroleum diagenesis. They also observed that in the simulation experiments involving montmorillonite the

porphyrins were strongly adsorbed by the clay and were not released even with ultrasonic treatment in the presence of 6 M HCl and ether. Metallated porphyrins were also formed when clays were present in the reaction mixtures. Hodgson¹⁸ has also shown that porphyrins are capable of extracting Cu(II) ions from the exchange sites of montmorillonite.

Studies¹⁹ on the adsorption of commercial K-Cu chlorophyllin by montmorillonite saturated with various metal ions show that the porphyrin monoanion is adsorbed only onto the external surfaces. Visible absorption spectra of the porphyrin adsorbed on the clay suggest that the cationic composition of the clay affects the state of aggregation and relative orientation of the clay particles which in turn affect the electronic arrangement of the porphyrin nucleus. Attempts^{20,21} to intercalate proteins from blood serum into the crystal lattice of montmorillonite resulted in the external surface adsorption of albumen, hemoglobin, and hemin; however, experiments²² with pure hemin show that in addition to external adsorption the hemin cation $C_{34}H_{32}N_4O_4Fe^+$ is intercalated into the interlamellar region. While the hemin cation could not be removed with boiling dioxane, the hemin cation was liberated with pyridine, which can be intercalated as a cation and swelling solvent.



2.3 meso-Tetraphenylporphyrin

Synthesis. meso-Tetraphenylporphyrin(TPPH_2)(Fig. 3a) is a synthetic porphyrin often employed as a model for the naturally occurring porphyrins. TPPH_2 readily adds two additional protons in acidic solutions to form the porphyrin dication(TPPH_4^{++})(Fig. 3b) and can be transformed into a metalloporphyrin(MTPP)(Fig. 3c) by replacement of the two inner protons by a monovalent, divalent, or trivalent metal ion. TPPH_2 of relatively high purity can be conveniently synthesized from pyrrole and benzaldehyde in highly acidic media such as propionic acid under reflux conditions.²³ The resulting purple crystals are contaminated with approximately 3 per cent tetraphenylchlorin by weight.

Mechanisms of formation. Initial mechanistic investigations of the Rothmund reaction²⁴ for meso-tetra(o-substituted phenyl)porphyrins²⁵ provided the proposed reaction scheme shown in Figure 4 for the formation of meso-tetraarylporphyrins. The initial condensation step between a molecule of pyrrole and benzaldehyde produces a carbinol(I) which undergoes oxidation to an aroylpyrrole(II). Condensation of the aroylpyrrole with another molecule of pyrrole yields another carbinol(III), which undergoes dehydration to a dipyrromethane(IV). Condensation with a further molecule of aldehyde produces the carbinol(V) which oxidizes to the aroyldipyrromethane(VI). Two molecules of this aroyldipyrromethane condense to form an α,γ -dihydroxyporphyrinogen(VII). The loss of two water molecules yields

Figure 3. Molecular structures of (a) meso-tetraphenylporphyrin, (b) meso-tetraphenylporphyrin dication, and (c) metal chelate of meso-tetraphenylporphyrin.

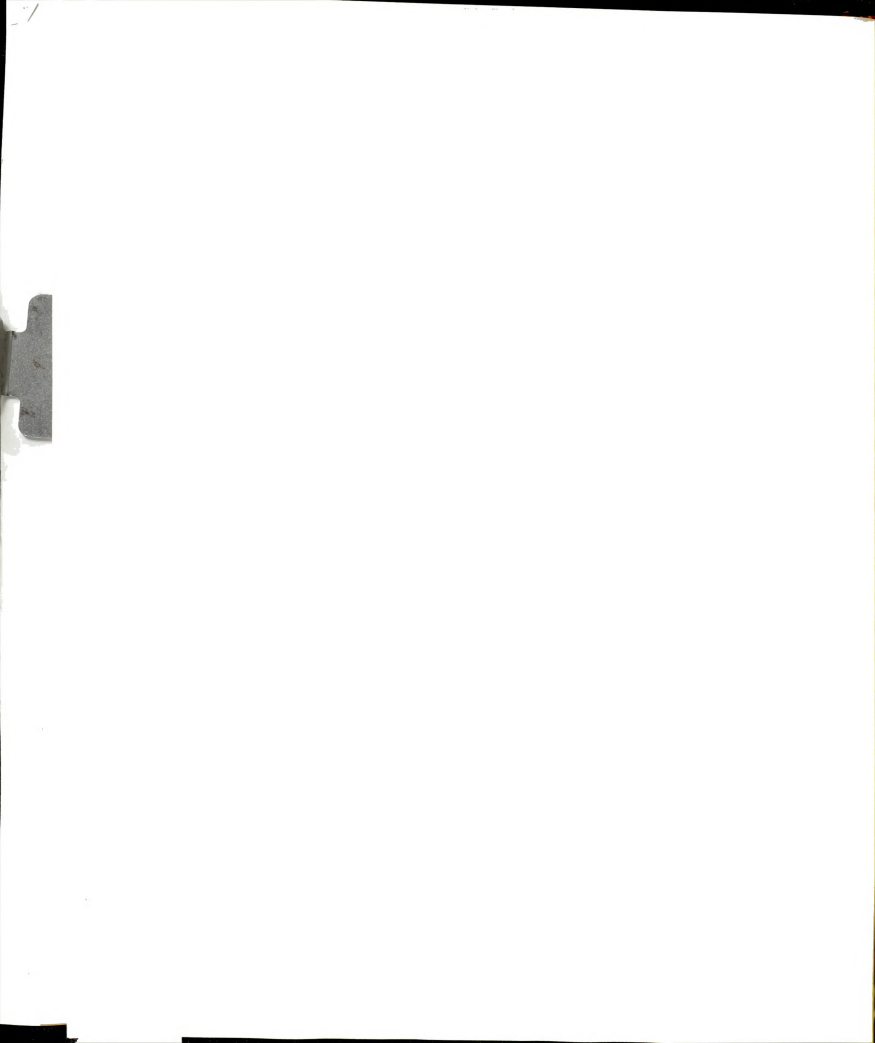
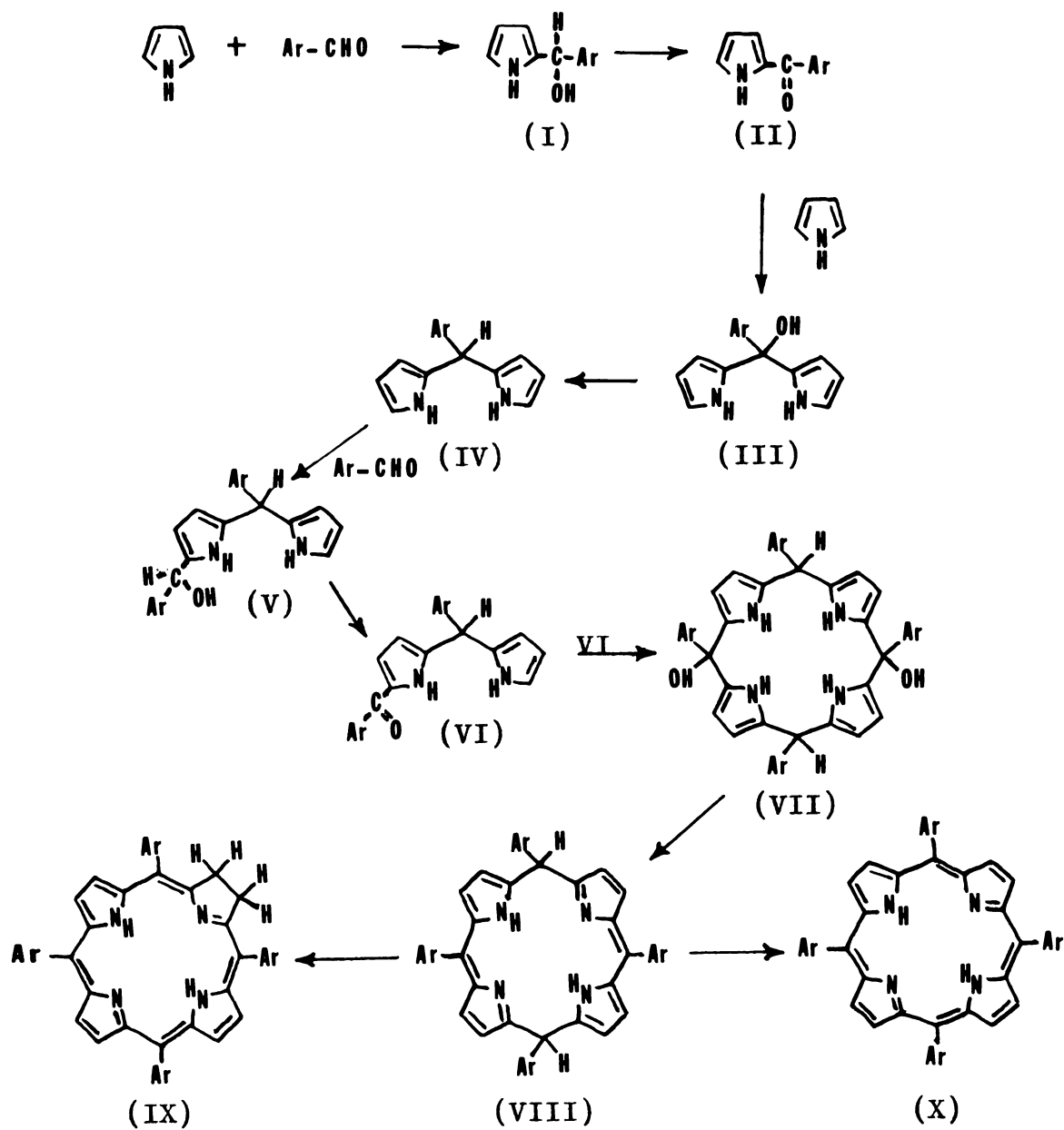


Figure 4. Mechanism proposed by Badger et al²⁵ for the Rothemund reaction.



the porphodimethene intermediate(VIII) which can either rearrange to a chlorin(IX) or undergo oxidation to the porphyrin(X).

The initial condensation step in the mechanism postulated by Adler et al^{1,2} for the synthesis of TPPH₂ also involves the formation of pyrrole-2-carbinol(I). The next reaction step, which is acid-catalyzed, becomes the condensation of two pyrrole-2-carbinols to form the dipyrromethane carbinol(V), which may undergo oxidation to a dipyrromethene carbinol. These carbinols then condense with molecules of carbinol(I) to form chainlike polypyrrole derivatives or polypyrrole carbinol derivatives. The tetrapyrrole carbinols cyclize to form saturated ring structures which undergo oxidation to phlorins, which either rearrange to chlorins or oxidize to porphyrins. A similar mechanism has been suggested for the reaction between substituted benzaldehydes and pyrrole.³

More recently Dolphin⁴ undertook a detailed mechanistic study of the formation of octamethyltetraphenylporphyrin (OMTPP) from 3,4-dimethylpyrrole and benzaldehyde in acetic acid. While the initial condensation steps are fast, the subsequent oxidations to "planar intermediates" are slow and allow the isolation and study of the intermediates. The principal intermediate isolated from the reaction was the porphyrinogen(XI)(Fig. 5), a colorless solid which absorbs near 200 nm. During the acid-catalyzed oxidation of porphyrinogen to porphyrin, the zinc(II) chelate of the porphodimethene(VIII) was isolated as an orange-red powder.

Figure 5. Summary of Dolphin's⁴ proposed mechanism for meso-tetraarylporphyrin formation.

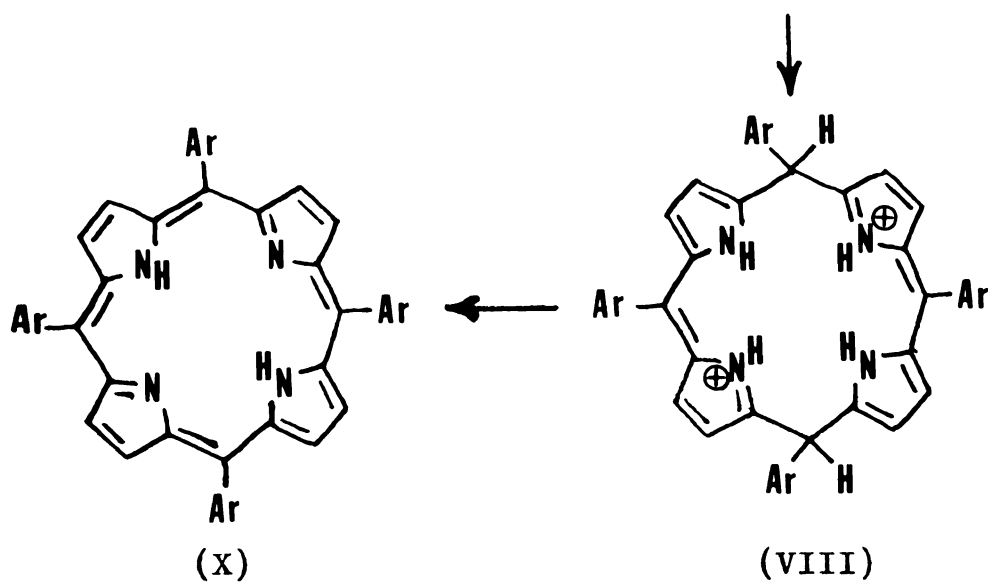
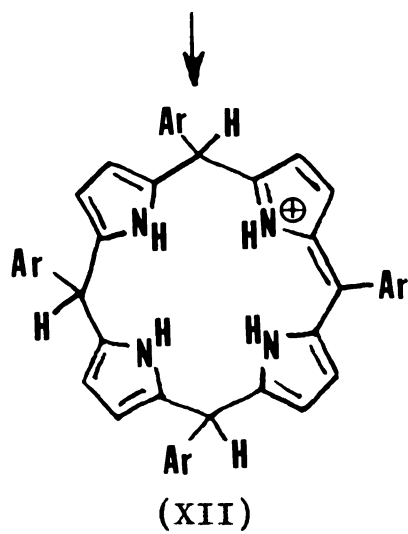
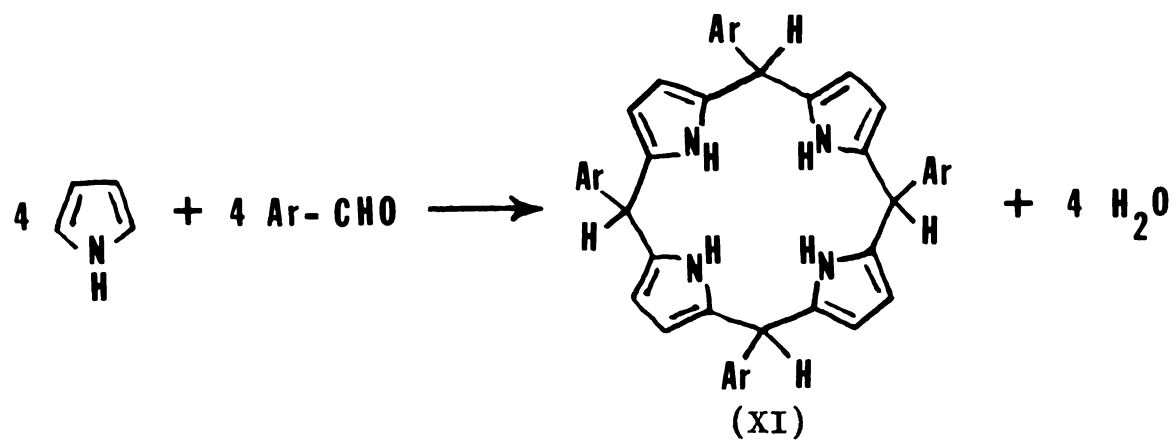


Figure 5 summarizes Dolphin's proposed mechanism for the formation of meso-substituted porphyrins from pyrroles and benzaldehydes. A porphomethene(XII) and a porphodimethene(VIII) are also believed to be intermediates in uroporphyrin formation.²⁶⁻²⁸

2.4 Chemical Evolution of Porphyrins

Chemical evolution refers to the chemical events that occurred approximately 4.5 to 3.5 billion years ago on the primitive, prebiotic Earth and which culminated in the formation of the first living cell. The concept of chemical evolution is based on the hypothesis that, due to the environmental conditions prevailing on the primitive Earth, biologically important monomers and polymers were synthesized from simple molecules which interacted with available sources of energy and/or came in contact with catalytic surfaces. The aggregation of these biomonomers and biopolymers to form the first living organism marks the start of biological evolution. It is believed that chemical and biological evolution continued simultaneously until the advent of oxygen in the Earth's atmosphere. As the Earth's atmosphere became more oxidizing in nature, chemical evolution presumably ceased and was completely replaced by biological evolution.

Most authors who theorize on the origin of life believe that at some stage of chemical evolution porphyrins were synthesized from precursors available during this period on the primitive Earth.²⁹⁻³⁶ This abiological

synthesis of porphyrins was crucial to the evolution of living systems at two stages: the evolution of porphyrin-dependent photosynthesis and the evolution of porphyrin-dependent respiration. It is also of interest that porphyrins may have been critical to the further progress of chemical evolution while the primitive Earth was undergoing the transition from a reducing atmosphere to an oxidizing one. Lemmon³⁷ has pointed out that the gradual accumulation of oxygen would have led to the formation of hydrogen peroxide which would have caused widespread oxidation and therefore destruction of organic compounds. However, Calvin³⁰ has shown that the incorporation of ferric ion into heme porphyrin increases the catalytic ability of iron to decompose hydrogen peroxide a thousand-fold.

Despite the prebiological and biological importance of porphyrins, very little experimental data has been collected on the mechanism of porphyrin abiosynthesis under simulated primitive Earth conditions. Early work by Rothmund³⁸ on porphyrin synthesis showed that when a mixture of 5 M pyrrole in methanol, 2 per cent formaldehyde in methanol, and pyridine solvent was heated for 30 hours at 90-95⁰ C in sealed tubes, a 0.1 per cent yield of free base porphine was obtained. Later Calvin et al³⁹ added zinc salts to the above mixture of reagents and achieved a more effective condensation. However, neither of these experiments simulated prebiotic chemistry.

In experiments designed to simulate conditions on the

prebiotic Earth, Szutka et al⁴⁰ exposed a mixture of pyrrole, benzaldehyde, pyridine, and zinc acetate to γ -radiation and obtained meso-tetraphenylporphyrin as a major product. More recently Szutka used a mixture of pyrrole, benzaldehyde, and water exposed to ultraviolet radiation⁴¹ and aqueous solutions of α -aminolevulinic acid exposed to uv radiation⁴² to produce porphyrin-like compounds. Krasnovsky and Umrikhina⁴³ studied the effects of atmospheric oxygen, water, catalysts, and electron donors and acceptors on the production of porphyrin-like material from the condensation of pyrrole and formaldehyde in methanol. Atmospheric oxygen, water, and catalysts increased the rate of porphyrin synthesis with catalysts increasing the yield of the end product. Electron donors and acceptors accelerated, inhibited, or had no effect on the rate. Hodgson and Baker⁴⁴ have reported the formation of metal porphyrin complexes from aqueous pyrrole and formaldehyde in the presence of metal cations and, under simulated geochemical conditions, in the presence of aqueous mineral suspensions; however, the absorption maxima and minima of the reaction products were shifted 100 Å toward shorter wavelengths. A satisfactory explanation for this shift has not yet been found. Porphyrins have also been generated from the action of electric discharges on a gaseous mixture of methane, ammonia, and water.⁴⁵

Although the above experiments show that the synthesis of porphyrins and/or porphyrin-like compounds occurs readily

under simulated prebiotic conditions, the yields of product materials obtained have not been significant enough to establish any one reaction as providing the mechanism for the prebiological formation of porphyrins. In addition, none of these experiments provides for the storage and concentration of biologically relevant molecules necessary for the formation of more complex molecules and, ultimately, the first living organism.

2.5 Prebiotic Syntheses on Clay Minerals

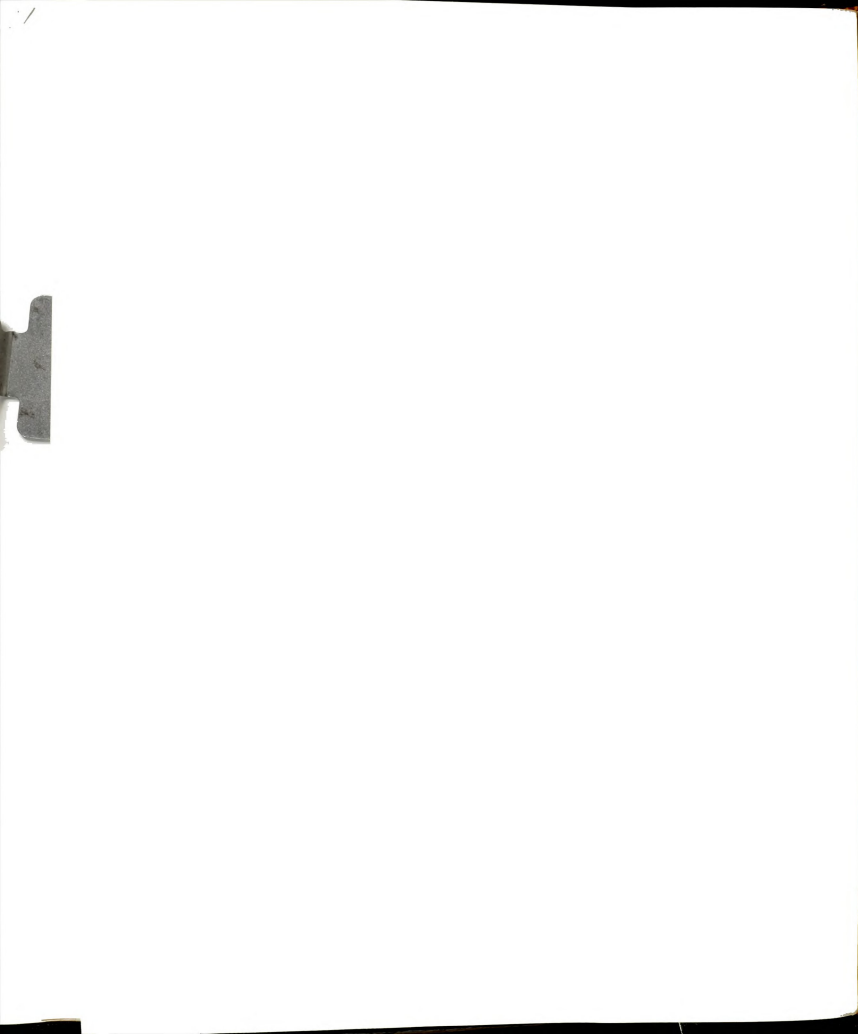
J. D. Bernal⁴⁶⁻⁴⁸ was the first to suggest that very fine clay deposits in marine and fresh water could have concentrated simple organic molecules by adsorption, catalyzed their condensation to more complex molecules, and stored the condensation products during chemical evolution. Recent research has shown that clay minerals, such as montmorillonite and kaolinite, can act as heterogeneous catalysts for the formation of polypeptides,⁴⁹⁻⁵⁴ polynucleotides,^{52,55} and monosaccharides.⁵⁶

A significant amount of research has been accumulated on the prebiotic synthesis of peptides on clay surfaces. Pavlovskaya et al⁵⁷ observed the formation of amino acids during the exposure of solutions of formaldehyde and ammonium nitrate to ultraviolet radiation in the presence of bentonite, kaolinite, and limonite. The formation of amino acids from the simple gases CO_2 and NH_3 in the presence of silicate lattices has also been observed.⁵²

Recently Degens and Matheja^{49,52,53} studied the adsorption, polymerization, and catalysis of amino acids on montmorillonite and kaolinite. They observed that while montmorillonite was a more efficient adsorbent for amino acids than kaolinite, kaolinite was a better catalyst. Both minerals were found to promote polymerization of amino acids under aqueous and dry conditions with peptides and polyphenolic compounds as the principal condensation products.

The amino acids are believed to be tightly bound to the silicate surface by strong electrostatic interactions. The amino groups are either hydrogen-bonded to the silica oxygens or occur as positive ions electrostatically bound to the silica oxygens. The carboxyl groups are generally believed to be bound to the positively charged Al-oxyhydroxy sites via ionic bridges. This electrostatic interaction results in the activation of the carboxyl group, which is necessary for polymerization to occur. It is postulated that a continuous flow of organic molecules across the catalytically effective mineral surface is also necessary for efficient polymerization.

Paecht-Horowitz et al^{50,51,54} showed that amino acid-phosphate anhydrides (amino acid adenylates) concentrated on clay surfaces polymerize to form polypeptides of different, but discrete sizes rather than a continuous distribution of molecular weights. Among the clays, illite and montmorillonite showed a marked catalytic activity while apatite, kaolinite,



and permutite displayed no catalytic activity. The dominant reaction in the heterogeneous polycondensation of amino acid adenylates on clay surfaces is supposed to involve the interaction between two active adenylates resulting in a still higher peptide.

Harvey et al⁵⁵ were able to synthesize the nucleic acid bases uracil and cytosine from CO_2 and NH_3 in the presence of kaolinite and water. The carbon dioxide is believed to bind to the clay surface to form an activated aluminum carbonate complex. The adsorption of nucleic acid bases on clay minerals and their subsequent polymerization to polynucleotides is determined by the amounts of phosphates present during the reaction.⁵²

There has been only one report to date on the formation of sugars in the presence of clay minerals. Gabel and Ponnampurama⁵⁶ refluxed an aqueous solution of formaldehyde in the presence of alumina, kaolinite, and illite and obtained a mixture of monosaccharides as condensation products. They proposed that the basic sites on the crystal lattices of the alumina and aluminosilicates were capable of accepting protons from the formaldehyde and various intermediates adsorbed on the mineral surfaces, thereby generating the necessary reactant molecules.

The foregoing experiments indicate that clay minerals provide a catalytically active and efficient surface for the heterogeneous catalysis of a variety of condensation reactions relevant to the prebiotic synthesis of biologically important molecules.

CHAPTER 3

EXPERIMENTAL SECTION

3.1 Preparation of Homoionic Montmorillonites

Mⁿ⁺ montmorillonites. The montmorillonite used throughout this research was a standard natural sample of Wyoming bentonite (Vol clay) obtained from the American Colloid Company, Skokie, Illinois. In order to remove the more dense components, a slurry of the clay in ethanol was prepared, and the clay particles were allowed to sediment. The top colloidal fraction was removed, an excess of the appropriate metal salt was added, and the suspension was stirred for 24 hours to saturate the exchange sites with the desired cation. The clay was removed by filtration, washed with solvent until the AgNO_3 test proved negative for Cl^- , and dried overnight in air. The chloride salts of Na(I), Mg(II), Co(II), Cu(II), Zn(II), and Fe(III) were used to prepare the corresponding metal-saturated exchange forms of montmorillonite.

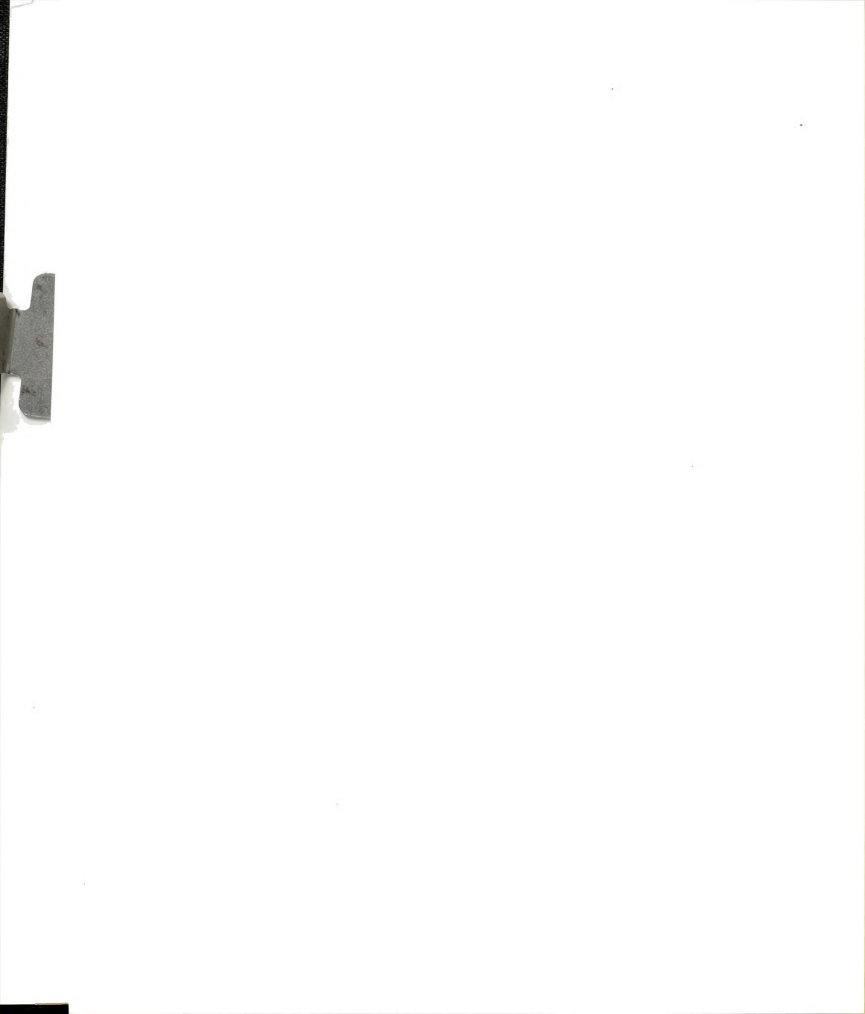
Vanadium oxysulfate obtained from Alfa Inorganics was used to prepare VO(II) montmorillonite. It should be remarked that if freshly prepared VO(II) montmorillonite is allowed to dry in air, the light blue color characteristic

of aqueous vanadyl ion, $\text{VO}(\text{H}_2\text{O})_5^{2+}$, is lost and a yellow-green color develops. $\text{VO}(\text{II})$ montmorillonite was therefore stored under methanol and filtered as needed.

TPA⁺ and H⁺ montmorillonites. Tetra(n-propyl)ammonium (TPA⁺) montmorillonite was prepared according to the above procedure with tetra(n-propyl)ammonium bromide obtained from Eastman Kodak Company.

Hydrogen(H⁺) montmorillonite was prepared by using Dowex 50W-X8, 20-50 mesh ion exchange resin from J. T. Baker Chemical Company. The hydrogen ion exchange form of the resin was prepared by stirring 5.0 g of the resin for one hour in 250 ml of a 1.0 M HCl solution, washing with distilled water to remove excess Cl⁻, and drying overnight in air. The resin was then added to a suspension of 2.0 g montmorillonite in 300 ml ethanol. After an hour of being stirred, the mixture was passed through a screen filter to remove the resin, which was washed several times with ethanol to remove the clay particles which had adhered to the resin. The clay-ethanol suspension was then filtered, and the clay was used immediately after being dried. It should be remarked that it is not possible to prepare a clay in which all the exchange sites are occupied by H⁺ since Al³⁺ moves from the lattice to the exchange sites before saturation with H⁺ becomes complete. It is necessary to use the clay immediately after it is dried since the movement of Al³⁺ from its lattice position is facilitated during drying.

TPPH₄⁺⁺ montmorillonite. The TPPH₄⁺⁺ exchange form of



montmorillonite was prepared by adding an excess of TPPH_2 in glacial acetic acid to a slurry of montmorillonite in ethanol. The mixture was stirred 24 hours, filtered, and washed with ethanol to remove excess acetate ion. The clay was bright green after being dried overnight in air. Its solid state absorption spectra in the visible and infrared regions are shown in Figures 6 and 7, respectively.

3.2 Synthesis of TPPH_2

A modified synthesis of that described by Adler²³ was used to prepare the TPPH_2 used in this research. Freshly distilled pyrrole(3.6 ml, 52 mmoles) and freshly distilled benzaldehyde(5.4 ml, 52 mmoles) were added to 250 ml refluxing propionic acid. After one hour, the reaction solution was transferred to a beaker and allowed to cool overnight. Filtration yielded purple crystals which were washed several times with methanol to remove impurities and then were dried at 110°C for two hours to remove adsorbed propionic acid. The final product is contaminated with 3 per cent tetraphenylchlorin by weight.

3.3 Adsorption of TPPH_2 onto Montmorillonite

Metal ion-exchanged montmorillonite(500 mg) was added to 10 mg(0.016 mmoles) of TPPH_2 dissolved in 500 ml reagent grade acetone at room temperature. Under these conditions, the molar ratio of M^{2+} to TPPH_2 was 14:1. The solution was stirred for 24 hours, and the adsorption of



Figure 6. Electronic absorption spectra of TPPH_4^{++} in glacial acetic acid(———), TPPH_4^{++} montmorillonite(-----), and Fe(III) montmorillonite after adsorption of TPPH_2 (-.-.-).

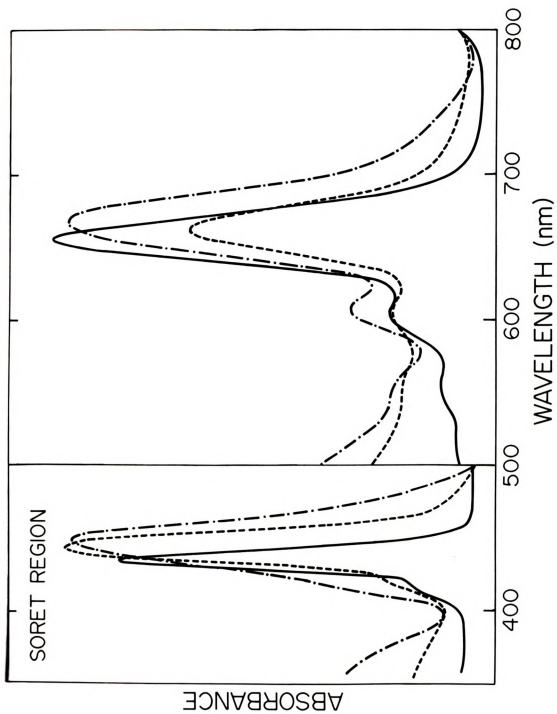
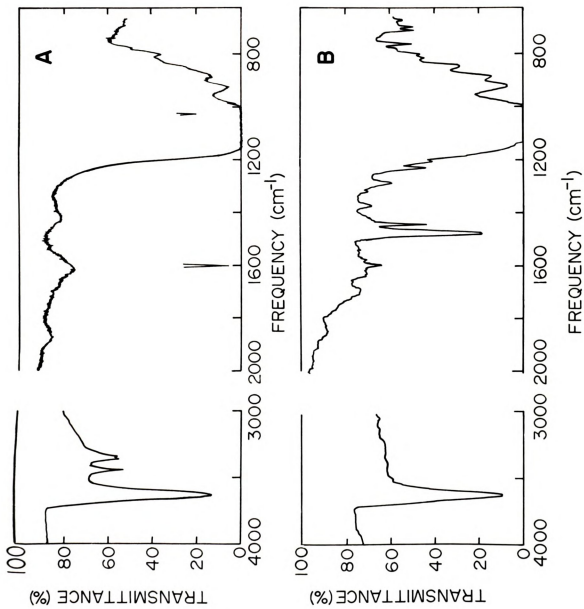




Figure 7. Infrared absorption spectra of (A) Cu(II) montmorillonite dried 1 week at 110° C and (B) Cu(II) montmorillonite after exchange with TPPH₄⁺ and drying 4 weeks at 130° C to remove adsorbed acetone.



TPPH₂ was followed spectroscopically by observing any changes in the intensities of the absorption peaks for TPPH₂ in the visible region and by noting the growth of any new visible absorption bands into the spectrum. The reaction mixtures were then filtered, the clays were washed several times with acetone and were then allowed to dry overnight in air.

3.4 Reaction between Pyrrole and Benzaldehyde in the Presence of Montmorillonite

Aerobic synthesis. Freshly distilled pyrrole(0.31 ml, 4.5 mmoles) and freshly distilled benzaldehyde(0.46 ml, 4.5 mmoles) were added to 5.0 g of the metal cation exchange form of montmorillonite suspended in 300 ml distilled water. The amounts of pyrrole and benzaldehyde were reduced to 0.19 ml(2.7 mmoles) and 0.28 ml(2.7 mmoles), respectively, for the reaction with 5.0 g Fe(III) montmorillonite. Under these conditions, the molar ratio of Mⁿ⁺ to pyrrole was 1:2.

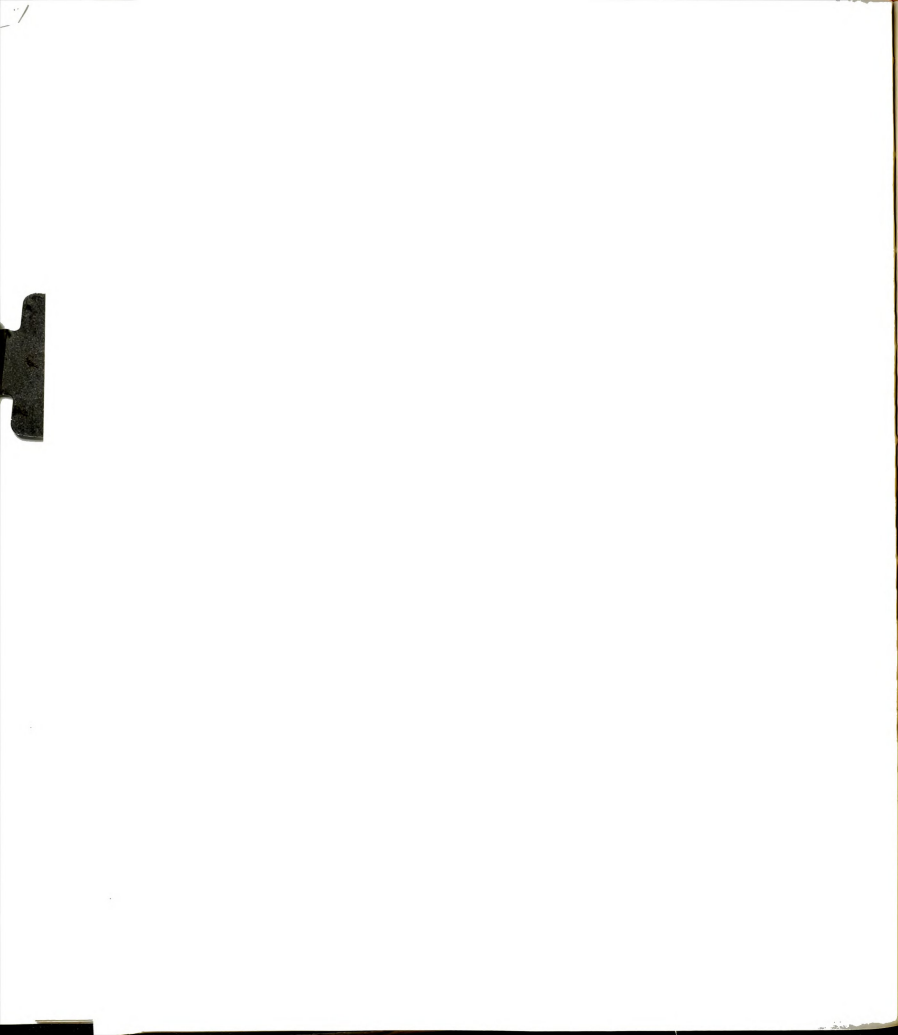
The reaction was also carried out at a 1:4 molar ratio by adding 0.12 ml(1.7 mmoles) pyrrole and 0.18 ml(1.7 mmoles) benzaldehyde to 1.0 g metal cation-exchanged montmorillonite suspended in 60 ml distilled water. One gram Fe(III) montmorillonite required 0.08 ml(1.2 mmoles) pyrrole and 0.12 ml(1.2 mmoles) benzaldehyde.

Each reaction was allowed to proceed while it was stirred continuously for 24 hours, during which time the colloidal

suspensions gradually changed from colorless to pale pink to deep purple in color. The elapsed time before the initial appearance of the pale pink color was dependent upon the metal ion occupying the exchange sites of the montmorillonite. The reaction between pyrrole and benzaldehyde progressed rapidly in the presence of Fe(III), VO(II), Cu(II), and H^+ , while the Zn(II), Co(II), and Mg(II) exchange forms of montmorillonite required a considerably longer period of time before a color change was observed. While the reaction which produces a purple-colored product occurred at the 1:2 molar ratio in the presence of Na(I) montmorillonite, only a gray-colored product believed to be a polymeric pyrrole compound similar to pyrrole black was obtained at the 1:1 molar ratio. No observable reaction between pyrrole and benzaldehyde occurred in the presence of TPA^+ montmorillonite at either molar ratio.

At the end of the reaction period, the clays and the adsorbed products were freeze-dried, and their solid state absorption spectra were recorded in the visible region.

Anaerobic synthesis. Pyrrole and benzaldehyde were distilled under argon and were stored under nitrogen in a glove box. Slurries of 5.0 g Cu(II) and 5.0 g Zn(II) montmorillonite in 300 ml distilled water were heated to reflux temperature for one hour under nitrogen and then were transferred to a glove box. Pyrrole(0.31 ml, 4.5 mmoles) and benzaldehyde(0.46 ml, 4.5 mmoles) were added to each slurry. Stirring the mixtures for 24 hours produced the



same gradual color changes as were observed during the aerobic syntheses. Exposure to the atmosphere after freeze-drying did not produce any changes in the color of the clays or their visible absorption spectra, which were similar to those obtained for the aerobic condensation reactions.

3.5 Reaction between Pyrrole and Benzaldehyde in Water

To establish the catalytic role of the montmorillonite surface during the condensation reaction, pyrrole and benzaldehyde were allowed to react in the absence of any clay surface. Pyrrole(0.06 ml, 0.87 mmoles) and benzaldehyde(0.09 ml, 0.87 mmoles) were added to 60 ml distilled water which had been acidified to a pH of approximately 5. The reaction was allowed to proceed while it was stirred continuously for 24 hours after which time the solution was transferred to a separatory funnel. The organic products were extracted with 200 ml chloroform. The organic layer was removed, dried over anhydrous sodium sulfate, and filtered. The filtrate was diluted to 250 ml in a volumetric flask, and the visible absorption spectrum was recorded. The Soret absorbance indicated a yield of less than one per cent porphyrin for the blank reaction.

3.6 Desorption of the Condensation Product

Method A. After the formation and adsorption of the reaction product onto the clay surface, attempts were made



to desorb it with a large organic ion capable of competing with it for the exchange sites on the clay. For this reason TPA^+ was selected as the exchange ion.

The general procedure for desorption was to add 72 mg (0.27 mmoles) $[\text{TPA}] \text{Br}$ to a suspension of 150 mg of reacted clay from the 1:4 molar reaction in 100 ml distilled water. The mixture was allowed to stir for 24 hours, and then 200 ml benzene were added to extract any desorbed product. After another hour of stirring, the mixture was transferred to a separatory funnel, the aqueous layer was removed, and the organic layer was dried over anhydrous sodium sulfate. Filtration yielded a darkly colored filtrate that was diluted to 500 ml in a volumetric flask. Further dilution was often required to obtain an absorbance value for the Soret band. The visible absorption spectrum was recorded, and a per cent yield of TPPH_2 was calculated based on the absorbance of the Soret band ($\epsilon = 449 \times 10^3$ for TPPH_2 and $\epsilon = 431 \times 10^3$ for TPPH_4^{++}) and one mole of TPPH_2 per mole of metal ion. This desorption method resulted in yields of only 2 per cent.

Method B. Approximately 100 mg of reacted clay from the 1:2 molar reaction was placed in a Soxhlet extractor with 300 ml pyridine. Pyridine can be intercalated as the neutral molecule or the cation into the interlamellar region of montmorillonite. Its ability to remove hemin cations from the intracrystal surfaces of montmorillonite has already been noted.²² The extraction was allowed to

proceed overnight. The intensely colored extract was diluted in a 500 ml volumetric flask and rediluted until an absorbance value for the Soret band ($\epsilon = 450 \times 10^3$ for TPPH_2) was obtained. Yields for the H^+ and Cu(II) exchange forms of montmorillonite were 4 to 5 per cent.

Method C. The Cu(II) exchange form of kaolinite was prepared as described for the montmorillonites. Conductometric titration yielded an exchange capacity of 4 meq/100 g Georgia kaolinite, which was obtained from the Ward's Natural Science Establishment. The Cu(II) exchange form (20 mg) and naturally occurring kaolinite (20 mg) were suspended in 300 ml distilled water. Pyrrole (0.06 ml, 0.87 mmoles) and benzaldehyde (0.09 ml, 0.87 mmoles) were added to each suspension. After being stirred for 24 hours, the reaction mixtures were freeze-dried, and 2.0 g of the resulting clay products were suspended in 200 ml chloroform in which 214 mg (0.80 mmoles) $[\text{TPA}] \text{Br}$ had been dissolved. The mixtures were allowed to stir for 24 hours and were then filtered. The filtrates were diluted in volumetric flasks, and the visible absorption spectra were recorded. Yields of 4 to 6 per cent were obtained ($\epsilon = 453 \times 10^3$ for TPPH_2). These yields were lower than expected since, unlike montmorillonite, kaolinite has an extremely low cation exchange capacity with virtually all adsorption occurring on the external surfaces.

Method D. This method attempted to desorb the condensation product from the interlamellar region as it

was formed. Distilled pyrrole(0.06 ml, 0.87 mmoles) and distilled benzaldehyde(0.09 ml, 0.87 mmoles) were added with 2.4 g(9.0 mmoles) [TPA] Br to 60 ml distilled water. The mixture was allowed to stir for 5 min to bring all the reagents into solution, and 1.0 g of clay was added. Stirring was continued for 24 hours. The reaction mixture was freeze-dried, and the clay product was resuspended in 200 ml chloroform. After 24 hours of continuous stirring, the suspension was filtered. The filtrate was diluted to 500 ml in a volumetric flask and rediluted until a Soret absorbance could be recorded. Yields for the H^+ , Cu(II), and Fe(III) exchange forms of montmorillonite were 10 to 12 per cent porphyrin. Esr absorption spectra and elemental analyses for Cu(II) montmorillonite indicate that the TPA⁺ cation undergoes ninety per cent exchange with the Cu(II) ions in the interlamellar region during the desorption process. However, total desorption of the product does not occur as evidenced by the fact that the clay retains a light purple color after the desorption process is complete.

3.7 Porphyrin Intermediates

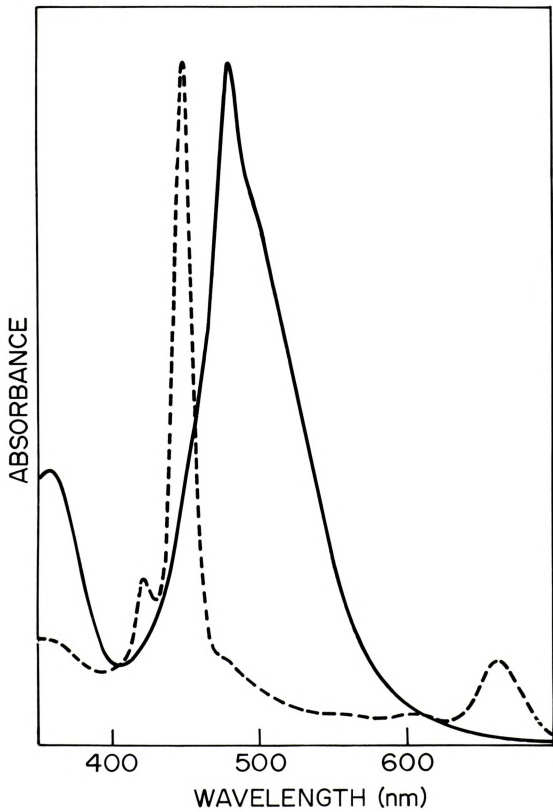
Synthesis. Distilled pyrrole(0.2 ml, 2.7 mmoles) and distilled benzaldehyde(0.3 ml, 2.7 mmoles) were dissolved in 250 ml chloroform. One drop of concentrated HCl was added as catalyst. The reaction solution was allowed to stir for 2 hours and was then purged with argon for an hour. The reaction solution was transferred to a glove box



containing a nitrogen atmosphere. The visible absorption spectrum of the solution exhibited an intense absorption at 477 nm (Fig. 8) which was assigned to the porphyrin intermediate. If an aliquot of the reaction solution was exposed to air overnight, the band at 477 nm disappeared and was replaced by two Soret absorptions at 421 nm and 447 nm for the free base porphyrin and dication, respectively. Attempts to isolate the intermediate either in crystalline or powder form were unsuccessful.

Adsorption on montmorillonite. The reaction solution was divided into two parts, and 1.0 g each of TPA^+ and Cu(II) montmorillonite was added to each part. Each mixture was allowed to stir overnight in the glove box, and filtration yielded purple-brown clays in both cases. The TPA^+ montmorillonite clay exhibited an intense absorption at 485 nm while the Cu(II) montmorillonite clay had its maximum absorption at 505 nm with shoulders at 475 nm and 447 nm (Fig. 9). The filtrate from the TPA^+ montmorillonite adsorption solution exhibited bands at 477 nm and 447 nm assigned to the intermediate and dication, respectively. The filtrate from the Cu(II) montmorillonite adsorption solution exhibited CuTPP absorptions at 535 nm and 415 nm and the intermediate absorption at 488 nm. Despite the presence of Cu(II) in the filtrate, the 001 spacing for the clay after adsorption was only $12.4 \overset{\circ}{\text{A}}$, which indicates that intercalation of the intermediate did not occur.

Figure 8. Electronic absorption spectra of an HCl-CHCl_3 solution of pyrrole and benzaldehyde after 2³ hours of reaction time(——) and after exposure to air overnight(-----).



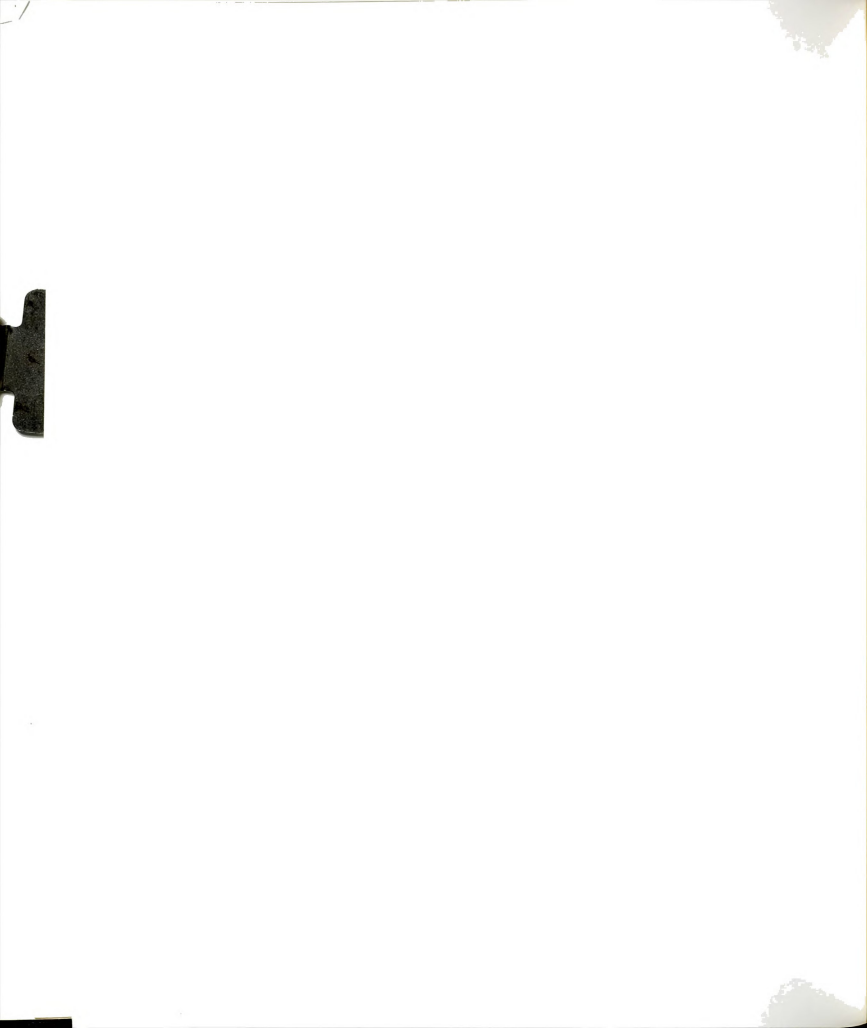
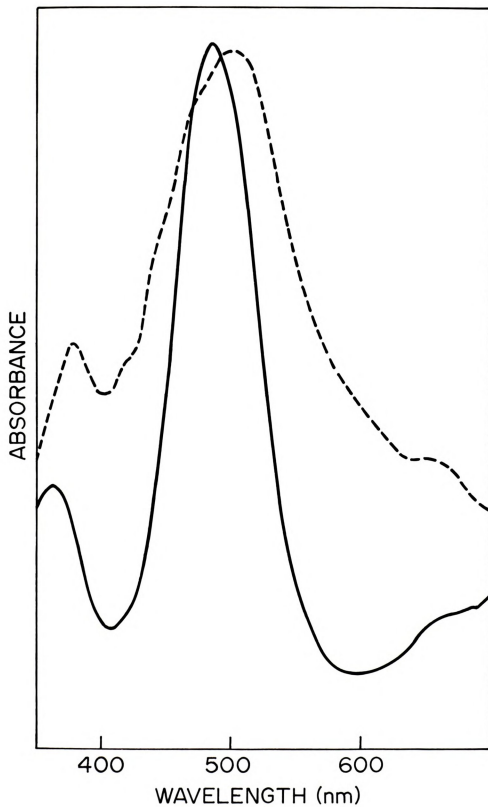


Figure 9. Electronic absorption spectra of TPA^+ montmorillonite after the adsorption of the porphyrin intermediate from HCl-CHCl_3 solution(——) and Cu(II) montmorillonite after adsorption of the intermediate from HCl-CHCl_3 solution(-----).



3.8 Spectroscopy

Visible absorption. All electronic absorption spectra were recorded by use of a Cary 17 recording spectrophotometer. Solid samples were recorded as Nujol mulls mounted between two quartz discs. Solution spectra were obtained with silica absorption cells having a path length of 1 cm.

Infrared absorption. Infrared spectra were recorded by use of a Perkin Elmer Model 237B grating infrared spectrophotometer. Solid samples were recorded as thin self-supporting films. A polystyrene film was employed as the standard sample for calibration of peak positions.

Electron spin resonance. Electron spin resonance spectra were recorded by use of a Varian E-4, X-band esr spectrophotometer. The powdered clay samples were placed in quartz esr tubes for measurement.

X-ray diffraction. The 001 basal spacings for the various montmorillonite clays were recorded by use of a Phillips X-ray diffractometer using Cu K(α) radiation and a Ni filter. The clay samples were deposited as slurries on microscope slides and allowed to dry overnight before measurements were obtained.

3.9 Chemical Analyses

Elemental analyses were performed on the clay samples by Galbraith Laboratories, Inc. and by the Michigan State University Soil Science Testing Laboratory.

CHAPTER 4

RESULTS AND DISCUSSION

4.1 Interaction of meso-Tetraphenylporphyrin with Montmorillonite

VO(II) and Fe(III) montmorillonite. The four free base porphyrin absorptions at 510 nm, 545 nm, 588 nm, and 645 nm rapidly decrease in intensity upon the addition of the vanadyl or Fe(III) exchange forms of montmorillonite to solutions of TPPH₂ in acetone. The absorptions virtually disappear from the spectrum within a few hours. No new absorption bands appear during the 24-hour reaction period.

Both clay exchange forms become bright green upon addition to the reaction solution and retain this color after filtration and air drying. The visible absorption spectrum of the Fe(III) exchange form is shown in Figure 6. The vanadyl exchange form exhibits a similar spectrum. Comparison of this absorption spectrum with those for TPPH₄⁺⁺ in glacial acetic acid and for the TPPH₄⁺⁺ exchange form of montmorillonite, both shown in Figure 6, indicates that the meso-tetraphenylporphyrin dication is formed upon adsorption of the free base porphyrin into the interlamellar region of vanadyl and Fe(III) montmorillonite.

Inspection of Table 1 reveals that bathochromic shifts of 10-15 nm occur in the Soret and band I absorptions for the dication in the adsorbed state. This suggests that the porphyrin molecule orients itself parallel to the silicate layers of the montmorillonite flake with the layers restricting the molecule to a more planar conformation in the interlamellar region (Fig. 10). Since the porphyrin molecule is a non-rigid aromatic system with low-energy barriers to a variety of angular distortions from planarity, the conformational change to a more planar structure is also easily effected, especially where packing effects, which often have a pronounced effect on porphyrin structures, are absent. The planar conformation of TPPH_4^{++} in the interlayer space is evident from X-ray diffraction data. A 001 reflection of $14.2 \overset{\circ}{\text{Å}}$ was obtained for a TPPH_4^{++} -saturated powder sample of montmorillonite. Because the basal spacing is about $9.6 \overset{\circ}{\text{Å}}$ when no interlamellar material is present, the separation between the silicate sheets is $4.6 \overset{\circ}{\text{Å}}$, which is the approximate thickness of the porphyrin nucleus.⁷ A similar interlayer spacing of $14.6 \overset{\circ}{\text{Å}}$ has been reported for pure hemin intercalated into the interlamellar region of montmorillonite as the monocation $\text{C}_{34}\text{H}_{32}\text{N}_4\text{O}_4\text{Fe}^+$.²² The infrared spectrum of TPPH_4^{++} exchanged onto montmorillonite (Fig. 7) lends further support to the planar conformation of TPPH_4^{++} in the interlamellar region. The bands at 1483 cm^{-1} , 1444 cm^{-1} , and 1239 cm^{-1} are similar to those previously reported for TPPH_4^{++} .⁵⁸ The bands at 767 cm^{-1} ,



Table 1. Ultraviolet and Visible Absorption Spectra for the Reaction of TPPH_2 with Montmorillonite

Compound(solvent)	Visible Bands(nm)	Soret Band(nm)
TPPH_2 (acetone)	510 545 588 645	415
TPPH_4^{++} (glacial acetic acid)	555(sh) 605(sh) 655	435
TPPH_4^{++} (montmorillonite)	555(sh) 605(sh) 665	448
TPPH_4^{++} (Fe(III) montmorillonite)	555(sh) 605(sh) 668	450
TPPH_4^{++} (VO(II) montmorillonite)	555(sh) 610(sh) 671	450
CuTPP(acetone)	500(sh) 538 570(sh)	412
CuTPP(Cu(II) montmorillonite)	545 575(sh)	416
ZnTPP(acetone)	515(sh) 555 593	421
CoTPP(acetone)	528	412
CoTPP(Co(II) montmorillonite)	538 570(sh)	429

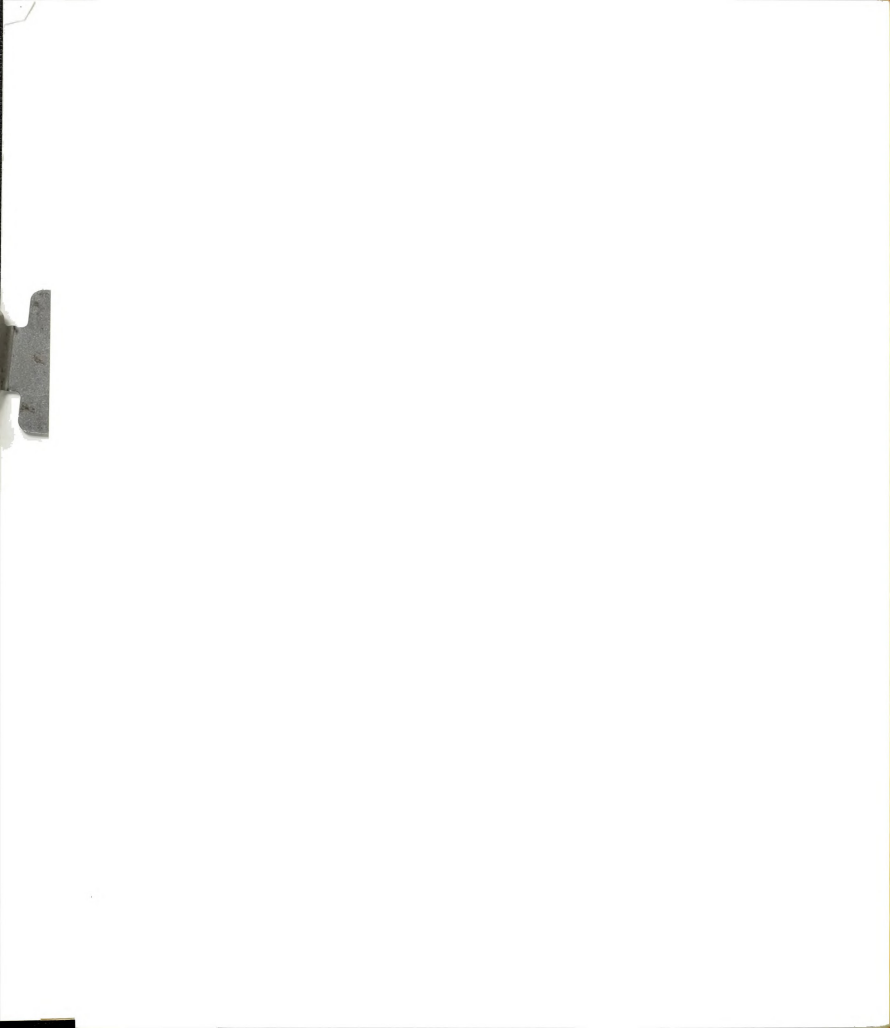
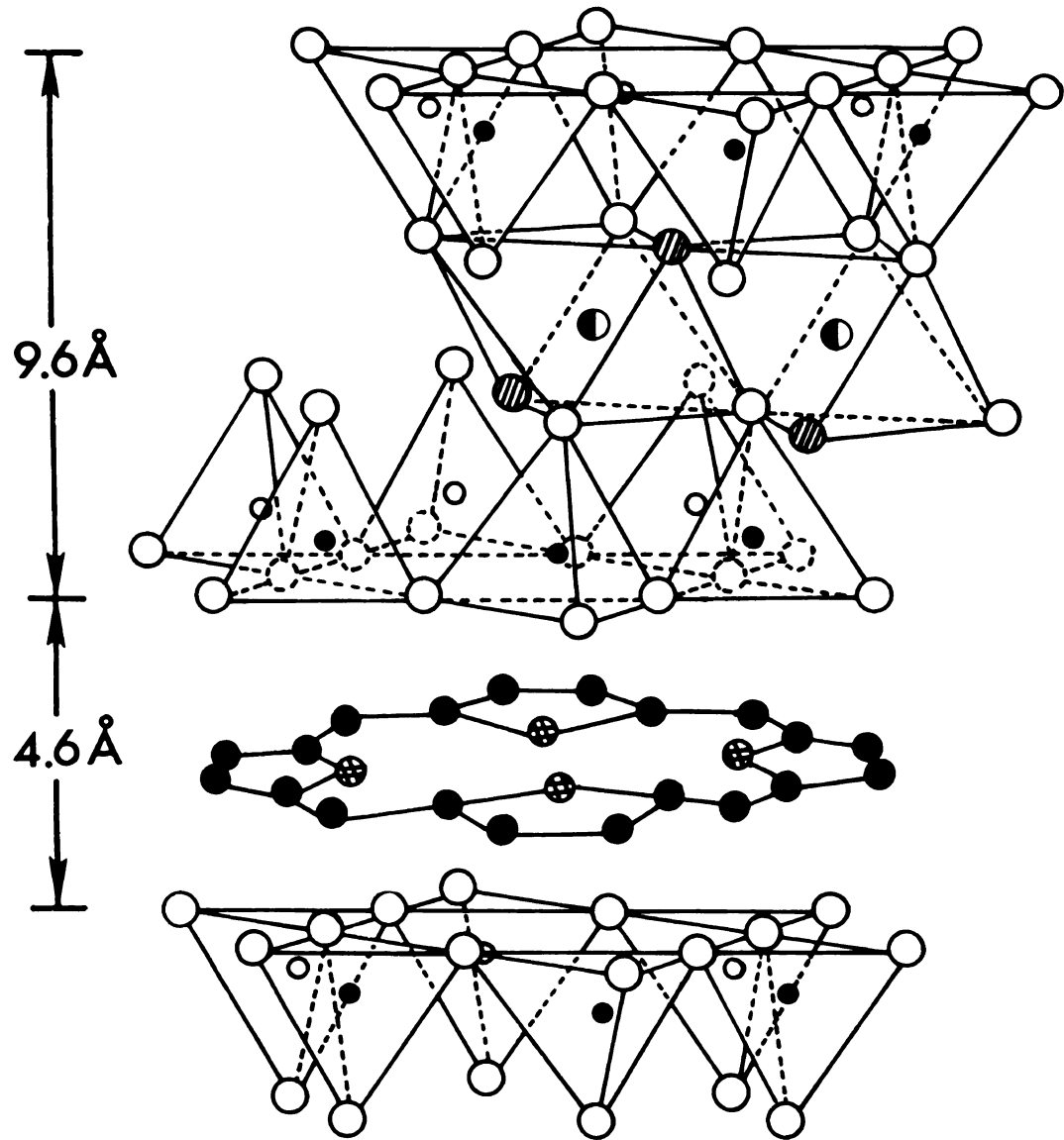




Figure 10. Schematic drawing showing the orientation of the porphyrin skeleton between montmorillonite layers.



- | Al³⁺, Mg²⁺, Fe³⁺
- / Hydroxyls
- Oxygens
- ⊗ Nitrogens
- Carbons
- } Si⁴⁺, occasionally Al³⁺
- }



717 cm^{-1} , and 700 cm^{-1} are assigned to out-of-plane C-H deformations characteristic of monosubstituted benzene.^{59,60} The 717 cm^{-1} and 700 cm^{-1} bands exhibit significant pleochroism when an oriented film is rotated in the infrared beam. The band at 700 cm^{-1} virtually disappears from the spectrum while the band at 717 cm^{-1} gains in intensity.

Cu(II) and Zn(II) montmorillonite. Figure 11 and Figure 12 show the spectrophotometric changes in the absorption spectrum of free base TPPH₂ after the addition of Cu(II) and Zn(II) montmorillonite, respectively. The free base porphyrin absorption bands are gradually replaced by an absorption band at 538 nm with shoulders at 500 nm and 570 nm in the case of Cu(II) montmorillonite. The Zn(II) montmorillonite reaction system behaves similarly with bands at 515 nm, 553 nm, and 593 nm replacing the TPPH₂ bands. The Soret absorption shifts slightly from 415 nm to 412 nm for Cu(II) and to 421 nm for Zn(II). It should be remarked that not all the absorption traces pass through the isosbestic points at 474 nm, 523 nm, 555 nm, 577 nm, and 668 nm for Cu(II) and 531 nm, 584 nm, 615 nm, and 668 nm for Zn(II) as a result of scattering caused by finely divided clay particles which remain suspended in the aliquot after centrifuging.

The new absorption bands which appear in the visible region are similar to those reported in the literature for meso-tetraphenylporphinatocopper(II)(CuTPP)^{61,62} and meso-tetraphenylporphinatozinc(II)(ZnTPP)⁶¹ in benzene solution.

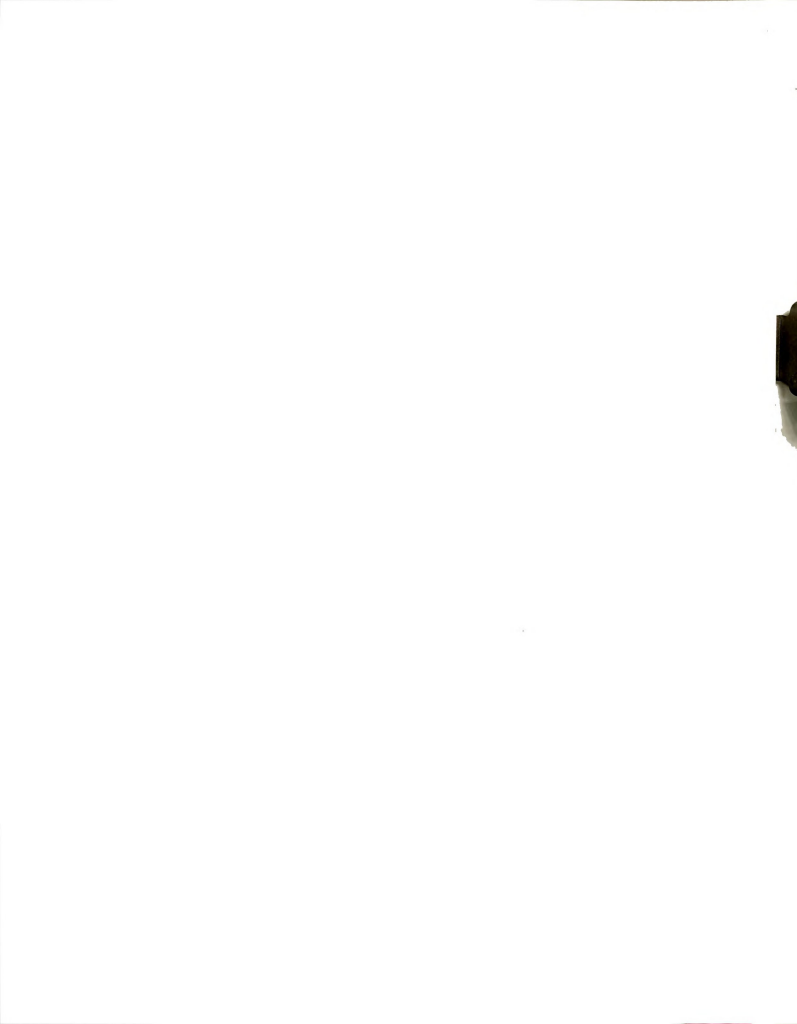
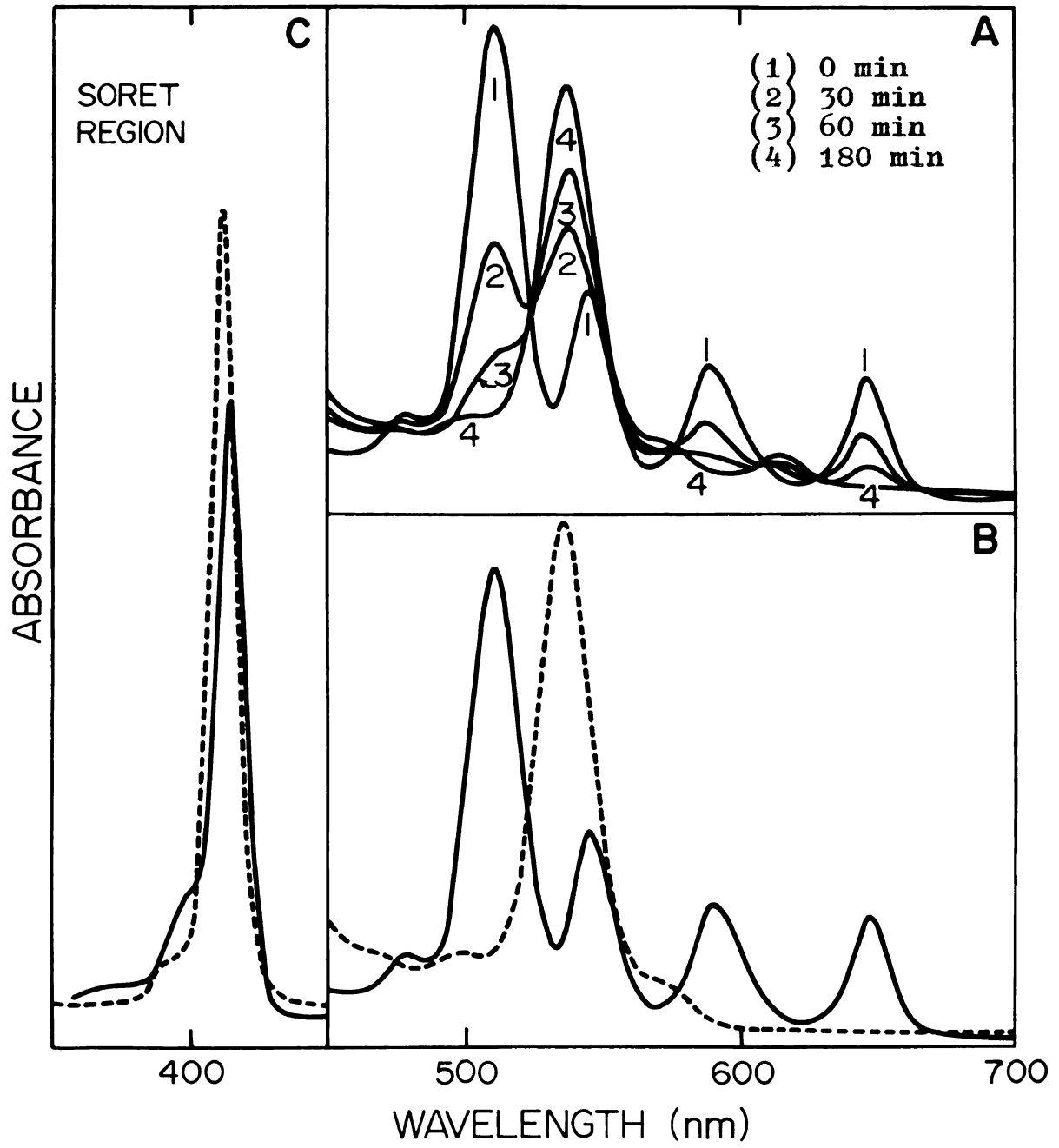


Figure 11. (A) Spectrophotometric changes after various time intervals in the absorption spectrum of the TPPH_2 -acetone solution after the addition of Cu(II) montmorillonite. (B) and (C) Visible and Soret absorptions of the TPPH_2 -acetone solution before(——) and 24 hours after(-----) the addition of Cu(II) montmorillonite.



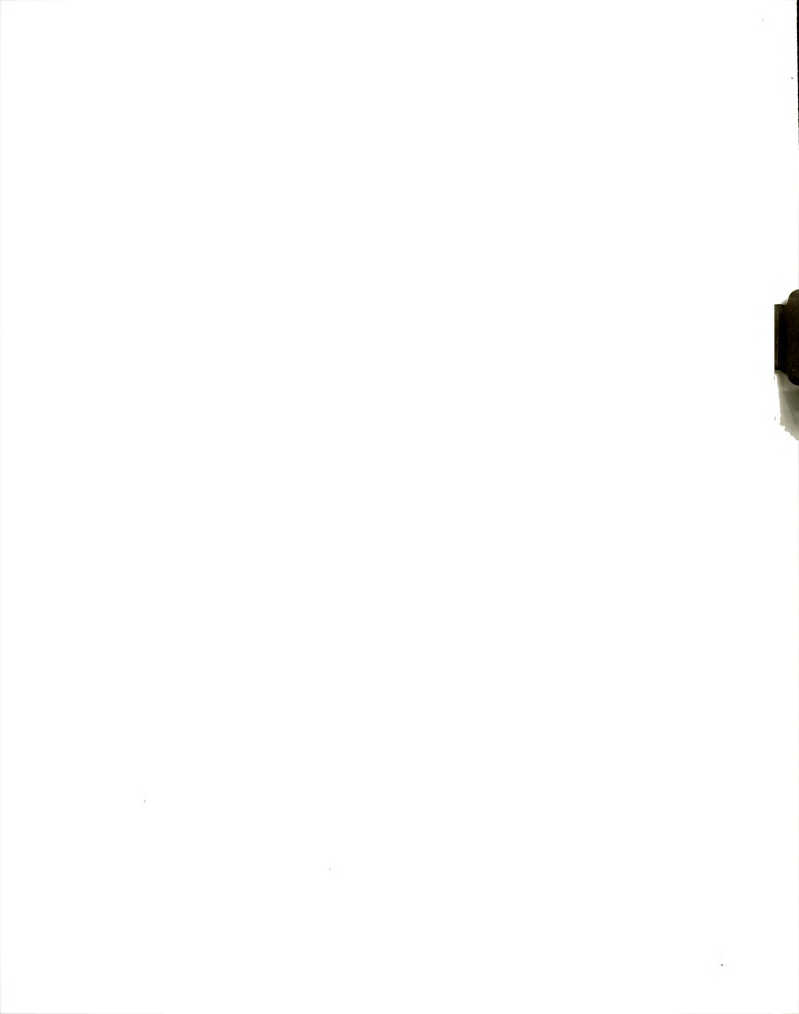
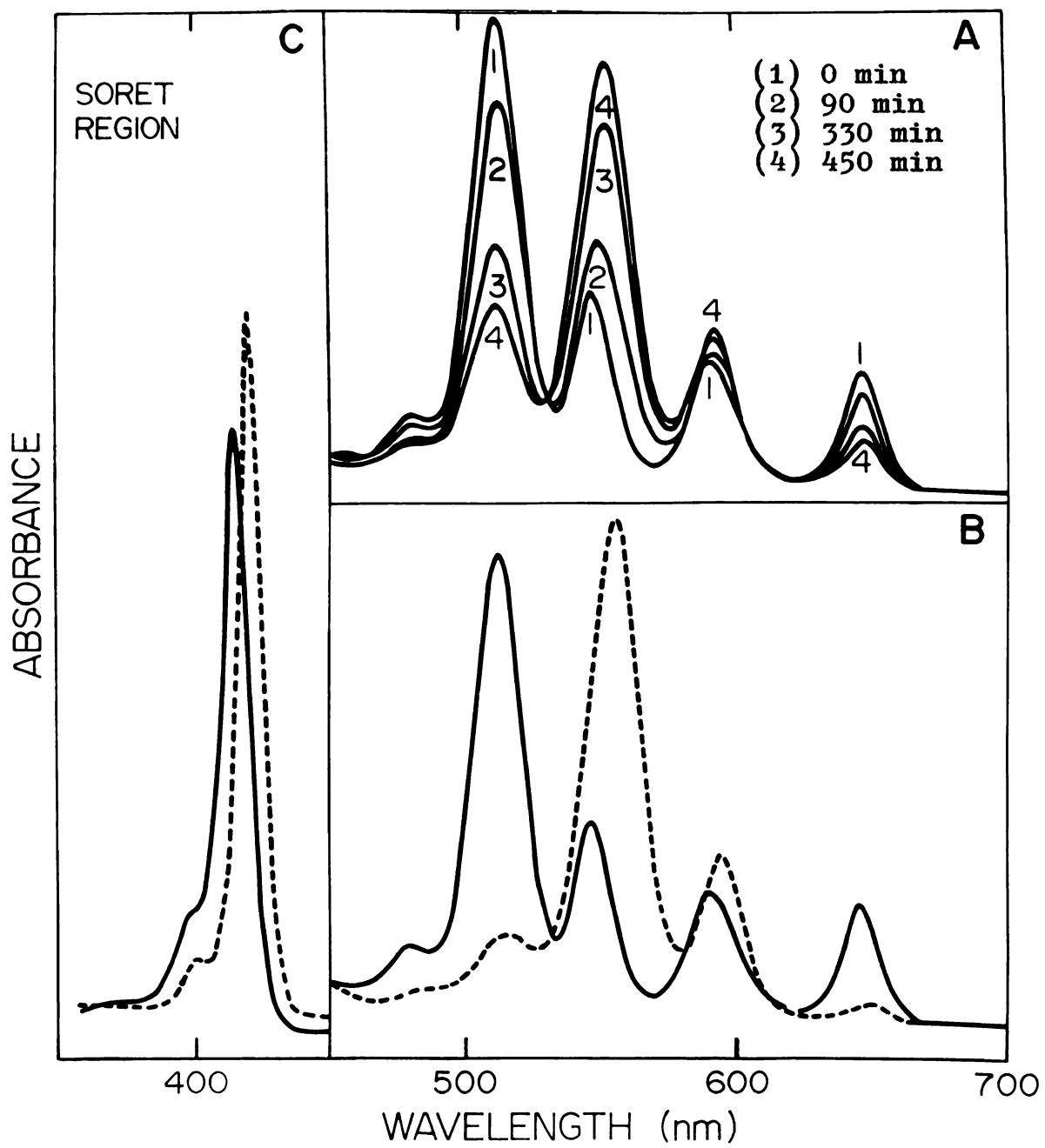


Figure 12. (A) Spectrophotometric changes after various time intervals in the absorption spectrum of the TPPH_2 -acetone solution after the addition of Zn(II) montmorillonite. (B) and (C) Visible and Soret absorptions of the TPPH_2 -acetone solution before(—) and 24 hours after(----) the addition of Zn(II) montmorillonite.

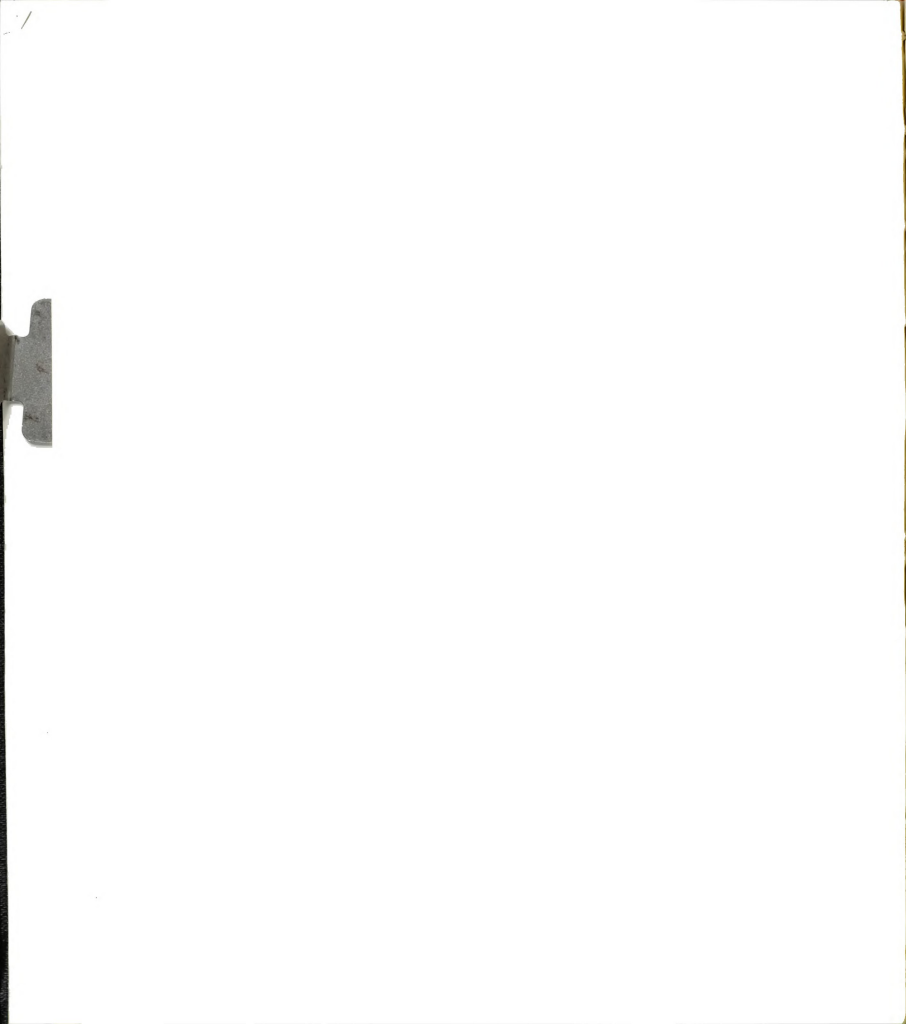




The fact that the metal chelates are desorbed from the montmorillonite surface probably results from the displacement of the neutral complexes from the exchange sites by the protons displaced from the porphyrin ring upon metalation.

Cu(II) montmorillonite exhibits a bright green color and Zn(II) montmorillonite a pale green color during the initial stages of the reaction; however, the pale blue and grayish white colors characteristic of the original clays, respectively, are present at the end of the reaction. If the amount of TPPH_2 dissolved in solution is increased to 70 mg, 140 mg, or 280 mg, the clays retain a bright green color at the completion of the reaction period. This phenomenon is apparently the result of an equilibrium established between the metal chelate and the dication on the clay surface.

If 500 mg Cu(II) montmorillonite is suspended in a concentrated acetone solution of TPPH_2 ($\sim 10^{-3}$ M) for 24 hours with continuous stirring, a light purple clay is obtained upon filtration. X-ray diffraction data indicate that the neutral porphyrin complex is adsorbed onto the external surfaces with some organic material interstratified in the interlamellar region. The small bathochromic shifts observed in the absorption spectrum of CuTPP adsorbed on montmorillonite also suggest that the adsorption is external: the markedly more pronounced spectral shifts which are found when TPPH_4^{++} is adsorbed into the interlamellar region



are absent.

Co(II) montmorillonite. The formation of a Co(II) chelate of TPPH_2 in solution is not observed spectroscopically at room temperature. However, filtration yields a yellow-tan clay whose absorption spectrum is shown in Figure 13. Although the Soret and visible absorptions are shifted 10-20 nm to the red from those observed for CoTPP in solution, the species adsorbed on montmorillonite is assigned to the Co(II) chelate of TPPH_2 . The bathochromic shifts are probably the result of an axial interaction between CoTPP and the silicate oxygens or a CoTPP complex with free diatomic oxygen trapped on the basal surfaces. A similar spectrum and bathochromic shifts have been observed for a CoTPP complex of O_2 in toluene glass at 77 K.⁶⁵ A 001 reflection of $12.6 \overset{\circ}{\text{A}}$ indicates that only external adsorption of the CoTPP complex occurs.

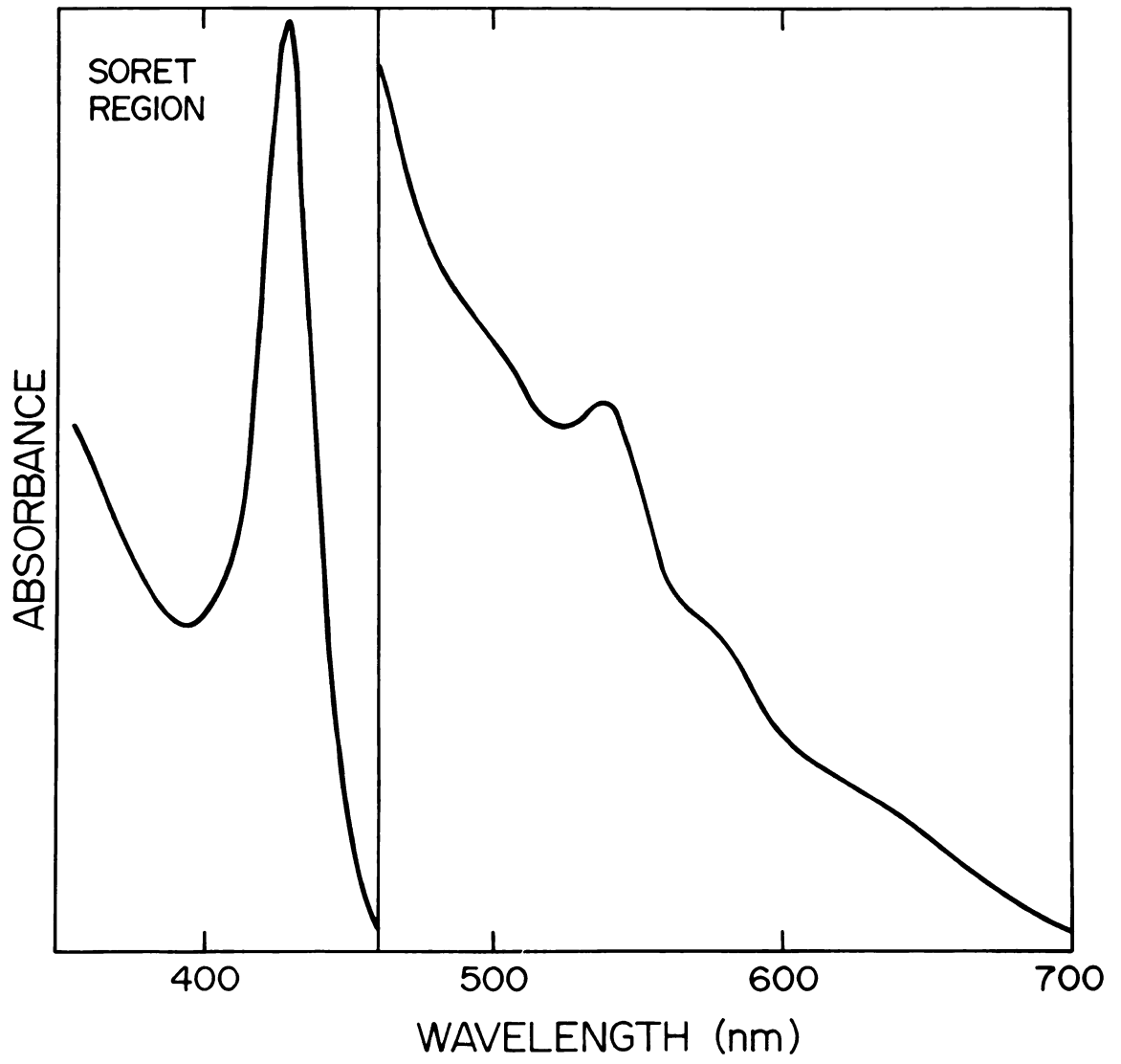
If the reaction between TPPH_2 and Co(II) montmorillonite is carried out in refluxing acetone, the formation of CoTPP occurs as indicated by a gradual increase in absorption at 528 nm (Fig. 14). Isosbestic points occur at 495 nm, 519 nm, 577 nm, and 668 nm.

Filtration yields the same clay as the room temperature reaction. When the amount of TPPH_2 is increased to 70 mg or 140 mg, the bright green clay characteristic of adsorbed TPPH_4^{++} is obtained.

Na(I) and Mg(II) montmorillonite. There are no



Figure 13. Electronic absorption spectrum of CoTPP on Co(II) montmorillonite.



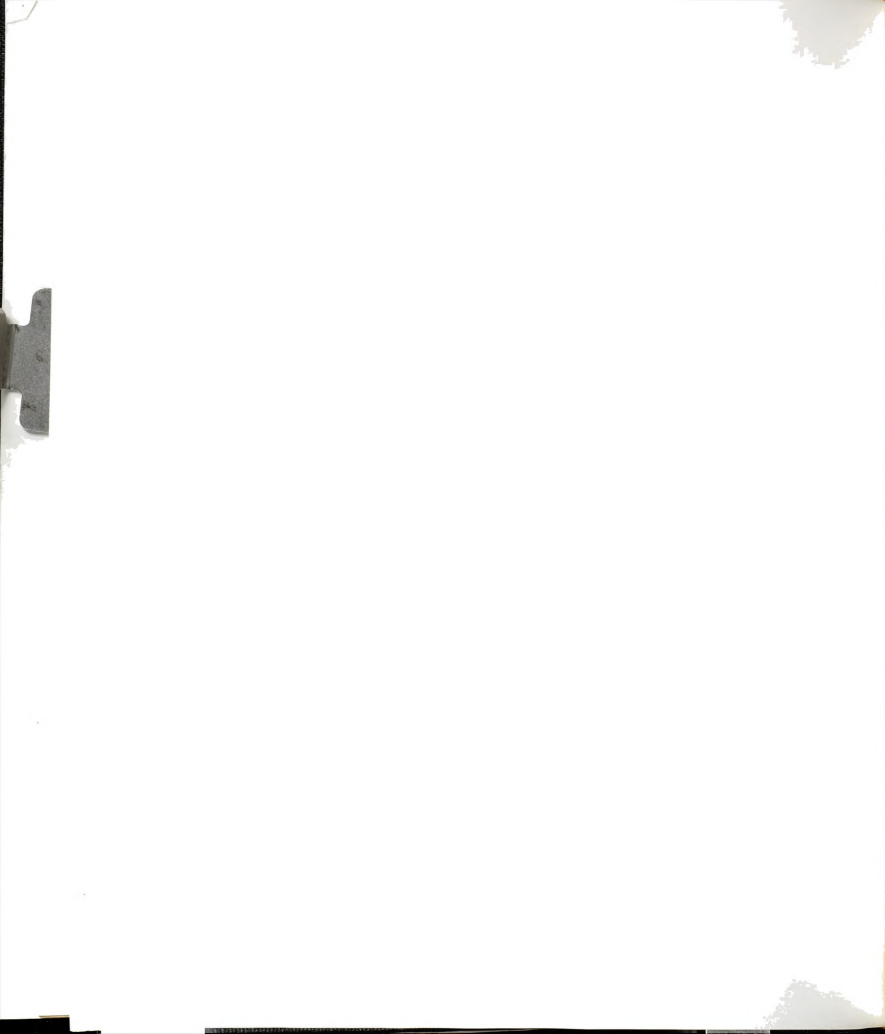
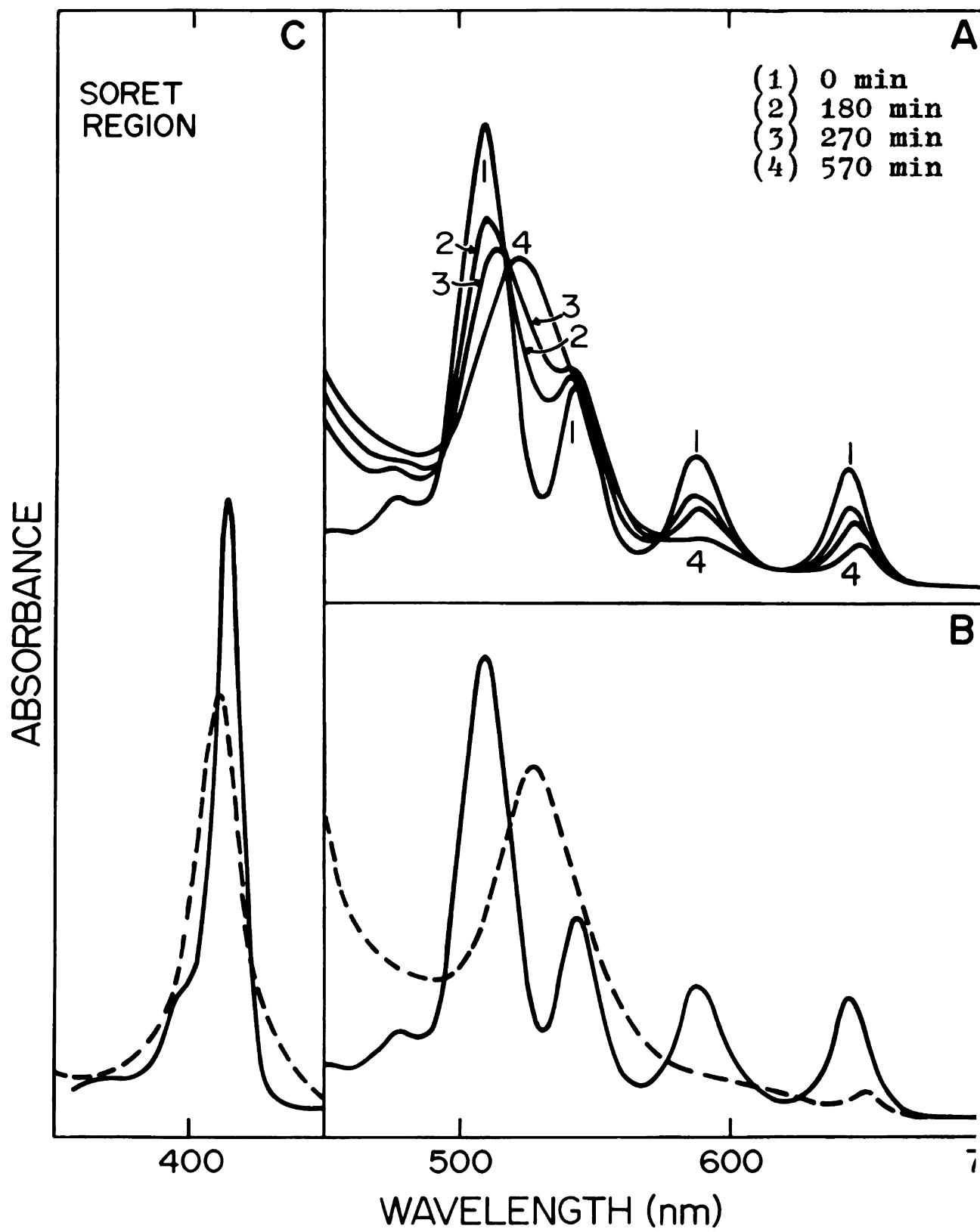
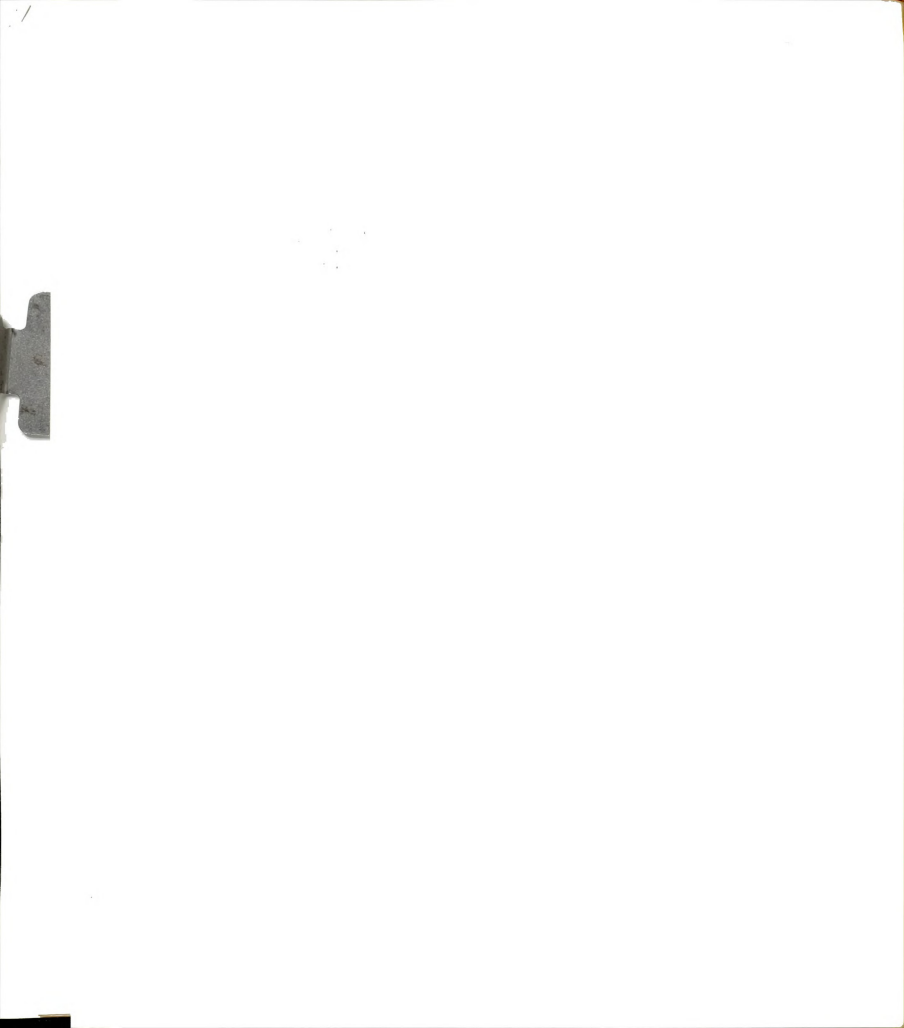


Figure 14. (A) Spectrophotometric changes after various time intervals in the absorption spectrum of the TPPH_2 -acetone solution after the addition of Co(II) montmorillonite at reflux temperature. (B) and (C) Visible and Soret absorptions of the TPPH_2 -acetone solution before (—) and 24 hours after (-----) the addition of Co(II) montmorillonite.

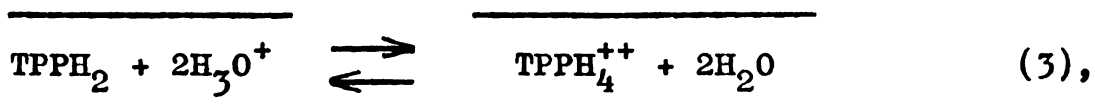
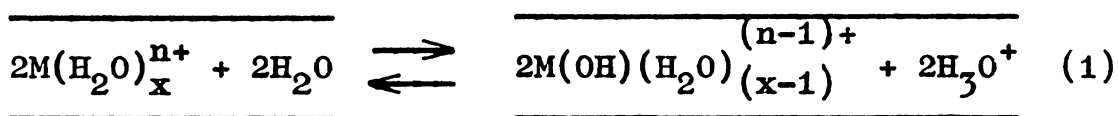




significant decreases in the intensities of the free base porphyrin absorptions after 24 hours when Na(I) or Mg(II) montmorillonite is the adsorbent. Filtration, in both cases, yields a pale green clay, which indicates that only trace amounts of TPPH_2 are adsorbed as the dication.

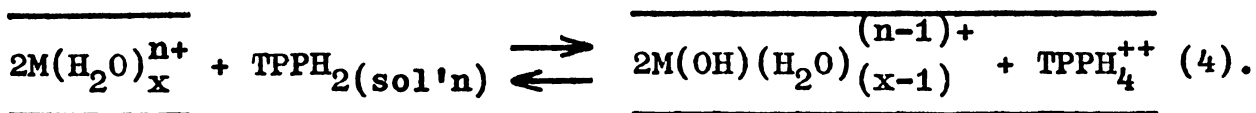
Mechanism of meso-tetraphenylporphyrin adsorption.

The formation of the meso-tetraphenylporphyrin dication in the interlamellar region of montmorillonite in the absence of metalloporphyrin formation can be described by the following set of equilibria:



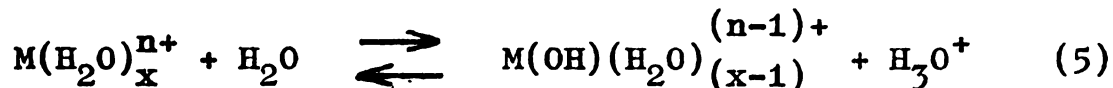
where $\frac{\quad}{\quad}$ represents surface or intercalated species.

The overall reaction for dication formation can then be represented by



From the above set of reactions, it is evident that the major factor governing the formation of the dication upon adsorption of the free base porphyrin is the ability

of the exchangeable metal cation to transfer protons to interlayer water molecules (Eq. 1). Hydrolysis constants measure the extent to which the reaction



occurs in water and are an indication of the acidity of the metal ion. Inspection of Table 2 reveals that $TPPH_4^{++}$ formation should occur most readily with the Fe(III) exchange form of montmorillonite and should become progressively more difficult as the pK_h values of the metal ions increase. This is observed experimentally as Fe(III) and VO(II) exchanged montmorillonites quantitatively adsorb $TPPH_2$ as the dication while Na(I) and Mg(II) montmorillonites convert only trace amounts of the free base porphyrin to the dication.

The acidity of interlayer water can also be increased by decreasing the water content in the interlamellar region of montmorillonite. As the number of coordinated water molecules decreases, the ability of the metal cation to polarize the remaining water molecules increases, which causes an increase in acidity. In experiments where the adsorption of $TPPH_2$ was performed in solvents immiscible with water, such as methylene chloride and benzene, all the metal ions listed in Table 2 became sufficiently acidic to allow dication formation upon adsorption of the $TPPH_2$ molecules as a result of the displacement of interlayer water molecules.

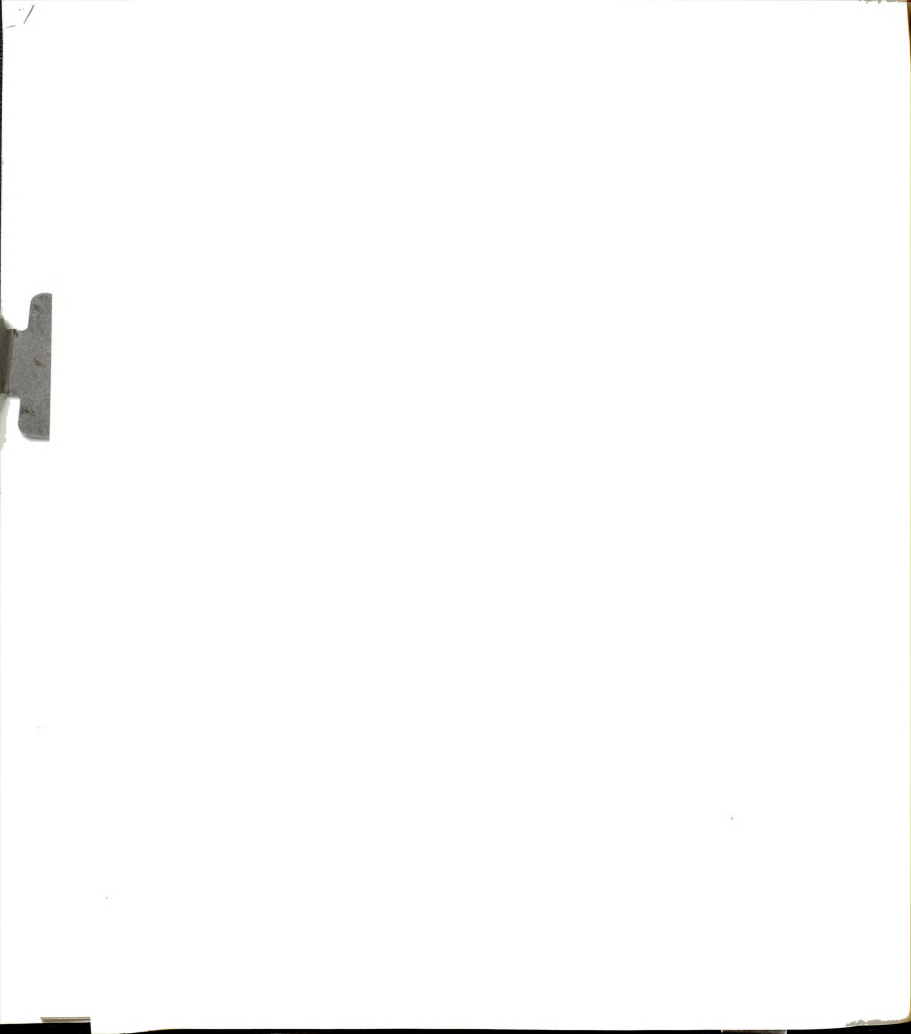


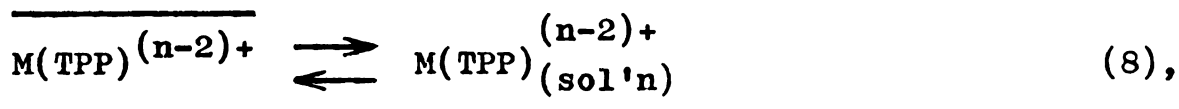
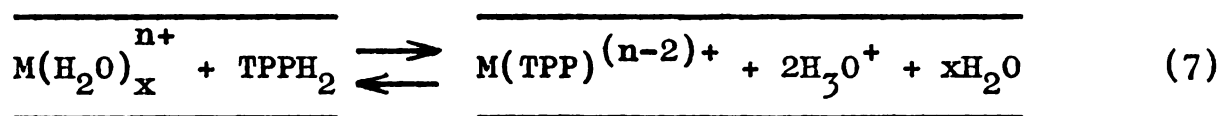
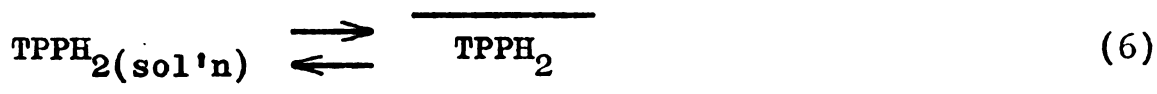
Table 2. Hydrolysis Constants for Selected Metal Ions^a

Metal Ion	pK _h
Fe(III)	2.19
VO(II)	4.77
Cu(II)	7.53
Co(II)	9.6
Zn(II)	9.60
Mg(II)	11.42
Na(I)	14.48

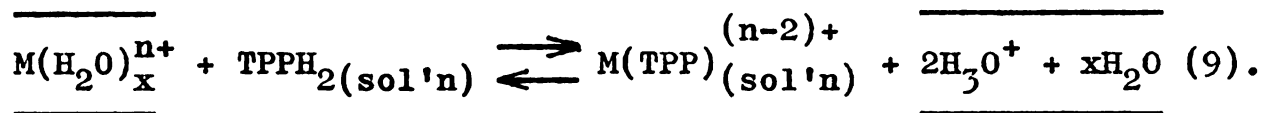
^aValues of pK_h are from J. E. Huheey, "Inorganic Chemistry: Principles of Structure and Reactivity," Harper and Row, New York, 1972 except for VO(II) which is from J. Bjerrum, G. Schwarzenbach, and L. G. Sillen, Eds., "Stability Constants of Metal-Ion Complexes: Part II, Inorganic Ligands," The Chemical Society, London, 1958.



Cu(II), Zn(II), and Co(II) are the only exchangeable ions which become incorporated into the porphyrin ring during adsorption. The following set of equilibria represent the metal chelation reaction:



where the overall reaction is

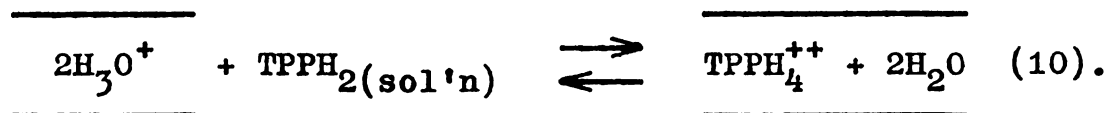


The above set of reactions indicate that the chelation of TPPH₂ is dependent on the metal ion occupying the exchange sites in the interlamellar region.

From Figures 11, 12, and 14 it can be seen that Cu(II) is the most rapidly incorporated ion followed by Zn(II) and Co(II), which reacts slowly even at reflux temperature. This reactivity order, Cu(II) > Zn(II) >> Co(II), is similar to that obtained for other porphyrins in aqueous environments.^{15,64} The rapid incorporation of Cu(II) into dimethyl protoporphyrin ester solubilized in aqueous detergent solution has been attributed to the electrostatic

attraction of Cu(II) ions to the anionic porphyrin micelle-water interface.⁶⁵ It is postulated that the porphyrin is mainly embedded in the hydrocarbon region of the micelle complex with the nitrogen atoms in contact with the aqueous phase. An analogous mechanism is proposed for metal chelate formation in the interlamellar region. The metal ion is electrostatically bonded to the negatively charged silicate layers. When the dipolar acetone-porphyrin micelle enters the interlamellar region, the positive end of the dipole is attracted to the negatively charged layers and the negative end is oriented towards the positive ions. Because acetone is miscible with water, the micelle is able to penetrate the hydrated coordination sphere of the metal ion so that metal insertion into the ring can occur.

The brightly colored green clays which appear during the course of the chelation reactions and are also obtained when the concentration of TPPH₂ in solution is increased result from the reaction between the displaced ring protons and the free base porphyrin molecules as represented by the reaction



At Cu(II) to TPPH₂ molar ratios of 14:1, 2:1, 1:1, and 1:2, the amounts of free base porphyrin converted to the metal chelate are approximately 95 %, 72 %, 71 %, and 50 %, respectively. This indicates that approximately 30 % of

the free base porphyrin is involved in reaction 10 when the molar ratios are 2:1 and 1:1 and accounts for the brightly colored green clays obtained at the end of the adsorption reaction.

The value of 50 % obtained for the 1:2 reaction represents the incorporation of all the exchangeable Cu(II) ions into the porphyrin ring. Spectroscopic measurements indicate that 25 % of the free base porphyrin is adsorbed as the dication. This figure corresponds to the complete coverage of the internal surface area of montmorillonite by porphyrin dications based on a theoretical surface area of $8 \times 10^6 \text{ cm}^2/\text{g}$ for montmorillonite and an area of 300 \AA^2 / molecule of TPPH_4^{++} . The calculated total internal surface area per Cu(II) exchange position is 150 \AA^2 , which indicates that one TPPH_4^{++} molecule occupies the area of two cation exchange positions. Because this figure leaves half the cation exchange positions charge deficient, the protons displaced from the porphyrin ring during metallation must maintain the conservation of charge in the interlamellar region.

Conclusion. Metal ion exchange forms of montmorillonite adsorb free base meso-tetraphenylporphyrin molecules and undergo two distinct reactions with the adsorbed molecules: dication formation and metalloporphyrin formation, as represented by Equations 4 and 9, respectively.

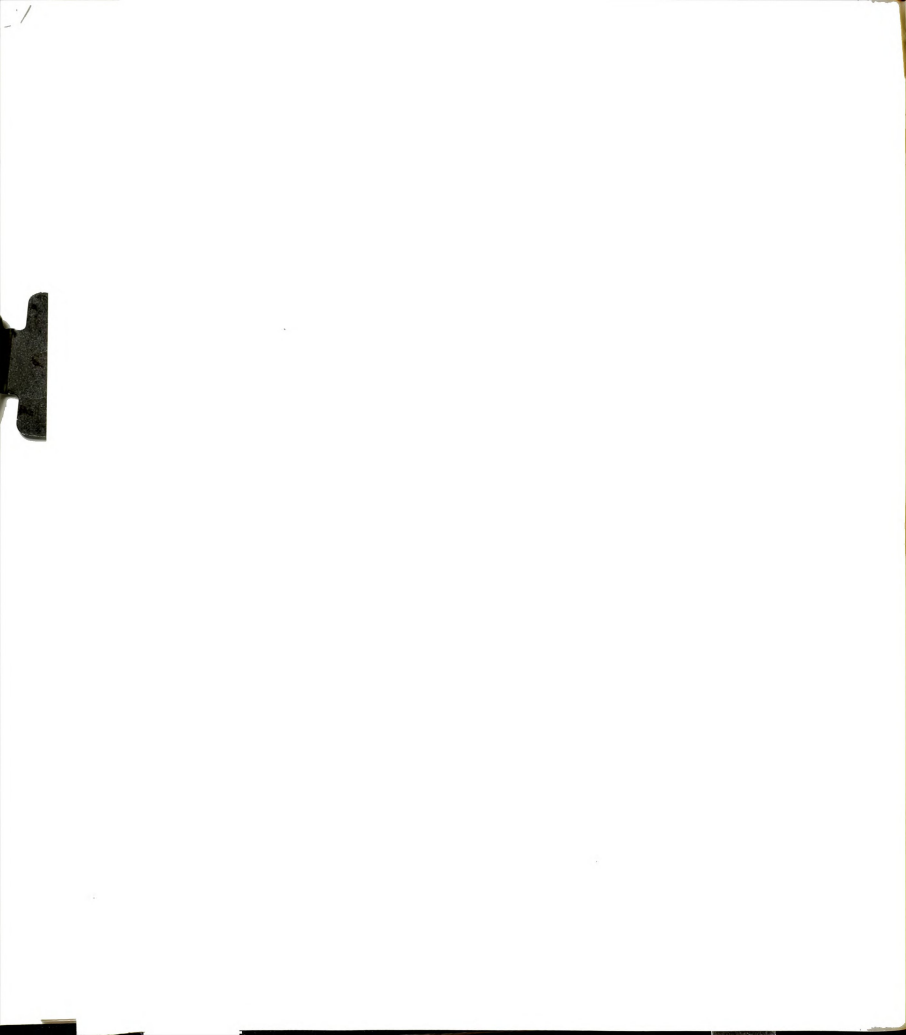
Dication formation is found to be dependent on the acidity of the exchangeable cation. The acidity of the metal ion can be increased by performing the adsorption in a

solvent which is immiscible with water. Visible absorption spectra, infrared pleochroic studies, and X-ray diffraction data indicate that TPPH_4^{++} assumes a more planar conformation in the adsorbed state than in the crystalline state. This suggests that the silicate layers of montmorillonite are capable of inducing conformational changes in the structures of porphyrins adsorbed into the interlamellar region.

Metalloporphyrin formation on clay surfaces also shows a metal-ion dependence with Cu(II), Zn(II), and Co(II) being the only exchangeable metal ions incorporated into the porphyrin ring. Dication formation also occurs during metalloporphyrin formation; however, the metallation reaction predominates. It is interesting that the same order of reactivity, $\text{Cu(II)} > \text{Zn(II)} \gg \text{Co(II)}$, is found for metal ions attached to clay surfaces as for other porphyrin model systems.

The neutral porphyrin complexes CuTPP and CoTPP are physically adsorbed only on the external surfaces of montmorillonite. Intercalation is apparently restricted to porphyrin cations such as TPPH_4^{++} and cationic metalloporphyrins.²² This selective intercalation arises from the ability of these positively charged porphyrins to function as exchangeable cations in the interlamellar region.

Bivalent transition metal complexes of TPPH_2 are known to act as heterogeneous catalysts for oxidative dehydrogenation.⁶⁶ The inability of neutral porphyrin complexes to become intercalated into montmorillonite precludes the use



of swelling layer silicates as inorganic supports for these porphyrin catalysts. However, the foregoing research does suggest that cationic metalloporphyrin catalysts such as FeTPP^+ , which is a homogeneous catalyst for the auto-oxidation of methylene compounds,⁶⁷ may be intercalated into clay minerals and function as heterogeneous catalysts.

4.2 Synthesis of Porphyrin Intermediates on the Intracrystal Surfaces of Montmorillonite

Visible absorption spectra. Sufficient clay is employed during the condensation reactions so that a single monolayer of pyrrole and benzaldehyde can be formed in the interlamellar region. In the case of M^{2+} and M^{3+} exchange ions, the amount of clay corresponds to a M^{n+} to pyrrole molar ratio of 1:2. Chemical analyses indicate that all the pyrrole and benzaldehyde molecules are adsorbed for all exchange forms of the clay.

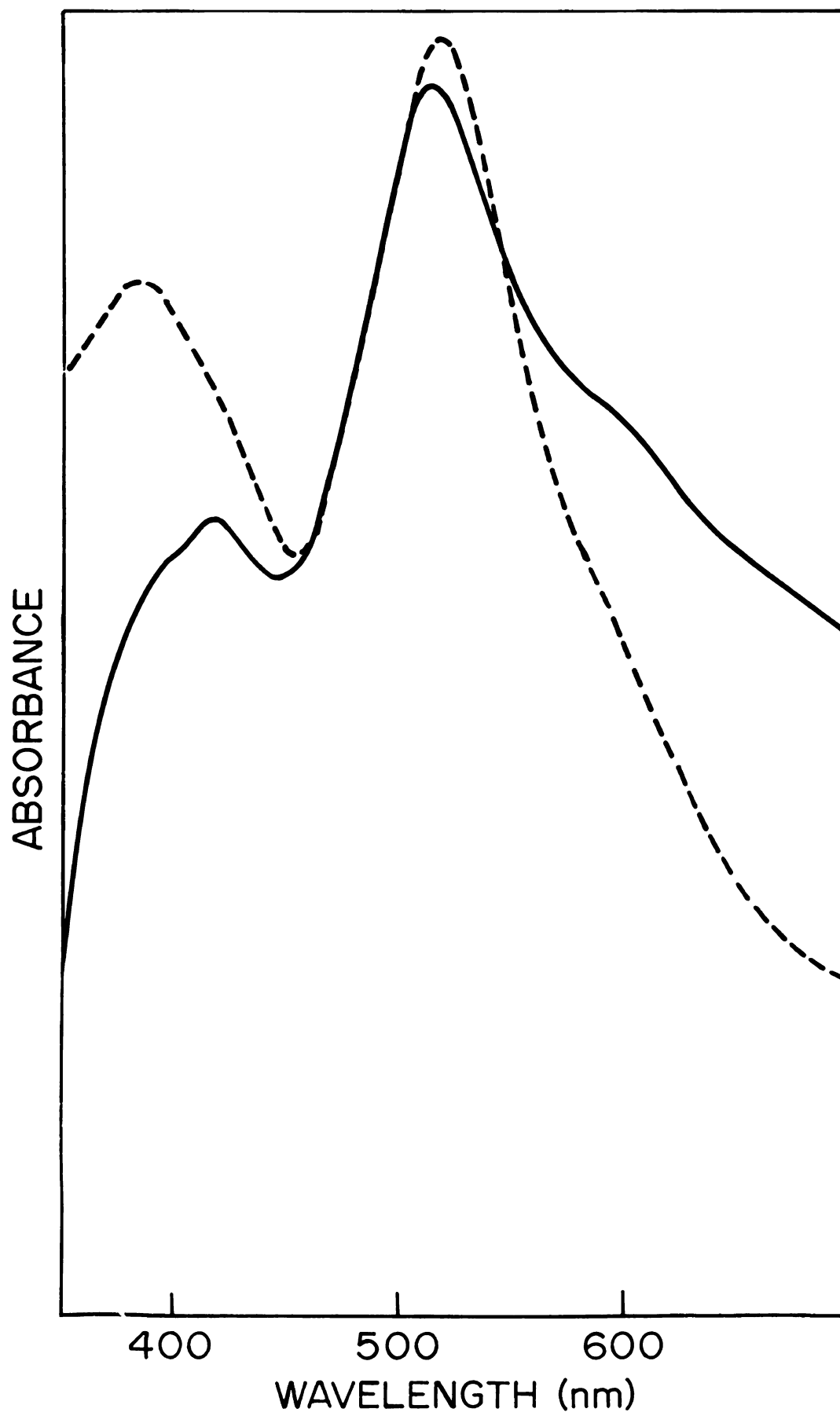
Table 3 and Figure 15 indicate that the product of the condensation reaction between equimolar amounts of pyrrole and benzaldehyde under aqueous conditions at a concentration of $1.5 \times 10^{-2} \text{ M}$ and in the presence of various cation saturated montmorillonites exhibits an intense absorption near 500 nm. The appearance of an intermediate absorbing near 500 nm has been observed during the oxidation of porphyrinogens in previous studies on porphyrin synthesis. Mauzerall and Granick²⁶ assigned porphomethene and porphodimethene structures to the intermediate absorbing at 500 nm

Table 3. Visible Absorption Spectra of the Pyrrole-Benzaldehyde Condensation Product Adsorbed on Various Montmorillonites

M^{n+} Montmorillonite	λ_{\max} (nm)
Fe(III)	518
Cu(II)	512
Zn(II)	511
Co(II)	506
Mg(II)	509
VO(II)	522
Na(I)	515 ^a
H ⁺	515
TPA ⁺	no reaction

^aThis value is for the reaction in which the M⁺:pyrrole ratio is 1:2.

Figure 15. Electronic absorption spectra of the pyrrole-benzaldehyde condensation product adsorbed on Cu(II) montmorillonite(——) and H⁺ montmorillonite(-----).

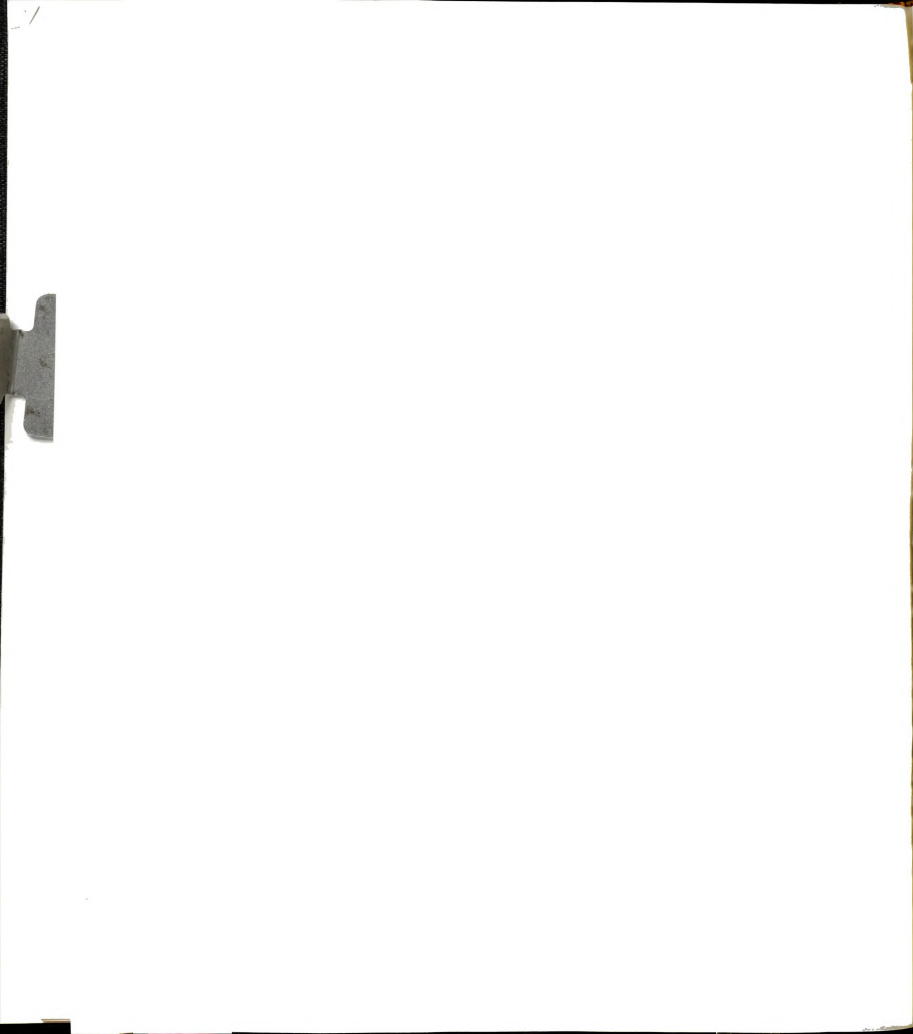




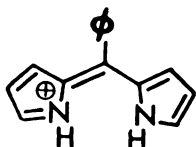
during the chemical oxidation of uroporphyrinogen to uroporphyrin. Later, in a study on the chemical and photoreduction of uroporphyrin, Mauzerall^{27,28} assigned the tetrahydroporphyrin intermediate a porphomethene structure. A second intermediate corresponding to a dihydroporphyrin absorbed at 440 nm and 735 nm and was assigned a phlorin structure. More recently Dolphin⁴ was able to isolate the zinc complex of the porphodimethene during the oxidation of octamethyltetraphenylporphyrinogen to OMTTP. The zinc chelate was found to absorb at 519 nm, which was in agreement with the transient absorption which appeared at 518 nm during the synthesis of OMTTP.

The formulation of the intermediate absorbing at 500 nm as a porphodimethene or porphomethene during uroporphyrin and OMTTP synthesis was based on its similarity to dipyrromethene. The spectral absorption properties,^{4,26-28} nmr chemical shifts,⁴ pK values,²⁶⁻²⁸ and the nature of the zinc, sulfite, and dithionite complexes^{4,26-28} of the intermediate were all found to be similar to those of the dipyrromethene. The porphomethene contains one isolated dipyrromethene unit while the porphodimethene consists of two separate dipyrromethene chromophores. The high degree of correlation between the properties of the intermediate and those of the dipyrromethene served to confirm the dipyrromethene type structure for the intermediate as either the porphomethene or porphodimethene.

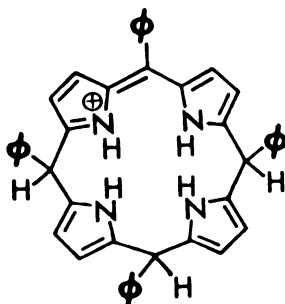
A similar dipyrromethene chromophore(XIII) is proposed



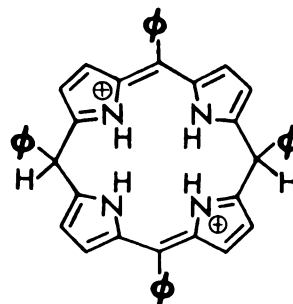
for the condensation of pyrrole and benzaldehyde on montmorillonite. A porphomethene or porphodimethene intermediate can then be represented by structures XIV and XV, respectively. Each of the species could exhibit



XIII



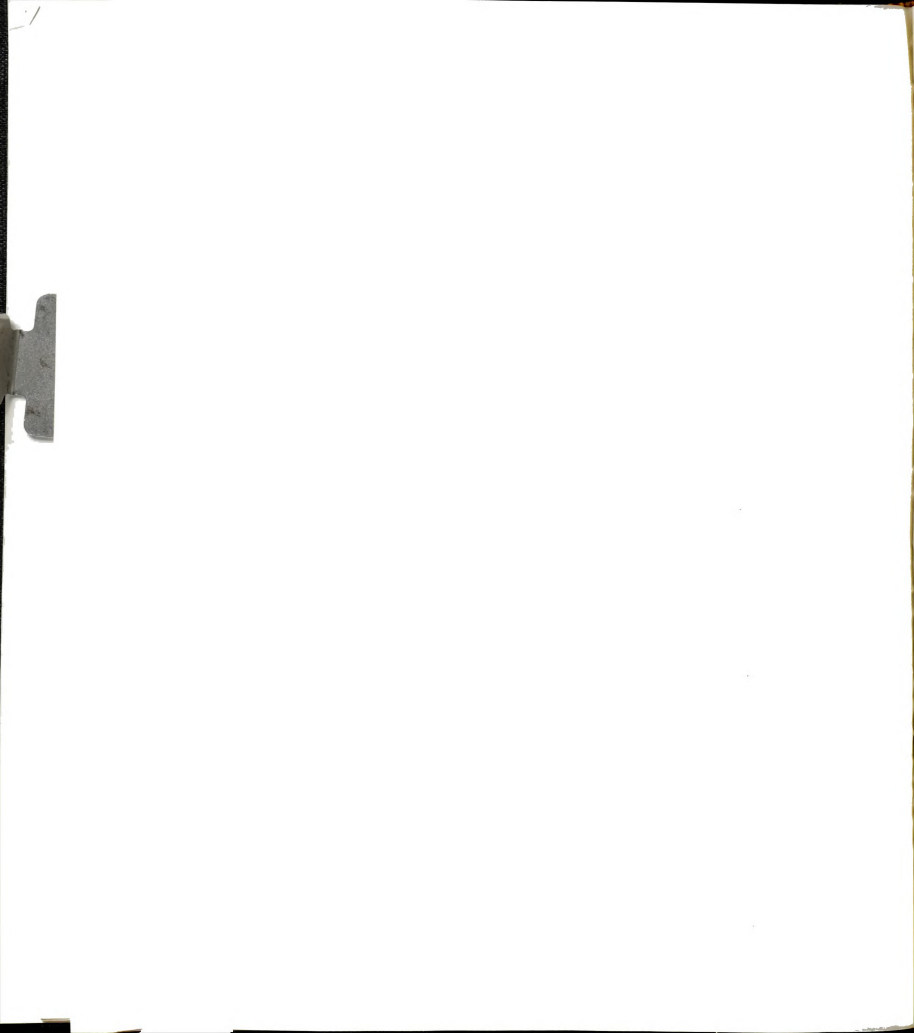
XIV



XV

the observed intense absorption near 500 nm. Although the visible absorption spectrum cannot distinguish between the porphomethene and porphodimethene structures, the intermediate on the montmorillonite surface is assigned the meso-tetraphenylporphodimethene (TPPDM) structure based on the similarity between the TPPH_2 reaction and the OMTTP reaction and the isolation of the porphodimethene intermediate from the OMTTP reaction as the zinc chelate. The presence of an additional dipyrromethene unit would also be expected to impart extra stability to the TPPDM structure because of the gain in resonance energy.

The shift of the TPPDM absorption band from 480 nm in acetic acid solution¹⁻⁴ to longer wavelengths when in the adsorbed state suggests that the intermediate assumes a more planar conformation in the interlamellar region than is possible in solution. The ability of the silicate layers



to restrict porphyrin molecules to a more planar conformation was noted previously for TPPH_4^{++} molecules exchanged into the interlamellar region of montmorillonite(cf., Section 4.1).

The 001 reflections for powdered samples of montmorillonite containing the adsorbed intermediate were 14.7 \AA° for Cu(II) and 17.7 \AA° for Fe(III) and H^+ after drying at 200° C . These basal spacings yield a separation between the silicate sheets of 5.1 \AA° and 8.1 \AA° ; however, broad, diffuse diffraction bands were obtained at the higher 001 reflections which indicates that interstratification of different layers was present. An accurate determination of the interlayer spacing due to TPPDM was therefore not possible at these particular reflections. The lower 001 reflection exhibited the sharp diffraction band indicative of a single organic layer. If the thickness of a porphyrin molecule is taken to be 4.7 \AA° ,⁷ then a basal spacing of 5.1 \AA° indicates that the TPPDM molecules are oriented parallel to the silicate sheets in a planar conformation.

Desorption studies. Further evidence for the existence of a porphyrin precursor on the montmorillonite is provided by the desorption experiments. Based on the yield of TPPH_2 obtained from various extraction methods(cf., Section 3.6), Method D, in which 10 to 12 per cent TPPH_2 can be obtained by forming the intermediate in the presence of TPA^+ , provided the most efficient means of displacing the adsorbed intermediate from the exchange sites of montmorillonite.

Figure 16 shows a typical absorption spectrum of the

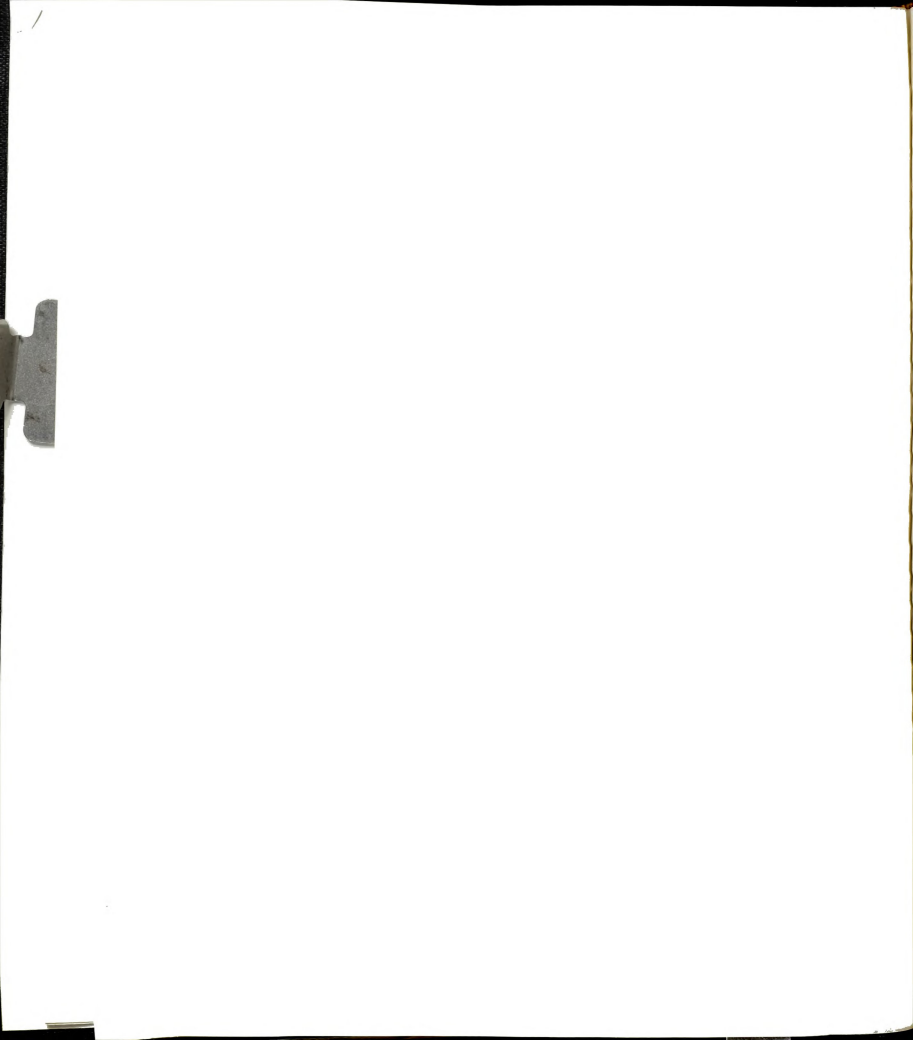
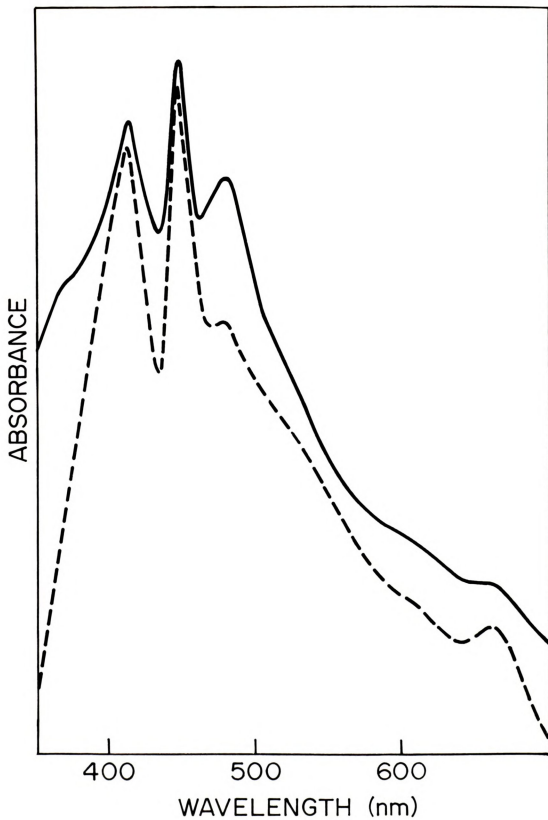
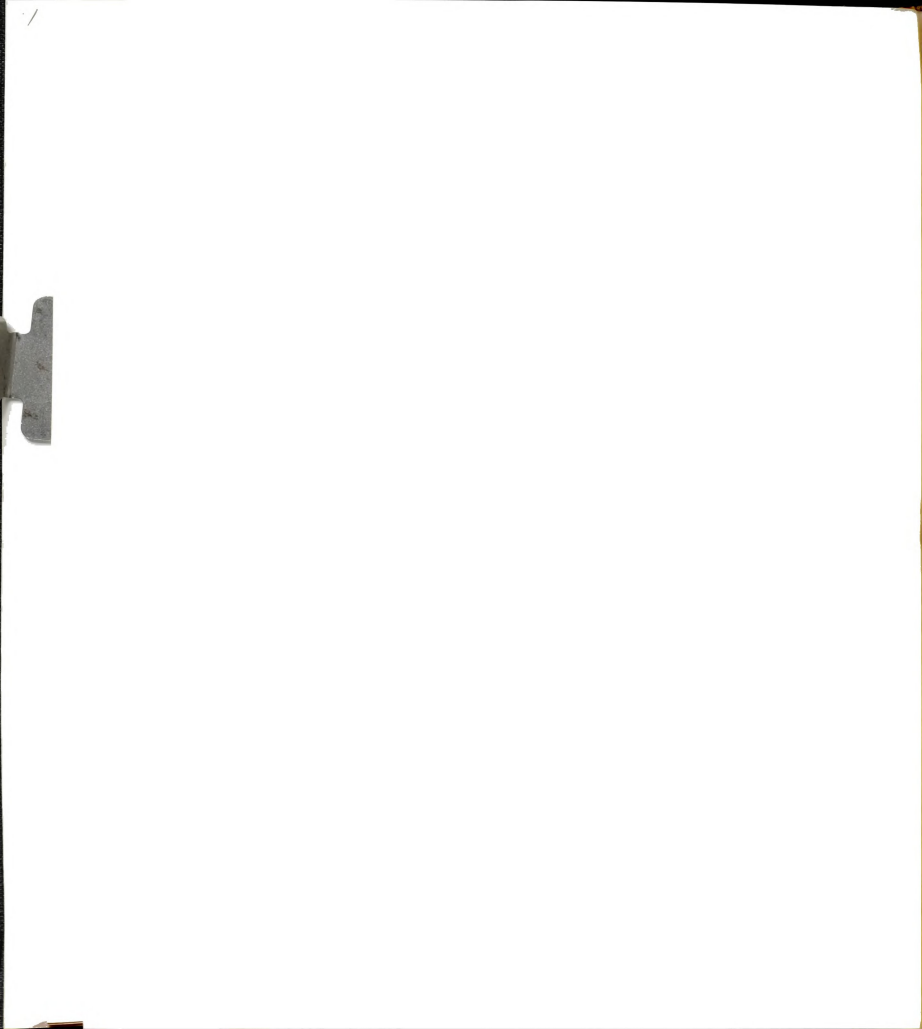


Figure 16. Electronic absorption spectra of the chloroform extraction solution 2 hours (——) and 24 hours (-----) after the desorption of the pyrrole-benzaldehyde condensation product from Cu(II) montmorillonite in the presence of TPA⁺.

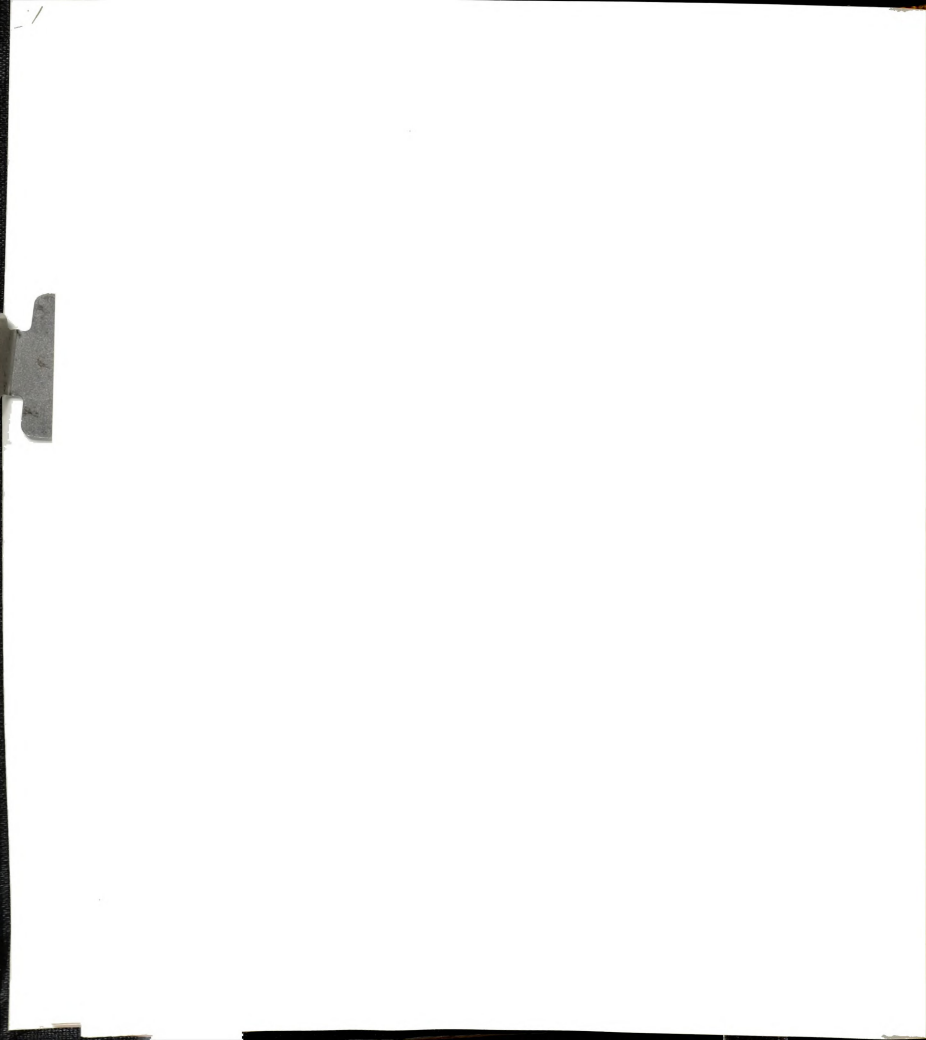




chloroform extract obtained by Method D. The absorption band at 485 nm, whose intensity decreases with time as the Soret absorptions increase, confirms the presence of the desorbed porphyrin intermediate in solution. The similarity in position of the intermediate absorption to that obtained for the intermediate during the synthesis of TPPH_2 in acetic acid¹⁻⁴ suggests that the same intermediate is formed in both cases, namely TPPDM. The bands at 415 nm and 447 nm are assigned to the Soret absorptions for TPPH_2 and TPPH_4^{++} , respectively. The appearance of an absorbance for diprotonated porphyrin is significant since an aprotic extraction solvent was employed, which suggests that the source of protons must be the clay surface itself. The acidic nature of the montmorillonite surface therefore is capable of maintaining the intermediate in the cationic form needed to satisfy the exchange sites on the clay. The presence of the Soret absorptions and the intermediate band in solution suggests that oxidation of the intermediate occurs after desorption from the montmorillonite surface.

Adsorption of the porphyrin intermediate from solution.

The synthesis of the porphyrin intermediate in solution and its subsequent adsorption onto the TPA^+ and Cu(II) exchange forms of montmorillonite provide additional evidence for assigning the TPPDM structure to the condensation product on the clay surface. Comparison of Figure 9 with Figure 15 shows the similarity in the shape and intensity of the absorption bands, with the bands in Figure 15 absorbing at



longer wavelenghts. The bathochromic shift that occurs when TPPDM is formed on the clay surface results from the intercalation of the condensation product during its synthesis while only external adsorption occurs during the adsorption of the intermediate from solution. That TPPDM is adsorbed from solution only onto external adsorption sites is supported by the X-ray diffraction data, which yielded 001 spacings of $12.4 \overset{\circ}{\text{Å}}$ and $14.7 \overset{\circ}{\text{Å}}$ for intercalated Cu(II) ions and TPA^+ ions, respectively.

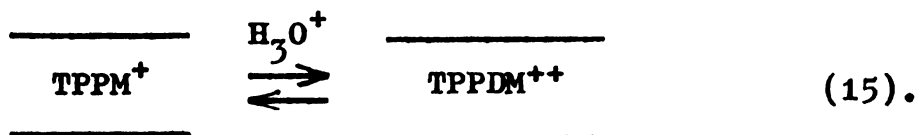
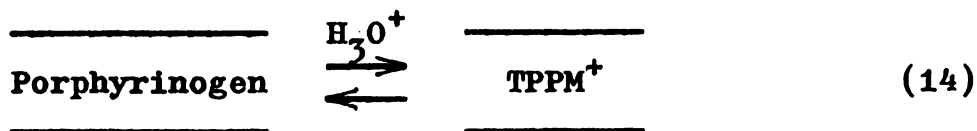
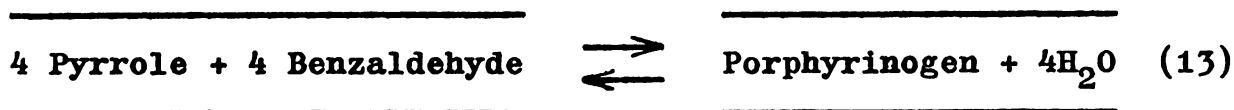
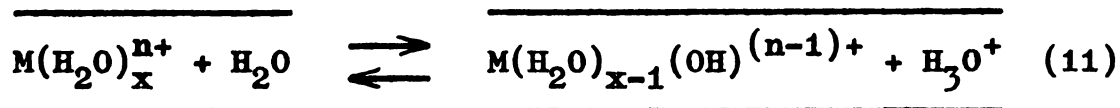
The adsorption of the porphyrin intermediate from acidic chloroform solution onto Cu(II) montmorillonite results in the formation of CuTPP in solution(cf., Section 3.7). The Cu(II) ions which become complexed with TPPH_2 in the filtrate are evidently replaced in the interlamellar region by the two protons which are displaced from the porphyrin molecule during chelation rather than the dipositive TPPDM intermediate. Since chloroform is a poor swelling solvent, the inability of TPPDM to penetrate the montmorillonite layers is not unexpected. Although the TPA^+ ions maintain a separation of $5.1 \overset{\circ}{\text{Å}}$ between the silicate layers, TPPDM, because of its larger size, does not compete favorably with TPA^+ for the exchange positions and intercalation does not occur.

The porphyrin intermediate when externally adsorbed on Cu(II) montmorillonite absorbs at 505 nm as compared to 485 nm when TPA^+ montmorillonite is the adsorbent. This shift of 20 nm to longer wavelength is believed to be the

result of chelation of TPPDM with Cu(II) ions. The shoulder at 475 nm is then assigned to the unchelated TPPDM molecules. The shoulder at 447 nm results from the Soret absorption for TPPH_4^{++} .

Mechanism of meso-tetraphenylporphodimethene formation.

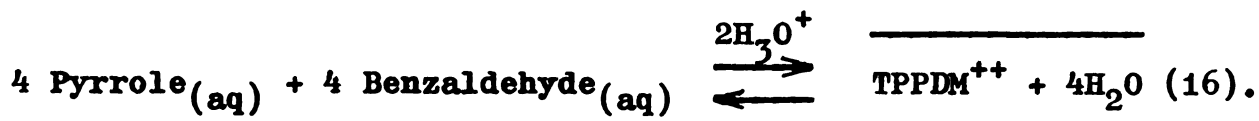
The mechanism proposed for the formation of TPPDM on the intracrystal surfaces of montmorillonite is an adaptation of the pathway described by Dolphin⁴ for the synthesis of meso-substituted porphyrins in acid solution. The following set of equilibria represent the synthesis of TPPDM on the montmorillonite surface:



The overall reaction for TPPDM formation can then be



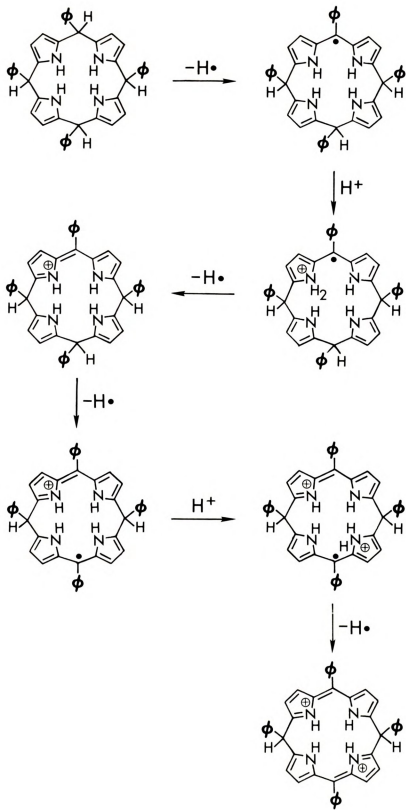
represented by the equation



The hydrolysis of the metal ion in the interlamellar region as represented by Equation 11 provides the protons needed to catalyze the autooxidation of the porphyrinogen to TPPM in Equation 14 and the oxidation of TPPM to TPPDM in Equation 15. The ability of the metal ion to hydrolyze, as measured by the pK_h values in Table 2, is an indication of the relative rate of TPPDM synthesis on the clay surface. The synthesis of TPPDM is found to proceed more rapidly in the presence of the more acidic metal ions such as Fe(III), VO(II), and Cu(II), which require only minutes to initiate the reaction, while the other metal ions require a half hour or more to produce the initial TPPDM condensation.

The oxidation of the porphyrinogen is believed to be either free radical in nature with acid catalysis being a function of protonation on a pyrrolic nitrogen or as a hydride transfer to the hydroperoxy(HO_2^+) cation.⁴ The formation of TPPDM in the absence of oxygen suggests that the acid catalysis of porphyrinogen oxidation follows a free radical pathway. The removal of a hydrogen atom from a methene bridge carbon generates a resonance stabilized free radical. Protonation of a pyrrolic nitrogen followed by the loss of another hydrogen atom produces an oxidized dipyrromethene unit. This oxidation is repeated a second time to

Figure 17. Mechanism of meso-tetraphenylporphodimethene formation on the intracrystal surfaces of montmorillonite.



1

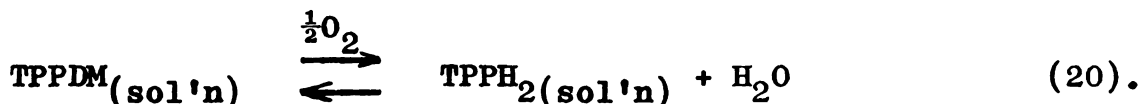
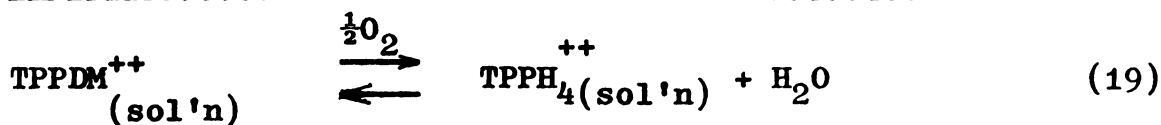


yield TPPDM(Fig. 17).

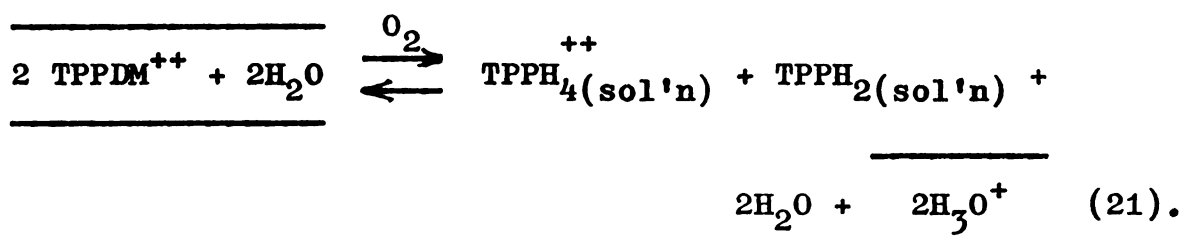
From Figure 15 it is evident that only a small amount of the TPPDM intermediate is oxidized to TPPH_2 while in the adsorbed state. This increased stability of TPPDM to air and photolytic oxidation while in the adsorbed state is believed to result from the ability of the negative charge on the silicate layers to stabilize the resonant dipositive charge on TPPDM. This electrostatic interaction is possible because the dicationic structure of TPPDM permits it to function as an exchangeable cation on the montmorillonite surface. The counter anion effect of the silicate layers is similar to that of the bromide ion used to stabilize and isolate the meso-phenyl-3,3',4,4',5,5'-hexamethyl-2,2'-dipyrromethene cation.⁴ It is significant that Dolphin⁴ reported the stability of the porphodimethene of OMTTP in the absence of oxygen for several days while Mauzerall²⁸ observed that the porphomethene of uroporphyrin was oxidized rapidly by iodine but only very slowly by oxygen. The slowness of TPPDM to oxidize in air was also observed during its synthesis in a weakly acidic chloroform solution. Several hours of reaction time were required before TPPH_4^{++} appeared in solution(cf., Section 3.7).

The formation of free base and diprotonated TPPH_2 during desorption of TPPDM can be represented by the following set of equilibria:

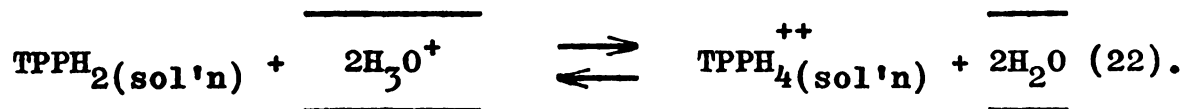




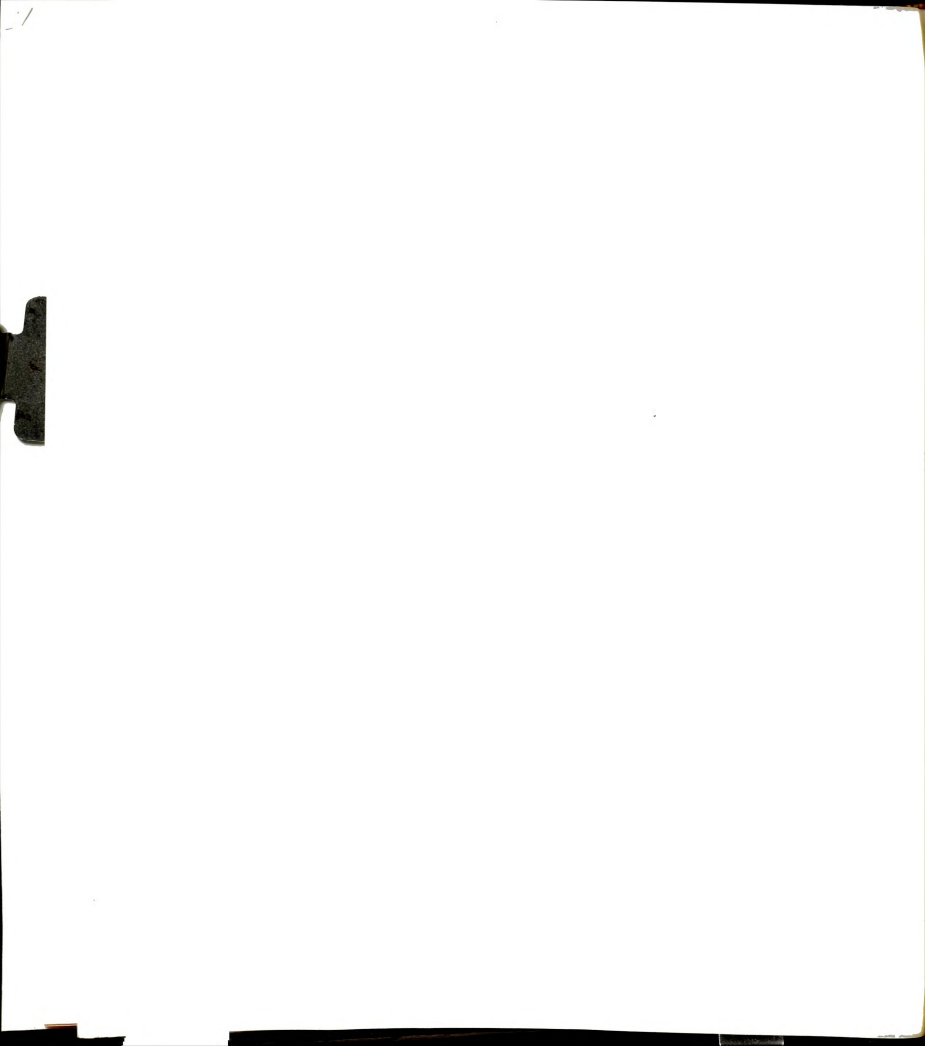
The overall reaction may then be written as



The above mechanism assumes that oxidation of TPPDM occurs only after its desorption from the montmorillonite surface. The trace amounts of TPPH_2 formed on the clay during the condensation reaction and the presence of TPPDM in the extraction solution and its subsequent oxidation to porphyrin would seem to support this assumption. It should be remarked that a small percentage of TPPH_4^{++} formed in solution may result from the protonation reaction



The release of TPPDM from the interlamellar region removes the silicate layers as counter anions and destabilizes the intermediate toward air oxidation. This destabilization results in the appearance of TPPH_2 and TPPH_4^{++} bands in the



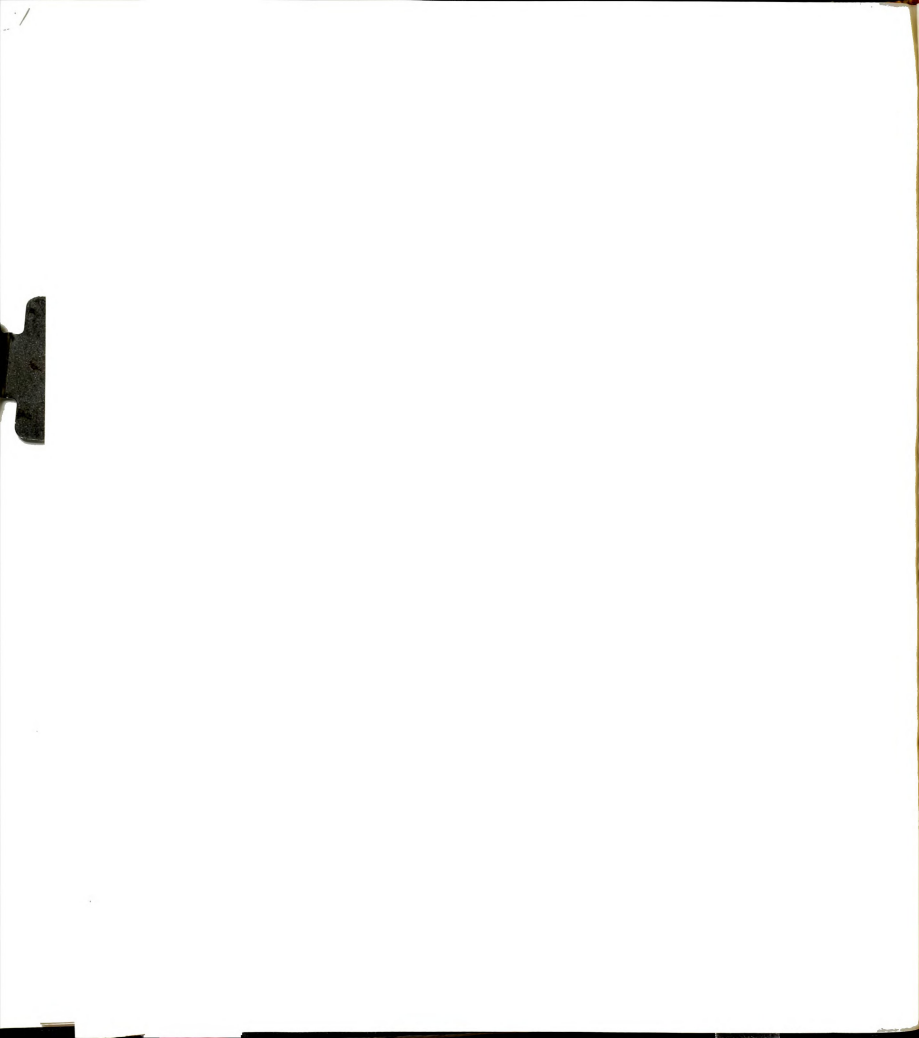
extraction solution. The yield of porphyrin is determined by the amount of TPPDM desorbed from the montmorillonite surface, which is severely limited by the ability of TPPDM⁺⁺ to function as an exchangeable cation in the interlamellar region.

Conclusion. It is probable that the prebiotic formation of porphyrins and porphyrin-like precursors occurred on the surfaces of clay minerals such as montmorillonite because of their ability to adsorb and concentrate smaller organic molecules from the primitive ocean. The presence of exchangeable metal cations and their ability to hydrolyze in the interlamellar region enabled the clay surface to function as a catalyst for the formation of biological monomers.

The formation of TPPDM from pyrrole and benzaldehyde in an aqueous environment is found to proceed quite easily in the presence of various cation exchanged montmorillonites under aerobic and anaerobic conditions. The negative charge of the silicate layers is believed to stabilize diprotonated TPPDM once it is formed on the clay surface. Appropriate organic solvents are capable of desorbing TPPDM in the presence of a suitable exchangeable cation with oxidation to porphyrin occurring after desorption. A free radical, acid-catalyzed mechanism which does not require the presence of oxygen for oxidation is proposed for the prebiotic formation of porphodimethenes on the intracrystal surfaces of clay minerals.

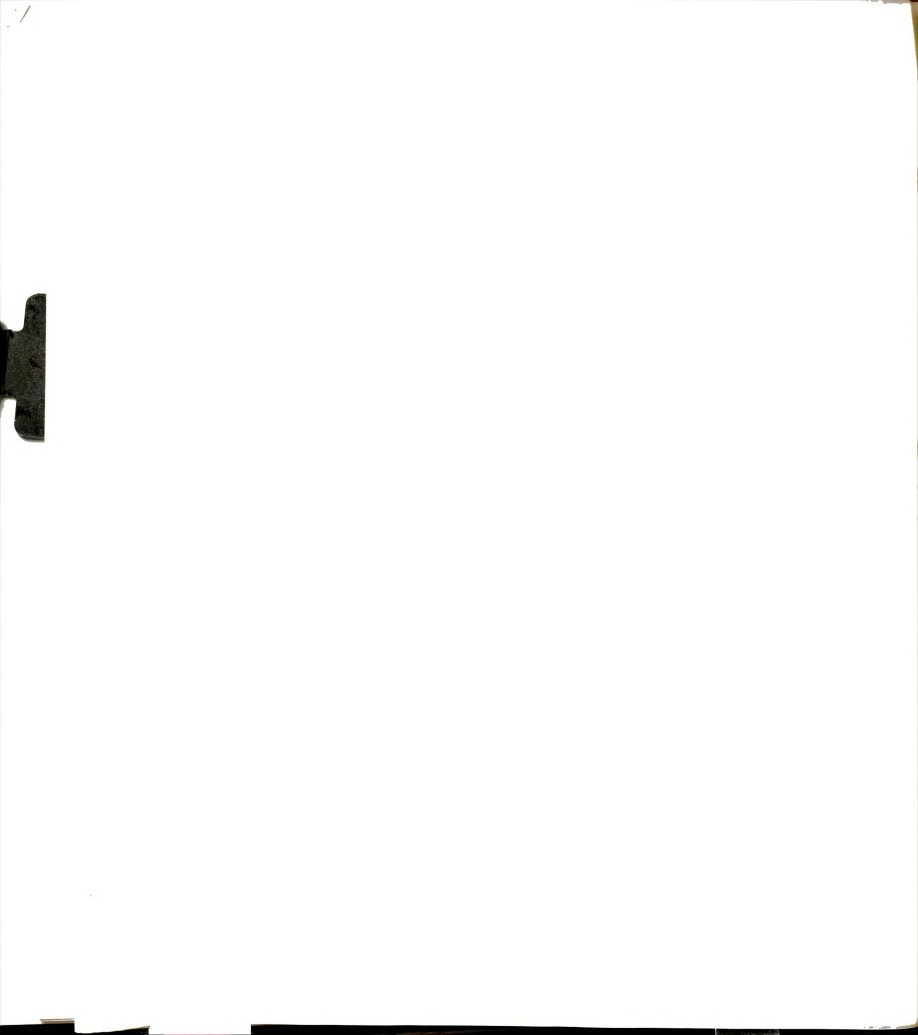


BIBLIOGRAPHY



BIBLIOGRAPHY

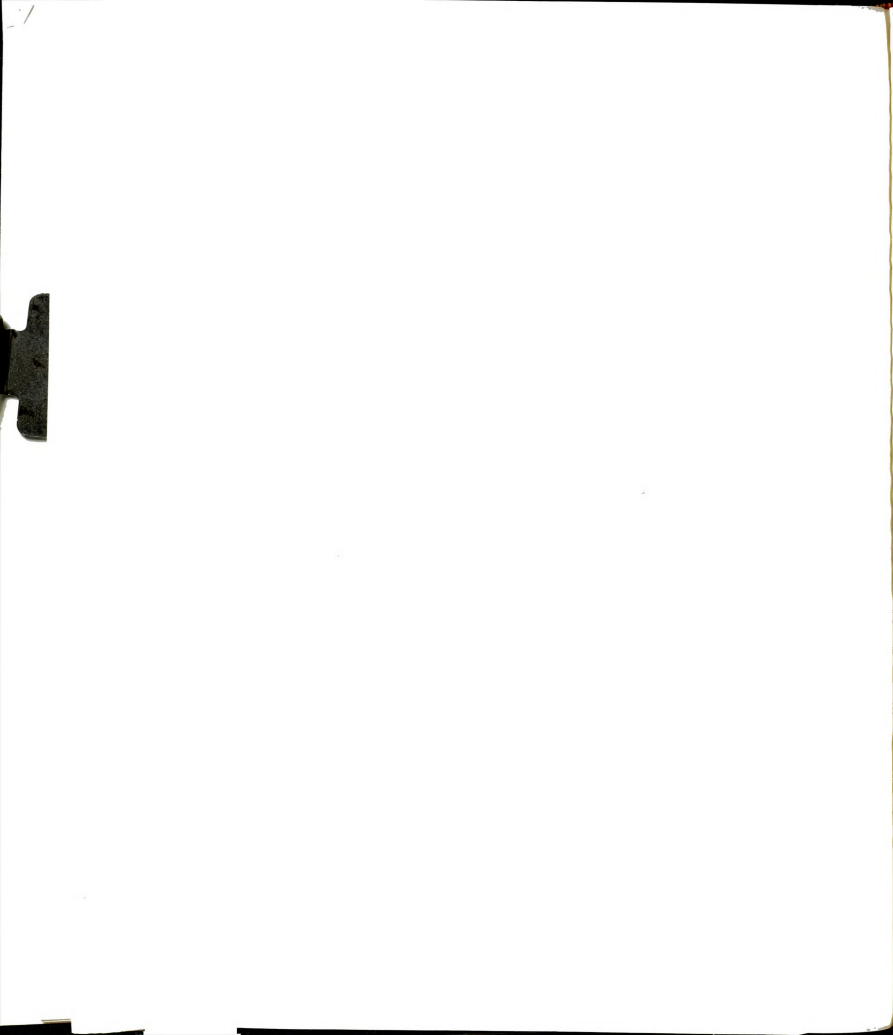
1. A. D. Adler, F. R. Longo, and W. Shergalis, J. Amer. Chem. Soc., 86, 3145(1964).
2. A. D. Adler, L. Sklar, F. R. Longo, J. D. Finarelli, and M. G. Finarelli, J. Heterocyclic Chem., 5, 669(1968).
3. J. B. Kim, J. J. Leonard, and F. R. Longo, J. Amer. Chem. Soc., 94, 3986(1972).
4. D. Dolphin, J. Heterocyclic Chem., 7, 275(1970).
5. L. E. Webb and E. B. Fleischer, J. Chem. Phys., 43, 3100(1965).
6. A. Tulinsky, Ann. N. Y. Acad. Sci., 206, 47(1973).
7. J. E. Falk, "Porphyrins and Metalloporphyrins," Elsevier, Amsterdam, 1964.
8. M. B. Crute, Acta Crystallogr., 12, 24(1959).
9. L. Bogorad, Federation Proc., 14, 184(1955).
10. S. Granick, in "Porphyrin Biosynthesis and Metabolism," G. E. Wolstenholme and E. C. P. Millar, Eds., Churchill, London, 1955.
11. L. Bogorad, J. Biol. Chem., 233, 501, 510, 516(1958).
12. D. Mauzerall and S. Granick, ibid., 232, 1141(1958).
13. R. B. Woodward, Ind. Chim. Belge, 27, 1293(1962).
14. J. N. Phillips, Rev. Pure Appl. Chem., 10, 35(1960).
15. E. B. Fleischer, E. I. Choi, P. Hambright, and A. Stone, Inorg. Chem., 3, 1284(1964).
16. D. J. Casagrande and G. W. Hodgson, Nature Phys. Sci., 233, 123(1971).
17. D. J. Casagrande and G. W. Hodgson, Geochim. Cosmochim. Acta, 38, 1745(1974).



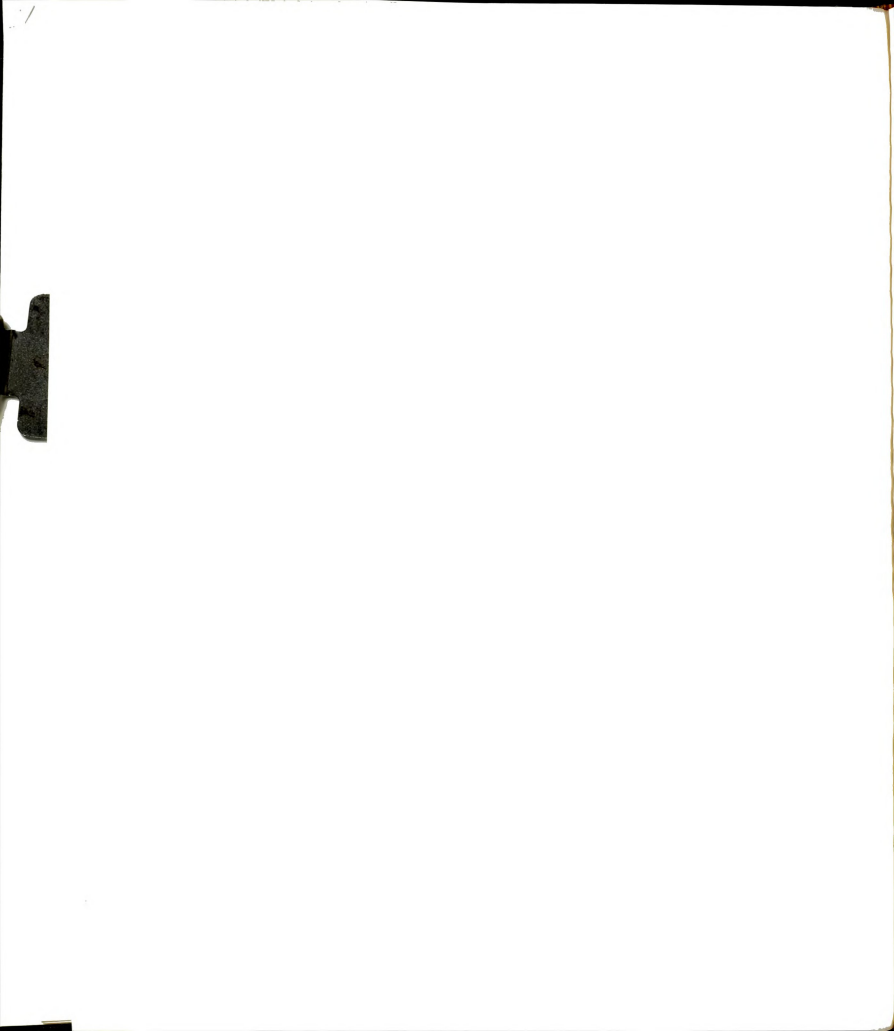
18. G. W. Hodgson, Bull. Geol. Soc. Amer., 71, 1888(1960).
19. N. Kaufherr, S. Yariv, and L. Heller, Clays Clay Minerals, 19, 193(1971).
20. A. Weiss, Dissertation, Darmstadt, 1953.
21. A. Weiss and G. Koch, Dissertation, Techn. Hochschule Darmstadt, 1960.
22. A. Weiss and G. Roloff, Z. Naturforschg., 19b, 533(1964).
23. A. D. Adler, F. R. Longo, J. D. Finarelli, J. Goldmacher, J. Assour, and L. Korsakoff, J. Org. Chem., 32, 476(1967).
24. (a) P. Rothemund, J. Amer. Chem. Soc., 57, 2010(1936).
(b) P. Rothemund, ibid., 61, 2912(1939).
(c) P. Rothemund and A. R. Menotti, ibid., 63, 267(1941).
(d) P. Rothemund and A. R. Menotti, ibid., 70, 1808(1948).
25. G. M. Badger, R. A. Jones, and R. L. Laslett, Aust. J. Chem., 17, 1028(1964).
26. D. Mauzerall and S. Granick, J. Biol. Chem., 232, 1141(1958).
27. D. Mauzerall, J. Amer. Chem. Soc., 82, 1832(1960).
28. D. Mauzerall, ibid., 84, 2437(1962).
29. A. I. Oparin, "The Origin of Life on the Earth"(translated by A. Syngé), 3rd Ed., Academic Press, New York, 1957.
30. M. Calvin, Science, 130, 1170(1959).
31. H. Gaffron, Perspectives Biol. Med., 3, 163(1960).
32. M. Calvin, Chem. Eng. News, 37, 96(1961).
33. C. Sagan, Radiation Res., 15, 174(1961).
34. M. Calvin, Perspectives Biol. Med., 5, 147(1962).
35. M. Calvin, ibid., 5, 399(1962).
36. A. I. Oparin, "Life, Its Nature, Origin and Development"(translated by A. Syngé), Academic Press, New York, 1962.
37. R. M. Lemmon, Chem. Rev., 70, 95(1970).
38. P. Rothemund, J. Amer. Chem. Soc., 58, 625(1936).



39. M. Calvin, R. H. Ball, and S. Aronoff, ibid., 65, 2259(1943).
40. A. Szutka, J. F. Hazel, and W. M. McNabb, Radiation Res., 10, 597(1959).
41. A. Szutka, in "The Origins of Prebiological Systems and of Their Molecular Matrices," S. W. Fox, Ed., Academic Press, New York, 1965.
42. A. Szutka, Nature, 212, 401(1966).
43. A. Krasnovsky and A. Umrikhina, in "Molecular Evolution: Prebiological and Biological," D. L. Rohlfsing and A. I. Oparin, Eds., Plenum Press, New York, 1972.
44. G. W. Hodgson and B. L. Baker, Nature, 216, 29(1967).
45. G. W. Hodgson and C. Ponnampereuma, Proc. Nat. Acad. Sci., 59, 22(1968).
46. J. D. Bernal, "The Physical Basis of Life," Routledge and Kegan Paul, London, 1951.
47. J. D. Bernal, Nature, 186, 694(1960).
48. J. D. Bernal, ibid., 190, 129(1961).
49. E. T. Degens and J. Matheja, J. Brit. Interplanet. Soc., 21, 52(1968).
50. M. Paecht-Horowitz, J. Berger, and A. Katchalsky, Nature, 228, 636(1970).
51. M. Paecht-Horowitz, in "Chemical Evolution and the Origin of Life," R. Buvet and C. Ponnampereuma, Eds., North-Holland, Amsterdam, 1971.
52. E. T. Degens and J. Matheja, in "Prebiotic and Biochemical Evolution," A. P. Kimball and J. Oro, Eds., North-Holland, Amsterdam, 1971.
53. E. T. Degens and J. Matheja, in "Organic Compounds in Aquatic Environments," S. Faust and J. Hunter, Eds., Dekker, New York, 1971.
54. M. Paecht-Horowitz, Angew. Chem. Internat. Ed. Engl., 12, 349(1973).
55. G. R. Harvey, E. T. Degens, and K. Mopper, Naturwissenschaften, 58, 624(1971).
56. N. W. Gabel and C. Ponnampereuma, Nature, 216, 453(1967).



57. T. E. Pavlovskaya, A. G. Pasynskii, and A. I. Grebenikova, Dokl. Akad. Nauk. SSSR, 135, 743(1960).
58. A. Stone and E. B. Fleischer, J. Amer. Chem. Soc., 90, 2735(1968).
59. D. W. Thomas and A. E. Martell, J. Amer. Chem. Soc., 78, 1338(1956).
60. D. W. Thomas and A. E. Martell, ibid., 81, 5111(1959).
61. G. D. Dorough, J. R. Miller, and F. M. Huennekens, ibid., 73, 4315(1951).
62. D. W. Thomas and A. E. Martell, Arch. Biochem. Biophys., 76, 2861(1958).
63. B. B. Wayland, J. V. Minkiewicz, and M. E. Abd-Elmageed, J. Amer. Chem. Soc., 96, 2795(1974).
64. B. Dempsey, M. B. Lowe, and J. N. Phillips, in "Haematin Enzymes," J. Falk, R. Lemberg, and R. Morton, Eds., Canberra, 1959.
65. M. B. Lowe and J. N. Phillips, Nature, 190, 262(1961).
66. J. Manassen and A. Bar-Ilan, J. Catal., 17, 86(1970).
67. D. R. Paulson, R. Ullman, and R. B. Sloane, Chem. Commun., 186(1974).











MICHIGAN STATE UNIVERSITY LIBRARIES



3 1293 03082 4225